

Cellular Mechanisms Regulating Single Lumen Formation in the Zebrafish Gut

by

Ashley Alvers Lento

Department of Cell Biology
Duke University

Date: _____

Approved:

Michel Bagnat, Advisor

Ken Poss, Supervisor

Blanche Capel

Dan Kiehart

Terry Lechler

Dissertation submitted in partial fulfillment of
the requirements for the degree of Doctor
of Philosophy, in the Department of
Cell Biology in the Graduate School
of Duke University

2014

ABSTRACT

Cellular Mechanisms Regulating Single Lumen Formation in the Zebrafish Gut

by

Ashley Alvers Lento

Department of Cell Biology
Duke University

Date: _____

Approved:

Michel Bagnat, Advisor

Ken Poss, Supervisor

Blanche Capel

Dan Kiehart

Terry Lechler

An abstract of a dissertation submitted in partial fulfillment of the requirements for the degree of Doctor of Philosophy, in the Department of Cell Biology in the Graduate School of Duke University

2014

Copyright by
Ashley Alvers Lento
2014

Abstract

The formation of a single lumen during tubulogenesis is crucial for the development and function of many organs. Although 3D cell culture models have identified molecular mechanisms controlling lumen formation *in vitro*, their function during vertebrate organogenesis is poorly understood. In this work we used the zebrafish gut as a model to investigate single lumen formation during tubulogenesis. Previous work has shown that multiple small lumens enlarge through fluid accumulation and coalesce into a single lumen. However, since lumen formation occurs in the absence of apoptosis, other cellular processes are necessary to facilitate single lumen formation.

Using light sheet microscopy and genetic approaches we identified a distinct intermediate stage in lumen formation, characterized by two adjacent un-fused lumens. These lumens are separated by cell contacts that contain basolateral adhesion proteins. We observed that lumens arise independently from each other along the length of the gut and do not share a continuous apical surface. Resolution of this intermediate phenotype into a single, continuous lumen requires the remodeling of basolateral contacts between adjacent lumens and subsequent lumen fusion.

Furthermore, we provide insight into the genetic mechanisms regulating lumen formation through the analysis of the Hedgehog pathway. We show that lumen resolution, but not lumen opening, is impaired in *smoothened (smo)* mutants, indicating that fluid-driven lumen enlargement and resolution are two distinct processes. We also show that *smo* mutants exhibit perturbations in the Rab11 trafficking pathway, which led

us to demonstrate that Rab11-mediated recycling, but not degradation, is necessary for single lumen formation. Taken together, this work demonstrates that lumen resolution is a distinct genetically-controlled process, requiring cellular rearrangement and lumen fusion events, to create a single, continuous lumen in the zebrafish gut.

Contents

Abstract.....	iv
List of Tables	ix
List of Figures.....	x
Acknowledgements.....	xii
1. Introduction.....	1
1.1 Tubulogenesis	1
1.2 Advantages of the zebrafish as a model.....	6
1.3 Zebrafish gut development	7
Anatomy of the zebrafish intestine	9
Formation of the intestinal lumen.....	11
Smooth Muscle	14
1.4 Hedgehog signaling during gut development	15
1.5 Intracellular trafficking.....	18
Intracellular recycling and morphogenesis	22
1.7 Summary.....	24
2. Materials and Methods.....	26
2.1 Fish Stocks.....	26
2.2 Transgenics	26
2.3 BAC Recombineering.....	27
2.4 RNA injection.....	27
2.5 Histology and Immunofluorescence	28

2.6 Live Imaging.....	29
2.7 Embryo dissociation and FACS.....	30
2.8 RNA isolation qPCR.....	30
2.9 In situ hybridization	31
2.10 Morpholino knockdown.....	32
2.11 Pharmacological treatment.....	32
2.12 Cell Culture.....	32
2.13 Membrane Association assay.....	32
2.14 Statistical analysis.....	33
3. Characterization of intestinal lumen formation	34
3.1 Introduction.....	34
3.2 Results.....	36
Time course analysis of lumen formation.....	36
Generation of Cldn15la-GFP	39
Live imaging the zebrafish gut	44
Epithelial morphology and polarity	44
Lumen fusion	48
3.3 Discussion.....	49
4. Molecular mechanisms regulating single lumen formation.....	54
4.1 Introduction.....	54
4.2 Results.....	55
smoothened mutants exhibit impaired lumen formation	55
Characterization of <i>smo</i> guts.....	58

Endocytic degradation and recycling during lumen resolution	63
Impaired Rab11a recycling in <i>smo</i> mutants	68
4.3 Discussion	73
5. The role of Clic5 in the zebrafish gut	77
5.1 Introduction.....	77
5.2 Results.....	80
In vitro analysis of Clic5	80
Is Clic5 a chloride channel?	84
In vivo analysis of Clic5	87
5.3 Discussion	89
6. Conclusion and Future Directions	94
6.1 Apical polarity and lumen initiation	94
6.2 The role of the mesenchyme in lumen formation	98
6.3 Regulation of Rab11	100
6.4 Claudin 15la and single lumen formation.....	101
6.5 Investigation of Array Targets	104
6.6 Conclusions.....	106
Appendix.....	108
Microarray data.....	108
References.....	119
Biography.....	131

List of Tables

Table 1- Downregulated genes in the intestinal epithelium.....	110
Table 2- Upregulated genes in intestinal epithelial cells	111
Table 3- Downregulated genes in <i>smo</i> mutant intestinal epithelial cells.....	114
Table 4- Upregulated genes in <i>smo</i> mutant intestinal epithelial cells.....	115

List of Figures

Figure 1-Mechanisms of tubulogenesis	3
Figure 2- Zebrafish gastrointestinal anatomy	8
Figure 3-Zebrafish intestinal lumen formation	12
Figure 4- The Hedgehog signaling pathway	16
Figure 5- Intracellular trafficking and acidification.....	21
Figure 6- Lumens enlarge and fuse during single lumen formation.....	37
Figure 7- Generation of an intestine specific transgenic line	40
Figure 8- Claudin 15-like a localizes to the basolateral membrane.....	42
Figure 9- Live imaging of <i>TgBAC(cldn15la-GFP)</i>	43
Figure 10- Basolateral contacts are found between lumens.....	46
Figure 11- Basolateral adhesions separate adhesions on A-P axis	47
Figure 12- Lumen resolution through luminal fusion.....	50
Figure 13- Lumen resolution through snapping.....	51
Figure 14- smoothed mutants exhibit a defect in lumen fusion	57
Figure 15- <i>smoothened</i> signaling acts in the surrounding mesenchyme.....	59
Figure 16- Gut tube shape and cell number are similar in WT and <i>smo</i> mutants.....	61
Figure 17- <i>smoothened</i> mutants do not display polarity defects.....	62
Figure 18- The degradation pathway is not involved in lumen formation	65
Figure 19- Rab11aDN embryos exhibit impaired lumen fusion.....	66
Figure 20- p120 expression impairs lumen fusion.....	69
Figure 21- Mesenchymal differentiation is not impaired in Rab11aDN embryos	70

Figure 22- Rab11a is abnormally localized in <i>smo</i> mutants	72
Figure 23- Lumens enlarge and fuse during single lumen formation.....	74
Figure 24- Zebrafish clic5.....	81
Figure 25- Gene expression analysis of clic5	83
Figure 26- in vitro expression of Clic5	85
Figure 27- Clic5 associates peripherally with the membrane.....	86
Figure 28- Clic5a1 localizes to the apical membrane in the gut.....	88
Figure 29- Expression of Tg(hsp70l:GFP-clic5a1) during gut development	90
Figure 30- Morpholino knockdown of clic5 impairs lumen formation	91
Figure 31- p-75 is unpolarized during early gut development.....	96
Figure 32- Claudin15la-GFP localization during development.....	102
Figure 33- Common biological pathways associated with upregulated genes in the intestinal epithelium.....	112
Figure 34- Common biological pathways associated with downregulated genes in the intestinal epithelium.....	113
Figure 35- Common biological pathways associated with upregulated genes in <i>smo</i>	116
Figure 36- Common biological pathways associated with downregulated genes in <i>smo</i> 117	
Figure 37- The endocytic pathway is downregulated in <i>smo</i> mutants.....	118

Acknowledgements

The completion of this work was made possible by the guidance and support of many people for which I am very grateful. First, I would like to thank my mentor, Michel Bagnat for taking me on as his first graduate student. He initiated this project and has since provided much direction and support through its completion. I would also like to thank him for creating a wonderful lab environment to work in. Each and every member of the Bagnat lab has been invaluable to my graduate work. I would like to thank Adam Navis for the tools and technologies that he is constantly developing for the lab. Without his technical expertise, much of this work would not be possible. I thank Lindsay Marjoram for thoughtful discussions and advice, and for the many resources she has brought to the lab. I would also like to acknowledge Sean Ryan who has generated many transgenic lines used in my studies as well and Kathryn Ellis and Jen Bagwell who have made the lab an enjoyable place to work.

I would next like to thank my thesis committee, Ken Poss, Blanche Capel, Terry Lechler, and Dan Kiehart who have provided thoughtful discussion and guidance during my graduate work. Additionally, I thank our collaborator, Jan Huisken for performing SPIM, which greatly enhanced the lumen formation study.

Finally, I would like to acknowledge my family and friends for their immeasurable support during my graduate work. Thank you to my parents who instilled in me a passion for science at an early age and to my sister who edited this work. I would especially like to thank my husband Bill for his support both scientifically and

emotionally. He has provided company during late night time courses, shared equipment and reagents, assisted in cell sorting experiments, and most importantly has provided encouragement every step of the way.

1. Introduction

1.1 Tubulogenesis

Tubes are critical to the form and function of many organs including the lungs, vasculature, kidney, and gut, and have become essential to the transport and distribution of fluids and gases throughout the body of multicellular organisms. Tubular organs vary greatly in their shape and function across organ systems. For example, they can range from small unicellular tubes like the *C. elegans* kidney cell, to the large multicellular mammalian gut tube. They can also vary considerably in complexity from simple cylinder shaped organs to complex tubular networks like the highly branched human lung. Despite their variability, tubes share common fundamental features. For example, all tubular organs are composed of cells with apical-basal polarity and contain a single central lumen. Within a tube, the apical membrane of cells face the central lumen, the basal surface is attached to the basement membrane, and lateral membranes contact neighboring cells through junctions to control barrier function. This organization allows for specialized membrane function and facilitates the delivery of ions and secretory vesicles to the proper surface (Iruela-Arispe and Beitel, 2013).

Tube formation occurs through several distinct mechanisms based on the initial architecture of the epithelial primordium. Tubes that develop from a polarized epithelium typically undergo the process of epithelial wrapping or budding. During epithelial wrapping, which occurs in the mammalian neural tube, cells within a flat epithelial sheet undergo apical constriction, causing a curvature in the sheet (Sawyer et al., 2010). This

bending continues until the ends of the sheet meet and fuse to form a tube with a single central lumen (Figure 1A). Alternatively, budding occurs when cells from an epithelial sheet invaginate to create a small tube that is then extended by cell elongation, migration, or division (Figure 1B). During this process, new buds frequently form off existing tubes to create a complex contiguous network as seen in the mammalian lung and vasculature. (Lubarsky and Krasnow, 2003).

Tubes can also form from unpolarized groups of cells as seen during the development of the pancreas and mammary gland. Unlike wrapping and budding, during the processes of cavitation and cord hollowing, cells must acquire polarity and undergo *de novo* lumen formation. Cavitation begins with a non-polarized solid rod of cells. Cells on the edge of then rod polarize while cells in the center of the rod are eliminated by apoptosis to form a central lumen (Figure 1C). This mechanism of tube formation is observed in the mammary gland and mammalian salivary gland (Melnick and Jaskoll, 2000). Another mechanism in which a tubular organ is formed from a solid rod of cells is cord hollowing. During cord hollowing a central lumen is formed by creating a space between cells within the rod, in the absence of apoptosis (Figure 1C). Cord hollowing is observed during the development of the neural tube and intestine in the zebrafish, yet the way in which cells polarize and form a lumen vary between the two organs. In the zebrafish gut, which will be discussed in detail later, polarity is established at multiple points within the rod of cells. Small lumens form at these points and merge to form a

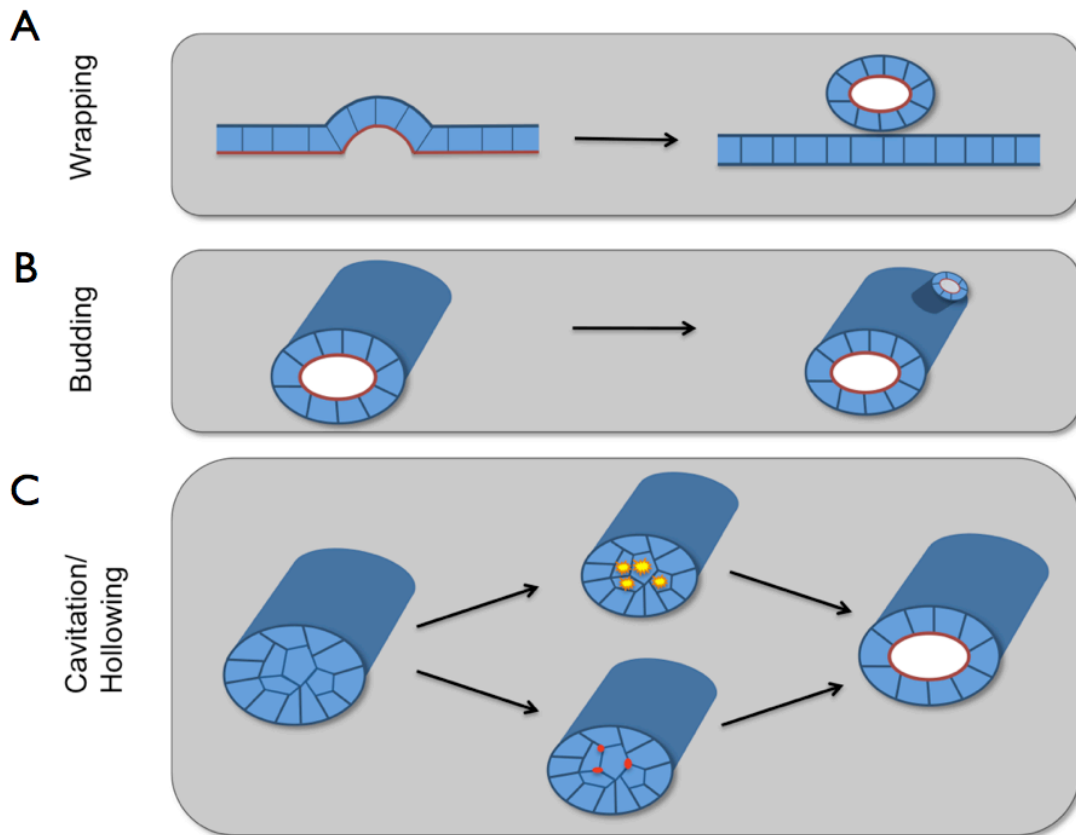


Figure 1-Mechanisms of tubulogenesis

There are four general mechanisms of tubulogenesis. **A-** A polarized epithelial sheet can undergo wrapping to form a tube. **B-** Cells can invaginate from an epithelial sheet to form a small tube or small tubes can bud off from an existing tube. **C-** A solid rod of cells can undergo cavitation in which central cells apoptose to form a lumen (top), or cells can undergo cord hollowing in which a central lumen is formed in the absence of cell loss (bottom).

single lumen (Bagnat et al., 2007; Horne-Badovinac et al., 2001). In contrast, neural tube formation begins with the establishment of apical-basal polarity through mirror symmetrical divisions. These cell divisions distribute apical proteins along the midline of the rod and a lumen is formed through fluid expansion (Buckley et al., 2013). The final mode of tube formation is cell hollowing, in which a luminal surface is created within a single cell by the fusion of intracellular vacuolar apical compartments. The *C. elegans* excretory canal and zebrafish vasculature typically form through this mechanism (Buechner, 2002; Kamei et al., 2006).

Understanding the molecular mechanisms regulating the process of tubulogenesis is critical to understanding several human diseases and disorders including atherosclerosis, spina bifida, and kidney disease which are all the result of defects in tube structure (Hogan and Kolodziej, 2002; Lubarsky and Krasnow, 2003). To study the cellular and molecular events controlling the formation of tubular organs, several model systems have been developed. The primary in vitro model of tubulogenesis utilizes MDCK cells, which when grown in a 3D matrix, form tube like cysts. In addition, in vivo systems have also been established to model different types of tube formation including the *Drosophila* trachea and salivary gland, the *C. elegans* excretory canal, and the zebrafish vasculature.

Given the relative simplicity of cell culture systems compared to in vivo systems, the in vitro MDCK cyst model of tubulogenesis has been extensively studied and has provided insight into the molecular regulators of polarity establishment, lumen formation,

and ECM interactions involved in tube morphogenesis. For example, findings from MDCK cyst models have identified that asymmetric membrane distribution of PIP2 and PIP3, together with Crumbs and Par3 complexes, is essential in establishing apical-basal polarity (Martin-Belmonte and Mostov, 2008). The correct distribution of these molecules is responsible for correct lipid and membrane protein targeting, as well as the localization of junctions within the epithelia. Furthermore, MDCK cysts studies have also shed light on the interactions between polarity and the ECM. Several studies have shown that B integrin, Rac-1, and laminin in the ECM orient epithelial cell polarity and that disruption of Rac-1 leads to a reversal in cyst polarity (O'Brien et al., 2001; Yu et al., 2005).

Lumenogenesis has also been well studied in the 3D cyst model. Lumen formation initiates in MDCK cysts with the accumulation of the apical protein podocalyxin in Rab11 and Rab8 positive vesicles. These vesicles are transported to the membrane between two opposing cells to establish an apical domain where a lumen soon forms (Bryant et al., 2010). However, this mechanism of lumen formation does not accurately represent single lumen formation in many *in vivo* systems. Unlike many *in vivo* systems, MDCK cysts polarize at the two-cell stage and a lumen forms in the presence of just these two cells. In contrast, tubular organs such as the mammary gland, salivary gland, and pancreas develop from a large cluster of unpolarized cells and have to coordinate lumen initiation and single lumen formation within a large tissue (Hogg et al., 1983; Villasenor et al., 2010). Furthermore, tube morphogenesis *in vivo* involves

interactions with surrounding tissues, and coordination with various cell types, which cannot be modeled in the 3D cyst system. Therefore, in vivo models of tubulogenesis are critical to understanding how tubular organs develop and function. The work presented here utilizes the zebrafish gut as a model to study the molecular mechanisms involved in single lumen formation during the process of cord hollowing.

1.2 Advantages of the zebrafish as a model

The zebrafish offers several unique advantages as a vertebrate model. One of the greatest advantages of the zebrafish compared to other vertebrates is the ability to image all internal organs together and intact. The optical transparency of zebrafish embryos and their rapid external development allows access to all developmental stages and real-time imaging of developmental processes. Most of the major organs including the heart, vasculature, intestine, liver, pancreas, and nervous system can be easily observed and screened for developmental abnormalities during the first few days after fertilization. Furthermore, the ability to generate tissue-specific fluorescent transgenic zebrafish has become relatively easy, fast, and inexpensive (Figure 2B-C). The transparency of zebrafish allows for real-time visualization of fluorescent transgenic animals during developmental processes such as cell division, differentiation and organogenesis. For example, confocal time-lapse imaging of *Tg(gutGFP)* embryos, which express GFP in endodermal tissue, has achieved a detailed characterization of the morphogenesis of all developing endodermal organs (Field et al., 2003). Finally, due to the genetic tractability of the zebrafish, forward and reverse genetic techniques are well established to

manipulate and study gene function. Notably, targeted gene mutation techniques are quickly being developed in zebrafish including Transcription activator like effector nucleases (TALENs). TALENs are a powerful new tool that induce mutations in endogenous zebrafish genes and enable targeted gene knockdown, which can be utilized in future studies of lumen formation (Huang et al., 2011; Miller et al., 2011). Thus, the transparent nature of the zebrafish together with the availability of a wide range of genetic tools, allows for easy genetic manipulation and real-time imaging of the gut throughout development, therefore making the zebrafish intestine an excellent model to study tubulogenesis.

1.3 Zebrafish gut development

The molecular pathways regulating endoderm development are well conserved between zebrafish and mammals. Gastrointestinal organogenesis in the zebrafish begins at 1 dpf when a thin layer of endoderm at the midline of the embryos gives rise to the primitive gut at 26-30 hpf (Ng et al., 2005). This rod of tissue soon gives rise to all the major organs of the digestive system including the pancreas, liver and intestine (Wallace and Pack, 2003) (Figure 2A-C). Development of the intestine begins at 24 hpf when the anterior portion of the endodermal rod thickens. Intestinal development continues over 5 days and undergoes stages of lumen formation, cell differentiation, epithelial folding, and gut motility.

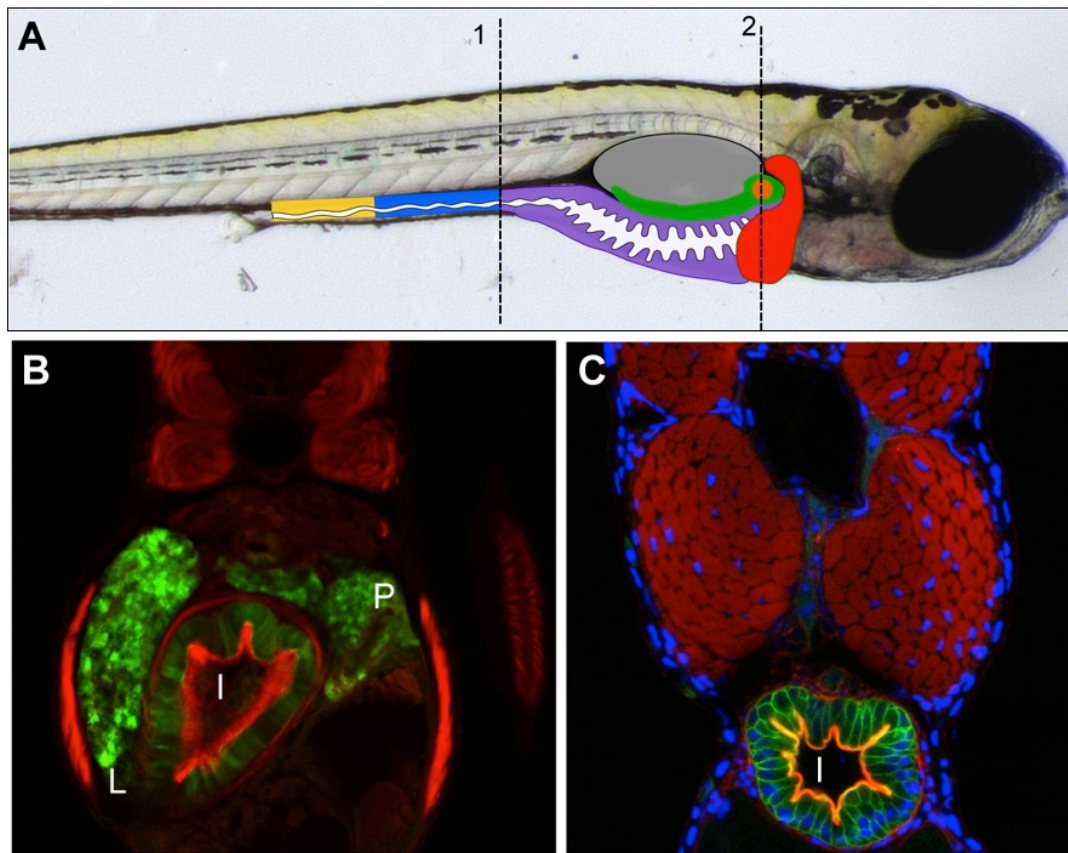


Figure 2- Zebrafish gastrointestinal anatomy

A-The zebrafish gastrointestinal tract is composed of a liver (red), exocrine pancreas (green), primary islet (orange), and an intestine that is divided into the intestinal bulb (purple), mid-intestine (blue), and posterior intestine (yellow). The swim bladder is in gray. **B-** Transverse cross section of a Tg(gutGFP) embryo expressing GFP in the liver (L), pancreas (P), and intestine (I). Section corresponds to line 2 in panel A. **C-** Transverse cross section of a transgenic embryo expressing an intestine specific membrane GFP marker. Section corresponds to line 1 in panel A.

Anatomy of the zebrafish intestine

As in mice, the zebrafish intestinal tract is compartmentalized in an anterior-posterior direction and is divided into three regions: the intestinal bulb, mid-intestine, and posterior intestine, each of which have specialized anatomical and physiological characteristics (Wallace et al., 2005). Morphogenesis of the three intestinal regions occurs during the fourth day of development and each region can be identified based on the specialized characteristics and functions acquired by cells within each region. The most anterior region of the gut is known as the intestinal bulb. Unlike most vertebrates, the zebrafish esophagus connects directly to the intestine and there is no true stomach. Instead, zebrafish develop an expanded portion of the intestine called the intestinal bulb that acts as the major site of lipid digestion (Pack et al., 1996). Compared to the rest of the intestinal tract, the luminal space in the intestinal bulb is quite expanded and rounded in appearance. The epithelium in this region exhibits folds that extend down the intestinal tube to the middle of the embryo and cell proliferation occurs in cells found at the base of these folds (Ng et al., 2005). The next region of the gut is the mid-intestine which is characterized by a reduced rate of proliferation and a large amount of cell differentiation. In this region goblet cells, identified by Alcian blue staining, are observed early in development and not seen in other regions of the gut. In addition, enterocytes containing large vacuoles are also specific to this region (Ng et al., 2005). Finally, the most posterior region of the gut tube is called the posterior intestine and is characterized by the absence of epithelial folds, a moderate amount of proliferation and a lack of goblet cells. This

region of the gut has been proposed to function, like the mammalian colon, in ion and water uptake (Wallace et al., 2005).

Cell proliferation in the zebrafish intestine only occurs at the base of the epithelial folds (Ng et al., 2005). Although the base of epithelial folds appears to be similar to mammalian crypts, zebrafish do not form true crypt-like structures. As the cells migrate up the folds, proliferation stops and cells begin to express differentiation markers. Cell differentiation in the epithelium occurs through lateral inhibition, which is regulated by the Notch signaling pathway. This signaling is critical to ensure cells become different fates, since in the absence of Notch signaling, all intestinal cells differentiate into a secretory fate (Crosnier et al., 2005)

The zebrafish intestinal epithelium differentiates into three major types of cells: enterocytes which are absorptive cells that display a brush border on their apical surface, mucus containing goblet cells, and enteroendocrine cells that contain secretory granules. These cells types are found within different regions of the gut with varying proportions. Enterocytes are the most abundant cell type in the zebrafish intestine and are found in the intestinal bulb and mid intestine. The second most populous cell type are the goblet cells which are found in all regions of the intestine, followed by enteroendocrine cells which are restricted to the anterior intestine. Unlike mammals, the zebrafish intestine does not contain Paneth cells during development or in adulthood (Wallace et al., 2005).

Formation of the intestinal lumen

The process by which lumen formation occurs in the zebrafish intestine differs widely from that seen in mammals. In mammals, the intestinal tube is formed through the wrapping of a flat epithelial sheet that forms a transiently stratified epithelium and undergoes apoptosis to form an epithelial monolayer (Wells and Melton, 1999). In contrast, tubulogenesis in zebrafish occurs through a process of cord hollowing (Wallace and Pack, 2003) in which a lumen is formed in between cells within a solid rod. Furthermore, unlike many tubular organs, the primitive zebrafish gut does not contain a lumen and the cells are not arranged in a radial pattern. Thus, the first stage of intestine development in the zebrafish involves the morphogenesis of a solid endodermal rod into a continuous tubular structure through a cord hollowing process. The process of lumen formation initiates in the anterior region of the endoderm and occurs in an anterior to posterior direction. The cells within the endodermal rod develop a bilayer arrangement and reconfigure into an epithelial monolayer as the lumen is formed. In contrast to the development of the mammalian intestine, which requires apoptosis for the formation of the epithelial monolayer, apoptosis is not involved in lumen formation in the zebrafish intestine (Ng et al., 2005).

Intestinal lumen formation begins around 40 hpf with the development of multiple actin rich foci within the endodermal rod. Next, junctional proteins such as ZO-1 localize to the foci which cluster and move toward the center of the gut. Small lumens form at these points then coalesce into a single continuous lumen that extends from the caudal

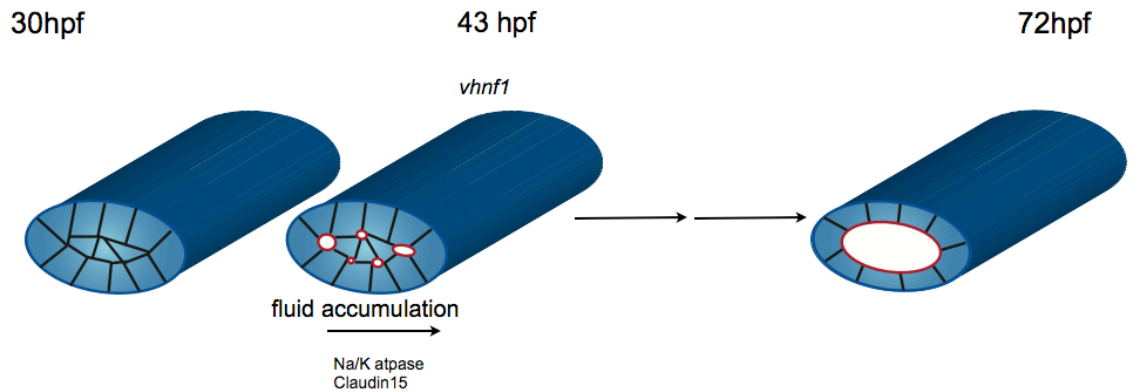


Figure 3-Zebrafish intestinal lumen formation

The zebrafish gut begins from a solid rod of endodermal cell. Lumen formation is initiated by the development of multiple actin rich foci and junctional clusters in between cells. Small lumens form at these points and *vhnf1* regulates Na/K⁺ atpase and Claudin15 to drive fluid accumulation within small lumens to promote lumen enlargement and coalescence. However other cellular processes are likely involved to facilitate cellular rearrangements and luminal coalescence during single lumen formation.

end of the intestine to the pharyngesophageal region of the larvae (Bagnat et al., 2007). Zebrafish mutant for atypical protein kinase C (aPCK) fail to undergo gut looping and develop multiple small lumens in the gut (Horne-Badovinac et al., 2001). This gene appears to be involved in the regulation of clustering and maintenance of apical adherens junctions. In the absence of aPCK, apical adherens junction clustering is delayed and overall less effective compared to wildtypes, resulting in the formation of small lumens prior to their convergence at the center of the gut (Horne-Badovinac et al., 2001).

Further insight into how multiple small lumens coalesce into a single lumen was gained by the examination of embryos mutant for the transcription factor *hnf1*. Analysis of *hnf1* mutant embryos revealed multiple small lumens within the intestinal bulb region at 72 hpf (Bagnat et al., 2007). However multiple lumens were never observed in wildtype embryos at this time point. Hnf1 regulates expression of Claudin15 and Na/K - Atpase which are required for proper lumen coalescence. It is proposed that Na/K-Atpase generates an electrochemical gradient that drives ions through Claudin15 junctions into the lumen (Bagnat et al., 2007). As a result, fluid accumulates within the lumens leading to their expansion and coalescence into a single lumen. However, additional cellular processes are likely involved in the coordination of a single lumen and need to be investigated further.

Although lumen formation is the major morphogenic process occurring during this period of gut development, several other events are simultaneously occurring and the intestine is undergoing a high rate of proliferation. The epithelial cells around the lumen

take on a columnar shape and the nuclei localize near the base of the cells. In addition, around the time of lumen opening, a thin layer of cells from the lateral plate mesoderm begin to surround the intestine, and eventually differentiate into connective tissue and form the muscle layers that surround the intestine (Ng et al., 2005).

Smooth Muscle

In addition to an epithelium, the gut is also composed of smooth muscle which is vital to proper intestinal form and function. The zebrafish develops two layers of smooth muscle surrounding the intestine: circular smooth muscle and longitudinal smooth muscle. These layers of muscle are critical to the stability, contractility and mobility of the gastrointestinal tract. Several smooth muscle markers are dynamically expressed in the mesenchyme during gut development, the earliest of which include *SM22- α* , *α SMA* and *non-muscle myosin heavy chain (myh11)* (Georgijevic et al., 2007). Smooth muscle cells differentiate from mesenchymal cells beginning at about 50 hpf based on the expression of *myh11* in the anterior intestine. However the protein is not found until 72 hpf. Following expression of differentiation markers, smooth muscle cells proliferate and expand to all regions of the intestine by 72 hpf. Finally, by 96 hpf a continuous layer of circular and longitudinal muscle is easily observed around the gut and motility begins (Wallace et al., 2005).

Interactions between the epithelium and mesenchyme are critical to the development of many vertebrate organs including the gut. In the gut, signaling from the intestinal epithelium regulates the differentiation of mesenchymal cells into smooth

muscle (Kedinger et al., 1998). In return, reciprocal signaling from the mesenchyme controls epithelial patterning, differentiation and morphogenesis of the intestinal endoderm. These epithelial-mesenchymal interactions are primarily regulated by secreted proteins. For example, hedgehog signaling from the gut epithelium promotes proliferation of the neighboring mesenchyme and is involved in villus formation, SMC differentiation, and the development of the enteric nervous system (Mao et al., 2010). Furthermore, in the zebrafish, interactions between Hh in the epithelium and Fgf10a in the mesenchyme have been shown to be critical during esophagus and swimbladder development (Korzhan et al., 2011). In addition to the Hh signaling pathway, bone morphogenic proteins (BMPs) secreted from the mesenchyme, are also known regulators of mesenchyme differentiation, and epithelial cell proliferation, differentiation and migration during gut development (Ishizuya-Oka and Hasebe, 2008). Therefore, understanding the cross talk between the epithelium and mesenchyme is critical to the understanding of the morphogenic processes regulating gut development.

1.4 Hedgehog signaling during gut development

The role of hedgehog signaling has been extensively studied in gastrointestinal development. Hedgehog signaling coordinates morphogenic patterning and regionalization of the gut tube across a wide range of the animal kingdom, including *Amphioxus*, *Drosophila*, sea urchin, zebrafish, chicken and mouse (Bitgood and McMahon, 1995; Mohler and Vani, 1992; Shimeld, 1999; Strahle et al., 1996; Walton et al., 2006). There are three Hh ligands in vertebrates- Sonic Hedgehog, Indian Hedgehog,

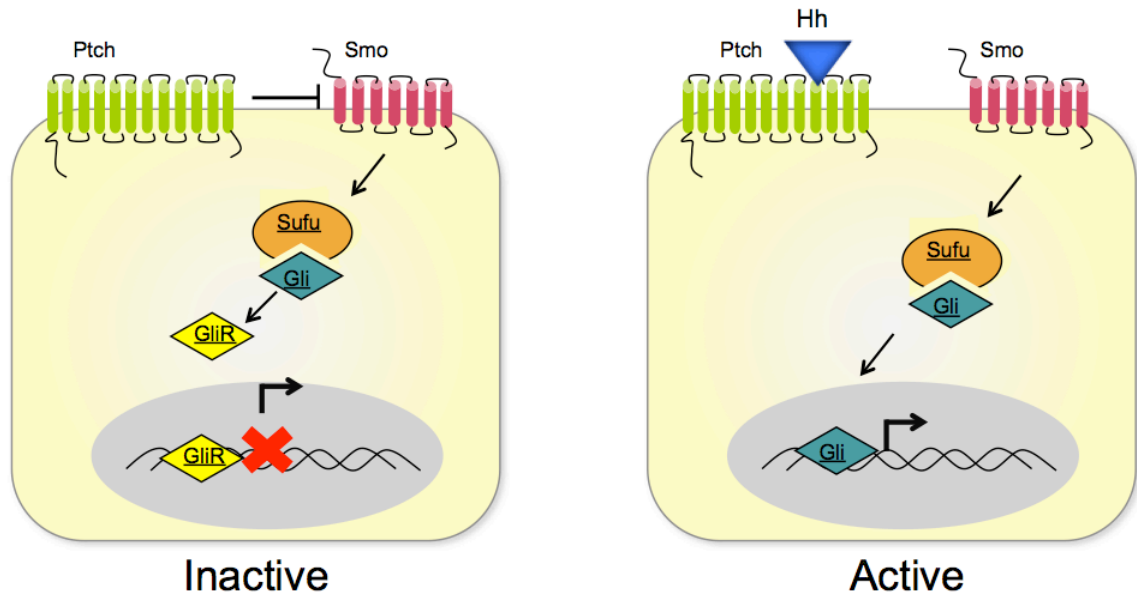


Figure 4- The Hedgehog signaling pathway

When the hedgehog ligand is absent, patched inhibits smoothened and Sufu generates a repressor form of Gli to inhibit transcription of target genes. In the presence of ligand, hedgehog binds to the patched receptor and relieves repression of smoothened. Gli can then translocate to the nucleus to activate transcription of target genes.

and Desert Hedgehog, all of which are expressed in the gut tube. These ligands bind to the receptors Patched 1 and Patched 2 (Ptch). In the absence of Hh binding, Ptch represses the membrane protein smoothened and the pathway is inactive. In the presence of ligand, Hh binds to the Ptch receptor relieving the inhibition of smoothened and in turn, activates pathway activity and transcription of target genes (Figure 4). Shh and Ihh are expressed in the gut epithelium, while Dhh is found in Schwann cells and peripheral nerves in the gut. Signaling between pathway members occurs in a paracrine fashion between Hh in the epithelium and target genes in the mesenchyme, which is critical for the proper development of both tissues (Kolterud et al., 2009).

Hedgehog signaling is involved in all major aspects of gut development including anterior-posterior patterning, radial patterning, and stem cell regulated proliferation and differentiation (Ramalho-Santos et al., 2000). Loss of Hh activity leads to a wide range of gastrointestinal defects and diseases. In mice, loss of Shh and Ihh results in malrotation of the gut, reduced smooth muscle, and esophageal atresia with tracheal esophageal fistula. In addition, loss of the Hh effector protein, Gli, results in morphogenesis defects in the esophagus and hindgut, as well as anal stenosis, and an extended distal stomach. In humans, impaired Hh signaling is also linked to GI malformations including Palister-Hall syndrome and VACTERL association (Ramalho-Santos et al., 2000).

Zebrafish have three Hh homologs that are expressed in the gut endoderm, including *shha*, *shhb* and *ihha*. Hh signaling has been shown to regulate morphogenesis of the esophagus, gut, and swimbladder in zebrafish. Fish mutant for Ihh exhibit reduced

expression of the endodermal marker *foxa2* in the esophagus, intestinal bulb and swimbladder, as well as a reduction in the gut epithelium (Korzsh et al., 2011). In addition, these mutants display a reduced or absent lumen and lack differentiated enterocytes. Studies in zebrafish mutant for *shh* also suggest a role for Shh in esophagus morphogenesis and differentiation, cloacal development, and for the development of the enteric nervous system (Parkin et al., 2009; Reichenbach et al., 2008; Wallace and Pack, 2003). Taken together, signaling between the intestinal epithelium and mesenchyme, particularly by the Hh signaling pathway, is vital to the proper morphogenesis and function of the gut.

1.5 Intracellular trafficking

Cells internalize ligands, membrane proteins, and extracellular material through the process of endocytosis. Endocytosis is in turn balanced by the process of endosomal recycling, in which many endocytosed proteins are recycled back to the plasma membrane. This balance between internalization and recycling is critical to a number of cellular processes including signal transduction, the formation of adhesions and junctions, cell polarity, and cell migration. For example, in epithelial cells, endocytic trafficking is essential for membrane proteins to be properly returned to the membrane from which they were removed in order to maintain the distinction between the apical and basolateral membrane (Wang et al., 2000).

Given the importance of protein endocytosis and recycling, the intracellular trafficking pathways regulating these processes are highly coordinated by a large family

of Rab GTPases. Rab proteins comprise the largest family of small GTPases and over 60 Rab proteins have been identified in vertebrates, highlighting a great need for intracellular transport throughout a range of organisms (Zerial and McBride, 2001). Rabs act as molecular switches that alternate between a GDP bound inactive state and a GTP bound active state. In their inactive state, Rabs are inserted into their target membrane. A GEF then converts the Rab to its active state, allowing the Rab to interact with effector proteins (Hutagalung and Novick, 2011). When active, Rabs regulate diverse cellular functions through their interaction with effector proteins, which are highly specialized for individual organelle and transport activities. Together with effector proteins, Rabs direct all stages of membrane transport including vesicle formation, vesicle transport, and the docking and fusing of vesicles to their intended compartment (Hutagalung and Novick, 2011).

The first step of the endocytic trafficking pathway involves the internalization of ligands from the plasma membrane. Ligands are sequestered into clathrin-coated vesicles and are transported from the plasma membrane where they fuse to early endosomes. This early endocytic pathway, including the homotypic fusion of early endosomes, is regulated by Rab5 and its effector EEA1 (Bucci et al., 1992; Gorvel et al., 1991). Due to the mild acidity of early endosomes, proteins in this compartment undergo conformational changes leading to the release of ligands from receptors. Proteins are then sorted and undergo either fast recycling back to the plasma membrane or are sent to the recycling endosome. Rab4 is thought to regulate the efflux of proteins from the early

endosome to the fast recycling pathway, however knockdown studies have been inconclusive (van der Sluijs et al., 1992; Yudowski et al., 2009). Proteins sent to the recycling endosome are recycled back to the plasma membrane through the slow recycling pathway regulated by Rab11. The slow recycling pathway was initially demonstrated to be important for transferrin recycling in non-polarized cells and has since been shown to also be critical for recycling from the apical recycling endosome in polarized epithelial cells (Calhoun et al., 1998; Ullrich et al., 1996). Alternatively, instead of being recycled, cargo proteins can also be endocytosed into early endocytic compartments and sent for degradation. In this case, cargo is trafficked from early to late endosomes and finally to lysosomes through regulation by Rab7 (Feng et al., 1995) (Figure 5A).

Acidification of endosomal compartments is critical for proper sorting and recycling along the endocytic trafficking pathways. Each endosomal compartment has a distinct pH and become increasingly acidic as they progress along the pathway from newly formed vesicles at the plasma membrane to the highly acidic lysosomal compartment (Marshansky and Futai, 2008). Acidification of intracellular compartments is driven primarily by the (V) H-ATPase pump which hydrolyses ATP to translocate protons into the lumen of the organelle. To maintain electroneutrality, additional ion channels, exchangers, and transporters are necessary to facilitate acidification, including ClC, NHE, and Ca²⁺ transporters (Scott and Gruenberg, 2011) (Figure 5B). Defects in

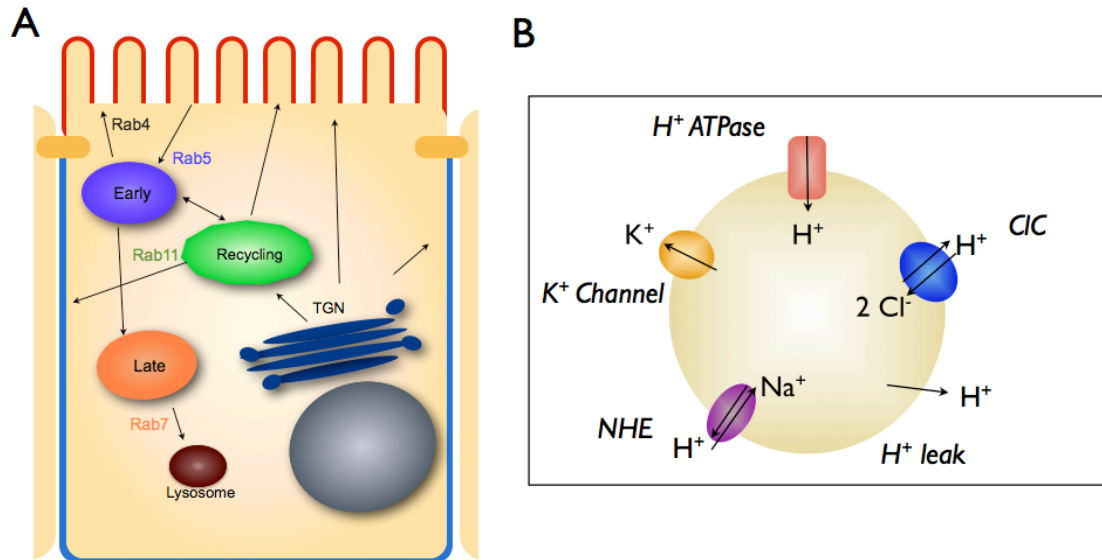


Figure 5- Intracellular trafficking and acidification

A- Membrane proteins can be internalized and degraded or recycled back the cell surface. When proteins are internalized they are transported from the plasma membrane and fuse with early endosomes (purple) which is regulated by Rab5. From here they can be recycled directly back to the membrane by Rab4 or they can be sent to the recycling endosome. The Rab11 mediated recycling endosome (green) sorts and recycles proteins back to the plasma membrane. If proteins are to be degraded, they are trafficked from the early endosome to the Rab7 mediated late endosome (orange) and finally to the lysosome (brown). **B-** Intracellular acidification is primarily regulated by the V- H⁺ATPase. Additional channels and transporters are also needed to maintain electroneutrality.

acidification inhibit endosomal transport, endosomal sorting, and intracellular vesicle fusion and are linked to various human diseases including cancer, neurological disorders, and diabetes (Aridor and Hannan, 2002).

Intracellular recycling and morphogenesis

The endocytic recycling pathway is critical to the continuous trafficking of the basolateral adhesion protein, cadherin, to and from the cell surface. This continual recycling is essential to the dynamic nature of adherens junction formation and is necessary for proper cell adhesion as well as a range of morphogenic events. E-Cadherin is an epithelial adhesion protein that forms dynamic adherens junctions during the processes of epithelial morphogenesis and polarization (Yap et al., 1997). It forms a complex with several other junctional proteins including B-catenin, p120-catenin, and a-catenin, at the adherens junction where it interacts with the actin cytoskeleton and signaling proteins (Pokutta and Weis, 2007). E-Cadherin is internalized from the surface of the cell by clathrin-mediated endocytosis and can be degraded or recycled back to the plasma membrane (Paterson et al., 2003). Recent work has shown that recycling endosomes and active Rab11 is necessary for the correct targeting of cadherin to the basolateral surface. When Rab11 function is impaired through expression of a dominant negative Rab11, cadherin missorts to the apical surface and lumen formation in MDCK cysts is compromised (Desclozeaux et al., 2008).

Several *in vivo* studies have also demonstrated that modulation of adhesions through intracellular recycling activities regulate morphogenic processes. In *Drosophila*

for example, cadherin removal and insertion at cell boundaries drives hexagonal packing of epithelial cells in the imaginal wing disc. This process is regulated by dynamin dependent endocytosis and Rab11 dependent recycling of cadherin. When endocytosis is blocked, cellular rearrangements are impaired, and the expression of a dominant negative Rab11 causes an accumulation of cadherin in intracellular compartments (Classen et al., 2005). Cadherin recycling has also been proposed to play a role in tube morphogenesis in the *Drosophila* trachea. The *Drosophila* trachea undergoes cellular rearrangements to promote a reduction in diameter of tracheal branches. It has recently been shown that Rab11 and its effector protein Rip11 modulate the trafficking of cadherin to specify which branches undergo morphogenesis. In this system, Rab11 and Rip11 accumulate in the dorsal trunk, causing a junctional accumulation of cadherin. It is proposed that increased levels of cadherin in the dorsal trunk inhibits cell intercalation, whereas low levels of Rab11 and Rip11 in other branches allow intercalation to proceed (Shaye et al., 2008). Adherens junctions are also regulated by the Cdc42, Par6, Par3, aPKC complex. During neuroectoderm development, Cdc42 and Par6 stabilize adherens junctions by slowing endocytosis of apical proteins from the plasma membrane and by accelerating the trafficking of apical proteins from the early to the late endosome (Harris and Tepass, 2008). Furthermore, this complex was also found to be essential in maintaining E-cadherin at junctions in the *Drosophila* dorsal thorax. In this system, loss of Cdc42-Par6-aPKC results in defects in junctional continuity and apical actin cytoskeletal organization (Georgiou et al., 2008). Taken together, these studies highlight the important role of

intracellular trafficking and adhesion dynamics during a variety of morphogenic processes.

1.7 Summary

Tubulogenesis is a complex process that occurs through a variety of mechanisms among different tissues and organisms. However, a defining feature among all tubes is the presence of a single continuous lumen. In this work, I will further investigate the process of single lumen formation using the zebrafish gut as a model. Compared to in vitro systems of lumen formation, which lack the complexity of an in vivo organ, the zebrafish gut is optically accessible and amenable to both physical and genetic manipulation, which makes it an ideal system to examine the development of a single continuous lumen within a large organ. Previous studies have shown how lumens initiate and enlarge, however additional cellular processes are likely involved in lumen coalescence. Since zebrafish lumen formation occurs in the absence of apoptosis, we hypothesize that cellular rearrangements within the endodermal rod are necessary for single lumen resolution. To address this hypothesis, I will thoroughly examine gene expression, cellular organization, and luminal arrangements during gut development. I will also examine the hedgehog pathway, which will provide insight into the genetic regulation of different stages of single lumen formation. Finally, given the importance of adhesion remodeling in tissue morphogenesis, I will address endocytic trafficking and recycling as possible mechanisms regulating cellular rearrangement during lumenogenesis in the zebrafish gut. Together, these studies will elucidate new

mechanisms regulating single lumen formation and will provide tools to further the study of gut morphogenesis in the zebrafish.

2. Materials and Methods

2.1 Fish Stocks

Zebrafish were maintained at 28°C and bred as previously described (Westerfield, 2000). Zebrafish lines used in this study include: EK, *smo*^{s294} (Aanstad et al., 2009), *Tg(UAS:mCherry-rab11a-S25N)mw35* (Clark et al., 2011), *Tg(hsp70l:Gal4)* (Scheer and Campos-Ortega, 1999), *Tg(hsp:GFP-podlx)pd1080* (Navis et al., 2013), *atp6v1e1b*^{hi577aTg/hi577aTg}, *atp6v1f*^{hi1988Tg/hi1988Tg} (Nuckels et al., 2009), *Tg(GBS-ptch2:EGFP)umz23* (Choi et al., 2013), *TgBAC(cldn15la-GFP)pd1034*, *Tg(-1.0ifabp:GFP-CaaX)pd1005*, *Tg(hsp70l:GFP-CaaX)pd1008*, *Tg(hsp70l:GFP-rab11bS25N)pd1090*, *Tg(hsp70l:GFP-RAB11a)pd1031*, *Tg(hsp70l:GFP-RAB7)pd1033*, *Tg(hsp70l:GFP-RAB7T22N)pd1032*, *Tg(hsp70l:GFP-p120)pd1091*, *Tg(hsp70l:Ras-RFP)pd1111*, *Tg(hsp70l:GFP-Clic5a1)pd1030* (this study). To induce expression, embryos under the *hsp70l* promoter were placed in 50ml conical tubes and heat-shocked for 40 minutes in a 40° C water bath.

2.2 Transgenics

Transgenic lines were generated using the Tol2kit gateway recombination system (Kwan et al., 2007). Plasmids used include p5E-MCS, p5E-hsp70l, pME-MCS, pME-EGFP-CaaX, p3E-polyA, pDestTol2pA2, and pDestTol2CG2. pME-RAB11a was generated from Addgene plasmid 12674: GFP-rab11WT. pMe-GFP-Rab7 and pMe-GFP-Rab7DN were generated from Addgene plasmids 12605 and 12660 respectively. *rab11b* was amplified from cDNA using primers with BamHI and NotI restriction sites:

Rab11b_BamHI_F, GGATCCATGGGGACCCGTGACGAC; Rab11b_NotI_R,
GCGGCCGCTCACAGGTCCTGACAGC and a point mutation was created using
QuikChange II XL site-directed mutagenesis kit (Agilent Technologies) to generate
Rab11bS25N. clic5a1 was amplified using the following primers with BamHI and NotI
restrictions site: Clic5a1_BamF,
GGATCCATGACCTCAAATGAAGAGGGCAAAGATCCT, Clic5a1_NotR,
GCGGCCGCTTATTTTCCGAGCCGCTTGGCCACGTCC.

2.3 BAC Recombineering

A BAC containing *cldn15la* was modified as previously described (Navis et al.,
2013). A C terminal fusion was created using a plasmid containing a 20-aa spacer
(DLPAEQKAASEEDLDPPVAT), GFP, and a SV-40 polyadenylation sequence.
Recombination was performed using the following homology primers: *cldn15la*-
spGFP_hom_F,
CCATCTATAACCACAGCTCAATCGAACGCAGAAACATCCAAAGCCTACGTCTGA
TCTCCCCGCCGAACAGAAA, and *cldn15la-spGFP_hom_R*,
TAAACAAACATCAACGTAACAACAGTTCAGCCTTGTTAAAATGGGAAATCAT
TGGAGCTCCACCGCGGTG. The *cldn15la-GFP* BAC was linearized using AsiSI
(NEB), injected into one cell stage embryos and a transgenic line *TgBAC(cldn15la*-
GFP)pd1034 was created.

2.4 RNA injection

RFP was fused to the N-terminus of Rab11fip1a and cloned into pCS2+ using
ClaI and XbaI sites. The plasmid was linearized using NotI and RNA was transcribed

using the mMESSAGE mMACHINE SP6 kit (Ambion). RFP-Rab11fip1a (294 pg/embryo) RNA was injected into embryos at the one cell stage.

2.5 Histology and Immunofluorescence

For cross sections, embryos were fixed in 4% paraformaldehyde overnight at 4°C, washed with PBS then embedded in 4% low melt agarose (GeneMate), sectioned with a vibratome (VT 1000S; Leica) and stained as described previously (Bagnat et al., 2007). Primary antibodies used were: pan-cadherin (Santa Cruz Biotechnology ; 1:1200), ZO-1 (Invitrogen; 1:500), 4e8 (AbCam; 1:500), β -catenin (Santa Cruz Biotechnology; 1:500), caspase 3 (Milipore, 1:500), Myh11 (Biomedical Technologies; 1:150) and BrdU (Invitrogen, 1:500). F-Actin was visualized with alexa-568 or 488 phalloidin (Invitrogen; 1:500). Goat anti mouse alexa568 and goat anti-rabbit alexa568 secondary antibodies (Molecular Probes) were used at 1:300. A custom Cldn15la antibody was generated in rabbit using a peptide derived from the C-terminus of Cldn15la (YQRFSKSKEKGAYYPYPC) and used at a concentration of 1:500. Cldn15la staining was performed as previously described (Dong et al., 2007). Briefly, embryos were fixed with 2% formaldehyde in 100mM PIPES, 1mM MgSO₄, 2mM EGTA overnight at 4°C. Embryos were washed with PBS, blocked in PBS plus 5% BSA, 10% FCS and 0.3% TritonX, and sectioned. Primary and secondary antibodies were diluted in PBS plus 5% BSA and 0.3% TritonX and sections were incubated overnight at 4°C. All sections were mounted on glass slides with Vectasheild mounting media with DAPI (Vector Laboratories) and imaged on a SP5 confocal microscope (Leica, Wetzlar, Germany) with 40×/1.25–0.75 HCX PL APO oil objective and Application Suit software (Leica). For

whole mount imaging, embryos were fixed, deyolked, permeablized in PBS with 0.4% TritonX for 1 hour at room temperature and stained as described above. Following staining embryos were washed in PBS and mounted on a glass slide in 0.8% low melt agarose (GeneMate). All images were acquired on a SP5 confocal microscope (Leica, Wetzlar, Germany) with a 20×/0.70 HC PL APO oil objective or 40×/1.25–0.75 HCX PL APO oil objective and Application Suit software (Leica).

To label proliferating cells 72 hpf embryos were incubated in 16mM BrdU with 10% DMSO in egg water for 1 hr at 28°C. Embryos were washed and fixed in 4% PFA overnight at 4°C. Embryos were then washed with water, rinsed with 2M HCl for 1 hr, washed with PBS and stained as described above. Percentage of proliferating cells was calculated by comparing the number of BrdU positive cells in a gut section versus total cells.

2.6 Live Imaging

Zebrafish embryos at 48 hpf were anesthetized and embedded in 1.5% agarose. Selective Plane Illumination Microscopy (SPIM) was performed using three 10×/0.3 water dipping lenses (Leica), two for illumination and one for detection in an mSPIM configuration (Huisken and Stainier, 2007). A 488nm laser (Coherent) was used for excitation. A stack of 100 planes (3µm apart) was recorded with an EMCCD camera (Andor) every 10min for a total duration of 24h at 24°C.

2.7 Embryo dissociation and FACS

Embryos were collected in 1.5 ml tubes and rinsed with 1 mL calcium free Ringer's solution for 10 minutes at room temperature. The Ringers solution was removed and embryos were incubated in 0.25% trypsin (Gibco) and 300 µg/mL collagenase (Sigma) for 45 minutes at 28°C with pipetting every 15 minutes until a single cell suspension was attained. Cells were spun, washed twice with ice cold PBS plus 5% FCS and passed through a 70 µm filter (BD Falcon). Cell suspensions were stained with propidium iodide (Invitrogen) prior to sorting. Cells were sorted on a BD FACS Diva sorter at the Flow Cytometry Shared Resource center (Duke University). GFP+/PI- and GFP-/PI- cells were collected in 1.5 ml tubes containing RLT buffer (Qiagen) and β-mercaptoethanol (Sigma) and stored at -80°C.

2.8 RNA isolation qPCR

RNA was extracted using the RNeasy micro kit (Qiagen) according to the manufacture's protocol and RNA was further concentrated by ethanol precipitation and eluted in 10µl water. cDNA was synthesized using the First Strand cDNA Synthesis Kit (Roche) with an anchored-oligo(dT) primer. Quantitative PCR was performed using a BioRad CFX96 Real TimeSystem C1000 Thermocycler and BioRad iQ SYBR Green Supermix. All reactions were performed in duplicate with an annealing temperature of 60°, and data from three independent runs were obtained. Primers used include: elfa_F, CTTCTCAGGCTGACTGTGC; elfa_R, CCGCTAGGATTACCCTCC; myoVb_F, AGGACATGCTGGACCACTTC; myoVb_R, TCCAGCTCTTGCACTTTCTTC;

rab11fip1a_F, TCAAACACGTTGGGACCATA; rab11fip1a_R,
TTTGGGCCTTGTAAGGACAG; rab11a_F, GAAAGACCGTCAAGGCTCAG;
rab11a_R, ACCTGGATGGACACCACATT; rab11b_F,
GGACAGGAACGCTACAGAGC; rab11b_R, TGCCCTTTAACCCGTCAGTA.
Expression levels of target genes were normalized to *elfa* for each cDNA set. Clic5a_F,
TGACAAAGGCACTCAAGAAGCTGG; Clic5a_R,
TCTTCTTGTGCATACGCACTGTT; Clic5a1_F, CAGCTTCCTAAACTCCCCTCT;
Clic5a1_R, CTCGGCTGTAGGCGTTCTG; Clic5b_F,
AGAGCCGATTTACAGCACTCTGGA; Clic5b_R,
ATCTCCATTGGACAGAGACGCCA, B-actin_F,
TGGACTTTGAGCAGGAGATGGGAA; B-actin_R,
AAGGTGGTCTCATGGATACCGCAA. All Clic expression levels were normalized to
B-actin.

2.9 In situ hybridization

To make an *in situ* probe, *cldn15la* was amplified from cDNA and ligated into pGEMT-Easy (Promega) using the following primers: *cldn_probe_F*,
GGGGCTGGTTGGTTTAGTTT; *cldn_probe_R*, CCGCATCCATGAAAATTGA. The
plasmid was linearized and DIG RNA Labeling Kit (Roche) was used to make
digoxigenin-labeled RNA. In situ hybridization for *cldn15la*, *foxa3* (Field et al., 2003)
and α SMA (Georgijevic et al., 2007) was performed as described previously (Navis,
2013) and images were acquired on a Discovery V20 stereoscope (Zeiss) with an
Achromat S 1.0x lens.

2.10 Morpholino knockdown

The following morpholinos against Clic5 isoforms were injected into one-cell stage embryos. Embryos were incubated at 28°C, fixed at 72hpf and analyzed for lumen defects. clic5a: ATCAGGCTCTTGACCGTCTCCCATT, clic5a1(zgc101827):

TGCCCTCTTCATTTGAGGTCATATC, clic5b:

GACGTTTGCAGCCATGATGGACCTC

2.11 Pharmacological treatment

Embryos were dechorionated at 48 hpf and placed in a 12 well dish with 1µM bafilomycin (Sigma) or 1µM DMSO (Sigma) in egg water. Embryos were incubated at 28°C and fixed at 72 hpf.

2.12 Cell Culture

MDCK-C7 cells and Caco2 cells were cultured in DMEM with 10% fetal bovine serum and 1% penicillin-streptomycin (Invitrogen). Cells were transfected with pcDNA3–GFP-CLIC5 using Lipofectamine 2000 (Invitrogen). To prepare cysts, cells were plated at 2×10^3 on matrigel in an 8 well chamber slide and covered with media plus 2% matrigel. Media was changed every 2 days and cells were grown for 7-10 days until lumens formed. Cysts were fixed in 4%PFA, stained with phalloidin and lumen formation is analyzed by confocal microscopy.

2.13 Membrane Association assay

Cells were washed with PBS, lifted and transferred to an eppendorf tube. Ice cold TNE buffer (150 mM NaCl, 2.5mM EDTA, 10 mM Tris pH 7.4), 250mM sucrose,

and 1mM PMSF was added and cells were homogenized with a dounce on ice. 0.5ml of homogenate was laid on top of a 35% sucrose cushion in TNE buffer and spun at 35 K rpm for 1 hr at 4 degrees. Four 0.5 ml fractions were collected from the top of the cushion and protein content from each layer was determined.

To determine integral versus peripheral membrane association the membrane (top) fraction from above was diluted in TNE buffer and centrifuged for 30 min at 100Kg at 4°C to pellet the membranes. The pellet was resuspended in TNE buffer or TNE plus 100 mM NaCO₃ pH11 and incubated on ice for 10 min. Tubes were spun for 30 min at 100Kg. Samples were collected from the supernatant, the pellet was resuspended in TNE plus 1% TritonX 100, and a sample was obtained. The resuspended pellet was transferred to a new tube, spun again for 30 min and supernatant and pellet samples were taken. Samples were mixed with Laemmli buffer, immunoblotted for anti-GFP primary antibody followed by goat anti-chicken HRP conjugated secondary antibody and detected by chemiluminescence (Amersham-Pharmacia).

2.14 Statistical analysis

Gut diameter and perimeter was determined using Image J software. Quantification of cell number within the gut were obtained by counting DAPI stained nuclei in A-P position matched sections. Statistical significance for all measurements was determined using Student's *t*-test.

3. Characterization of intestinal lumen formation

In this chapter I provide a detailed analysis of lumen formation in the zebrafish gut. I discuss the generation of a novel intestine-specific reporter transgenic line and show that single lumen formation occurs through luminal enlargement and fusion in an anterior to posterior (AP) manner. In collaboration with Jan Huisken from MPI in Desden, I provide a high-resolution *in vivo* imaging of the process of lumen formation in the zebrafish intestine and identify contact remodeling as a critical step in lumenogenesis that is distinct from fluid driven lumen enlargement.

3.1 Introduction

Tubulogenesis is a crucial process during the formation of many organs including the pancreas, lungs, vasculature, mammary gland and gut. Tube formation mechanisms are diverse across organ systems, but they all result in a structure with a single lumen. Tubes arising from a polarized epithelium typically undergo a process of epithelial wrapping or budding that is driven primarily by changes in cell shape. On the other hand, tubes originating from unpolarized cells form through a process of cord hollowing or cavitation that requires the establishment of cell polarity and *de novo* lumen formation (Lubarsky and Krasnow, 2003; Martin-Belmonte and Mostov, 2008).

The zebrafish has been used to study tubulogenesis in a variety of organs and is a powerful vertebrate model of *de novo* lumen formation. Live imaging of the zebrafish vasculature has revealed two mechanisms of tubulogenesis involving cellular rearrangements and cell invagination (Herwig et al., 2011). The isolation of a zebrafish

par6γ mutation identified a role for spindle orientation in the forming neural tube (Munson et al., 2008). In addition, examination of the zebrafish intestine and Kupffer's vesicle has demonstrated the role of fluid secretion in lumen expansion (Bagnat et al., 2010; Navis et al., 2013). Furthermore, optical accessibility and a vast array of transgenics make zebrafish an ideal vertebrate system in which live imaging and functional studies can provide insight into the molecular and developmental mechanisms involved in tube morphogenesis.

The zebrafish intestine begins as a solid rod of endodermal cells that differentiate into epithelial cells and undergo a cord hollowing process to form a tube. Lumen formation initiates with the development of multiple actin-rich foci between cells and is followed by the localization of junctional proteins at multiple points within the intestine (Horne-Badovinac et al., 2001). Small lumens then form at these points and expand, coalesce and eventually form a single continuous lumen. Interestingly, intestinal villus formation in the rat epithelium has also been suggested to form through the fusion of small secondary lumens (Madara et al., 1981). Previous work in zebrafish showed that paracellular ion transport regulated by Claudin15 and the Na⁺/K⁺-ATPase drives fluid accumulation, thus promoting lumen expansion and coalescence in to a single lumen (Bagnat et al., 2007). However, since the gut lumen forms without apoptosis (Ng et al., 2005), other cellular processes such as epithelial remodeling must occur to facilitate lumen coalescence.

3.2 Results

Time course analysis of lumen formation

Lumen formation in the zebrafish gut begins with the appearance of multiple small lumens that enlarge through fluid accumulation and then coalesce to form a single lumen (Bagnat et al., 2007). However, fluid accumulation alone cannot drive the cellular rearrangements necessary for lumen coalescence. The complexity of the tissue suggests that other processes are required. To elucidate the process of lumen formation in the zebrafish intestine we performed a time course analysis from 48 hpf to 72 hpf and characterized the appearance of the lumen at four hour intervals. Analysis of fixed, thick transverse sections by confocal microscopy revealed a range of lumen morphologies during this 24-hour period. We classified the intestinal tubes into three categories: Class I, containing multiple small lumens, in which 2-4 actin foci or small lumens spanned the intestine (Figure 6A); Class II, represented by enlarged, un-fused lumens, in which a bridge of cells separate open lumens (Figure 6B); Class III, single lumens, characterized by one enlarged continuous lumen (Figure 6C). In 48 hpf embryos all three lumen types are apparent with relatively similar frequency. Both class I and class III lumens were found in 38% of embryos whereas class II lumens were found in 24% of gut sections. Over the next 12 hours the appearance of class I lumens decreased, while the frequency of class II lumens increased to 30% and class III lumens increased to 70% at 60 hpf. During the subsequent 12 hrs, the number of embryos with class II lumens decreased and by 68 hpf only single lumen guts (class III) were observed (Figure 6D). Thus, single

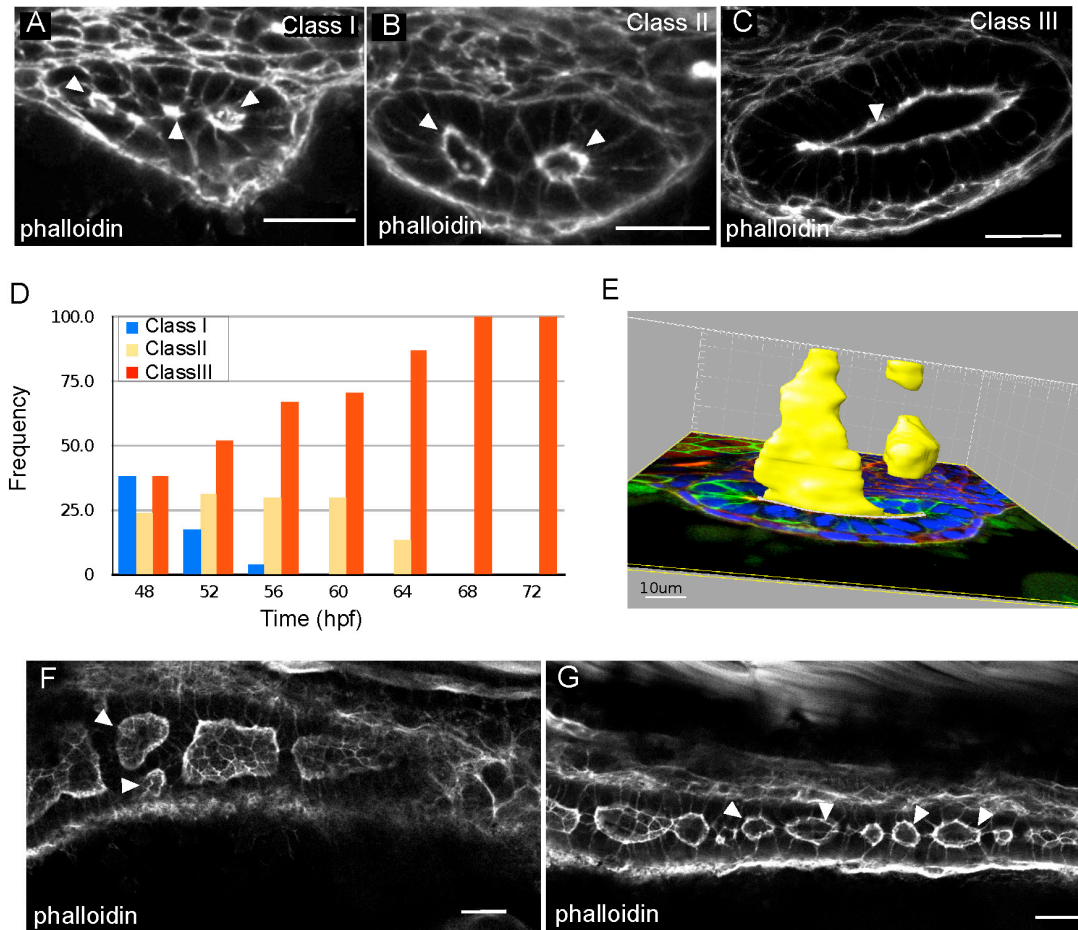


Figure 6- Lumens enlarge and fuse during single lumen formation

A-C Confocal images of cross sections of WT embryos exhibiting class I (A), class II (B), and class III (C) lumens, stained with phalloidin. Arrowheads indicate lumens. Scale bars= 20 μ m. **D-** Quantification of lumen phenotypes between 48 hpf and 72 hpf. 48 hpf n=21, 52 hpf n=29, 56 hpf n=27, 60 hpf n=27, 64 hpf n=30, 68 hpf n=21, 72 hpf n=26. **E-** Space fill projection from a 200 μ m confocal stack of an intestine section at the resolution stage. Yellow- Lumen, Green- GFP-CaaX, Blue- DAPI. Scale bar = 10 μ m **F-** Confocal whole-mount image of the anterior gut at 58 hpf stained with phalloidin (red). Arrowheads indicate adjacent un-fused lumens. **G-** Confocal whole-mount image of the posterior gut at 58 hpf stained with phalloidin (red). Arrowheads indicate the lumens. Scale bars = 20 μ m

lumen formation is preceded by two stereotypic luminal arrangements that include both multiple small lumens and enlarged, un-fused double lumens.

The most frequently observed luminal arrangement prior to single lumen formation is two enlarged lumens. When two lumens are observed in cross section they are typically located at the foci of the ellipsoid-shaped intestinal tube. However, this arrangement is not simply the result of two parallel lumens spanning the intestine. Using Imaris imaging software we generated a 3D rendering of lumen size and shape from a 200-micron transverse confocal stack. Even within this small region, lumens are discontinuous and highly dynamic in shape and size (Figure 6E). To gain a better understanding of how these discontinuous lumens are arranged along the AP axis we performed whole-mount confocal imaging. Analysis of the anterior intestinal bulb at 58 hpf revealed two enlarged lumens side by side (Figure 6F), which is representative of the un-fused lumens (class II) we observed in transverse cross section. These adjacently arranged lumens are most frequently observed in the anterior gut, likely due to the larger diameter and number of cells in this region of the intestine. Enlarged discontinuous lumens were found along the AP length of the intestine. Toward the posterior end of the intestine discontinuous lumens were more abundant and of smaller size (Figure 6G). The un-fused lumen phenotype (class II) occurs most frequently between 52 and 60 hpf and represents a previously uncharacterized stage in normal lumen formation. We have termed this phase of single lumen formation the ‘lumen resolution stage’. Together, these data suggest that lumen formation occurs through stages of multiple small, and expanded un-fused lumens before resolving into a single continuous lumen.

Generation of Cldn15la-GFP

Analysis of fixed tissue sections suggested that initial lumen expansion and coalescence, and lumen resolution are distinct phases of intestinal lumen formation. Since sectional analysis only offers a static snapshot of lumen formation, we wanted to monitor the process of lumen formation in the intestine using live imaging. To image lumen coalescence *in vivo*, we required a new transgenic line that is intestine-specific and expresses prior to single lumen formation. To identify intestine-specific genes we isolated intestinal epithelial cells using a *Tg(-1.0ifabp:GFP-CaaX)* line which expresses membrane-GFP in the intestinal cells starting around 120 hpf. Using RNA isolated from these cells we performed a microarray analysis to identify highly expressed genes in the gut. We found that one of the most highly intestine-enriched genes was *claudin15-like a (cldn15la)*, a member of the Claudin family of tetraspanning membrane proteins (Furuse et al., 1998). At day 5, *cldn15a* was upregulated in the gut 120 fold. By in situ hybridization, *cldn15la* was highly expressed and restricted to the intestine by 50 hpf. (Figure 7A-B). To generate a transgenic line expressing Cldn15la-GFP we obtained a BAC containing *cldn15la* with 80kb and 40kb of its upstream and downstream genomic DNA, respectively. A C-terminal fusion protein was created by replacing the stop codon of *cldn15la* with GFP, and a transgenic line, *TgBAC(cldn15la-GFP)pd1034*, was established (Figure 7C).

Cldn15la-GFP expression was first observed at 48 hpf in the intestinal epithelium and remained expressed throughout the course of lumen formation (Figure 8D-E). An analysis of transverse sections revealed that Cldn15la-GFP is restricted to the intestine

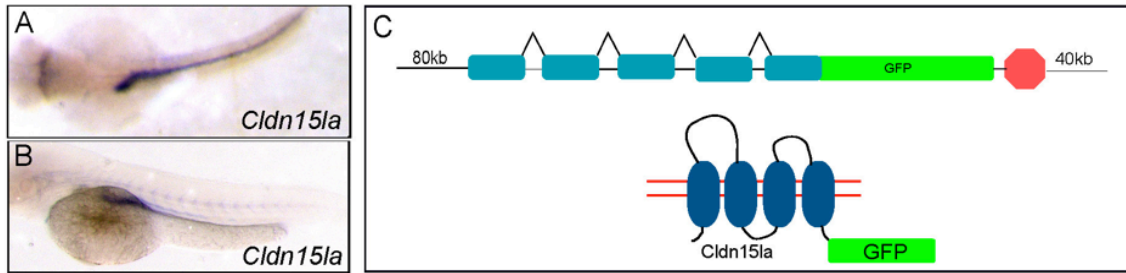


Figure 7- Generation of an intestine specific transgenic line

A-B Dorsal, top panel, and lateral view, bottom panel, *in situ* hybridization showing *claudin 15-like a* expressed specifically in the intestine at 56 hpf. **C-** Schematic representation of *TgBAC(cldn15la-GFP)* generation. The recombination target is shown on top, and the expected protein structure is shown on the bottom.

and is not expressed in other endoderm-derived organs (Figure 8A). Cldn15la-GFP was unexpectedly found localized to the lateral surface of the intestinal epithelium. The spacer sequence between Cldn15 and GFP (DLPAEQKLISEEDLDPPVAT) contained potential basolateral targeting motif, therefore we generated an additional transgenic line with a different linker sequence between GFP and Cldn15la (DLPAEQKAGSEEDLDPPVAT), yet observed a similar basolateral localization pattern (Figure 8B). Although Claudin proteins are components of tight junctions and typically localize to the subapical region (Furuse et al., 1998), recent studies have shown that several members of this protein family also localize to lateral membranes during morphogenesis (Gregory et al., 2001; Inai et al., 2007; Westmoreland et al., 2012) including the closely related zebrafish claudin Cldn15lb (Cheung et al., 2012). To determine whether Cldn15la-GFP lateral membrane localization represented the endogenous protein localization we generated an antibody against the C terminus of Cldn15la. Similar to the BAC transgenic construct, the Cldn15la antibody localized to the lateral membrane in intestinal epithelial cells, indicating that the Cldn15la-GFP fusion recapitulates endogenous expression and localization (Figure 8C). Despite the unexpected localization pattern, the Cldn15la-GFP transgene allowed for improved examination of the cellular and luminal arrangements within the intestine. Whole-mount imaging of the entire intestine revealed that lumen fusion begins in the anterior region and proceeds in an anterior to posterior direction (Figure 8F). In addition, we observed that un-fused lumens were frequently separated by single cell-cell contacts expressing Cldn15la-GFP (Figure 8G).

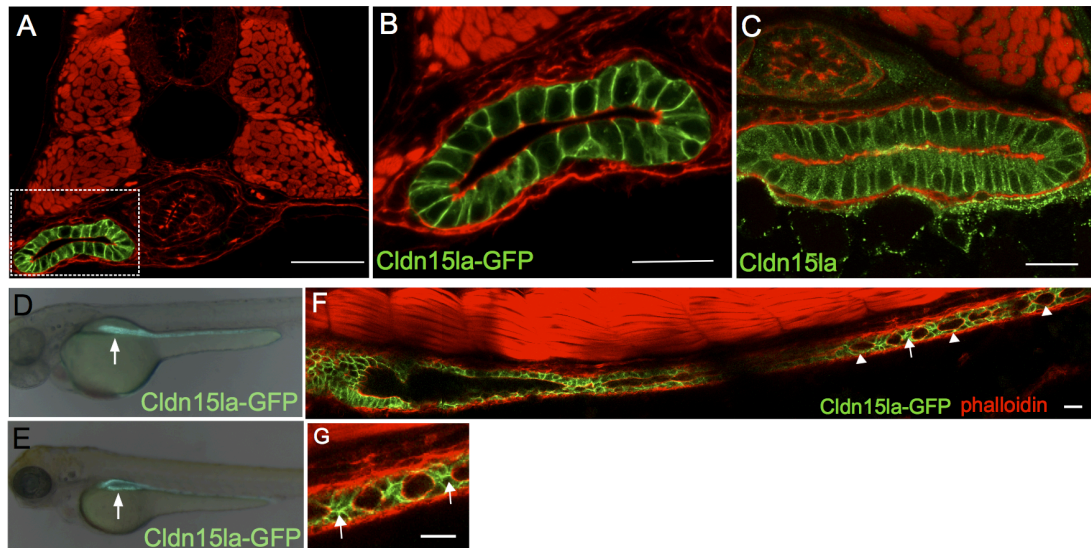


Figure 8- Claudin 15-like a localizes to the basolateral membrane

A- Confocal cross section of a 72 hpf *TgBAC(cldn15la-GFP)* embryo. Scale bar = 50 μ m. **B-** Magnification of box from A. **C-** Immunolocalization of Claudin15la to the basolateral membranes of intestinal epithelial cells. **D-E** Whole-mount fluorescent images of 55 hpf and 75 hpf embryos expressing *TgBAC(cldn15la-GFP)*. Arrows indicate the gut tube. **F-** Stitched confocal whole-mount images of a *TgBAC(cldn15la-GFP)* embryo show un-fused lumens (arrowhead) in the posterior intestine at 68 hpf that are separated by cell-cell contacts (arrow). **G-** Magnification of cell-cell contacts from Fig. F. Arrows indicate contacts. Phalloidin (red). Scale bar = 20 μ m

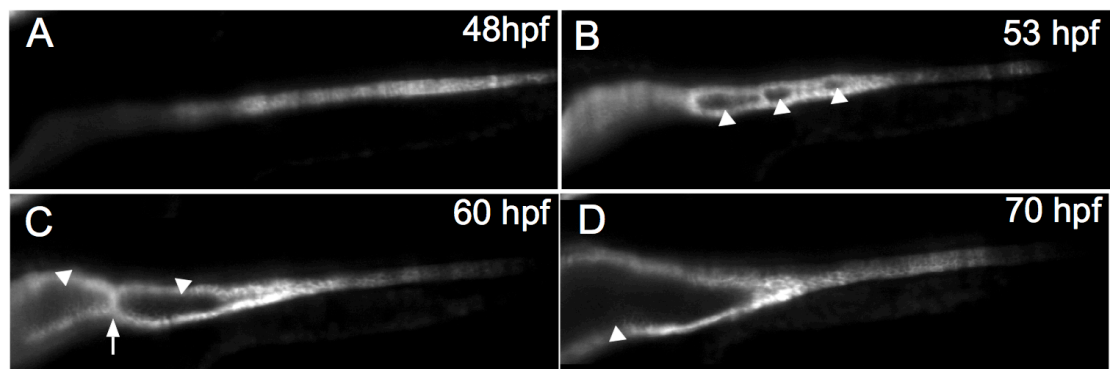


Figure 9- Live imaging of *TgBAC(cldn15la-GFP)*

A-D- Live imaging was performed from 48-70 hpf. Snapshots of a single plane at 48, 53, 60, and 70 hpf show lumens enlarging and fusing into a single lumen. Arrowheads indicate lumens, arrows point to cell-cell contacts between lumens.

Live imaging the zebrafish gut

To visualize the process of lumen formation live, we used Selective Plane Illumination Microscopy (SPIM) (Huisken and Stainier, 2007) to image *TgBAC(cldn15la-GFP)* embryos. Initially, several small lumens were seen opening along the AP length of the intestine (Figure 9B). These lumens were often separated by a few cells, which is similar to those observed in fixed whole mount embryos at the resolution stage. Initially, the expansion of these lumens was rapid and directly followed by local fusion events that resulted in two to three large luminal compartments along the AP axis of the tube. The larger lumens remained separated by a one or two cell-thick cellular bridge, and did not fuse for an extended period of time, yielding a distinct intermediate (Figure 9C). Ultimately, these large lumens resolve into one (Figure 9D). Taken together, our morphological and live imaging studies reveal that single lumen formation in the zebrafish intestine involves two distinct morphological and kinetic phases and identify a previously unknown stage characterized by the presence of large, un-fused lumens.

Epithelial morphology and polarity

Previous work has shown that fluid accumulation promotes lumen enlargement and coalescence during single lumen formation (Bagnat et al., 2007; Navis et al., 2013). However, because lumen coalescence occurs in the absence of apoptosis (Ng et al., 2005), additional processes must also be involved to facilitate tissue remodeling during lumen resolution. To address the process of lumen fusion, I further characterized the resolution stage. Analysis of the cellular architecture of transverse intestinal sections at

the resolution stage using a membrane GFP marker, *Tg(hsp70l:GFP-CaaX)pd1008*, revealed that lateral lumens were often separated by a bridge of cells whose contacts form a Y- or T-shaped arrangement between two adjacent lumens (Figure 10A,A'). To determine the identity of the bridge contacts, I examined the localization of specific apical and basolateral proteins. Using a *Tg(hsp70l:GFP-podxl)pd1080* line, we found that the apical membrane protein podocalyxin localized to the apical surface surrounding the lumens and was absent from the connecting bridge (Figure 10B-B'). Similarly, the tight junction protein ZO-1 was restricted to the subluminal area and was not found at the membrane between lumens (Figure 10C-C'). In contrast, the adhesion proteins cadherin and β -catenin were localized to all basolateral membranes and were also located on the bridge membrane separating the two lumens (Figure 10D-E'). These data reveal that during the resolution stage, intestinal epithelial cells surrounding the lumens are polarized and adjacently arranged lumens within an intestinal cross section are separated by basolateral contacts that exclude apical proteins.

Next we examined the process of lumen resolution along the length of the intestine. The generation of a single continuous lumen is a more complex process involving the coordination of several lumens along the entire gut. There are two possible scenarios in which a single continuous lumen can resolve from multiple discontinuous lumens (Figure 11A). One possibility is that apical membrane can be deposited at bridge contacts between lumens, forming a continuous path and acting as a linker connecting the enlarging lumens. Alternatively, each lumen may be an autonomous unit separated by basolateral contacts, similar to adjacently arranged lumens. In this case, single lumen

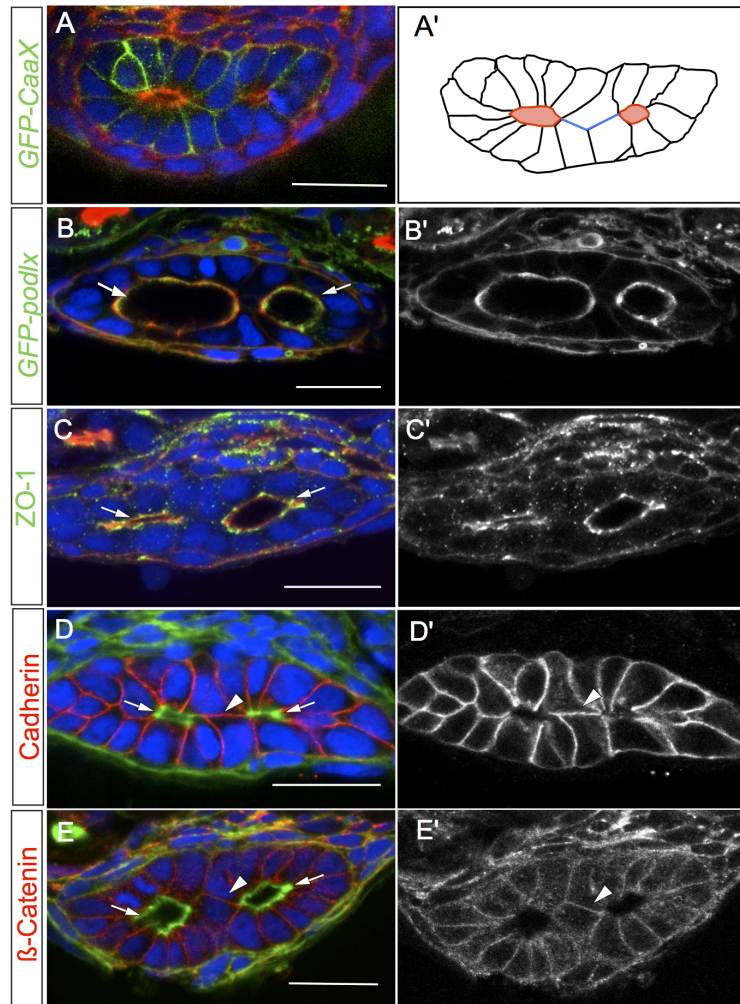


Figure 10- Basolateral contacts are found between lumens

A-E Confocal cross sections of embryos at the lumen resolution stage. **A-** *Tg(hsp70l:GFP-CaaX)* labels all cell membranes. **A'**- Cartoon diagram of Fig 3A depicting laterally arranged lumens in red and ‘bridge’ contacts in green. **B-B'** Apical protein, GFP-Podocalyxin surrounds the lumen but is not found at bridge contacts. Phalloidin (red). **C,C'** Antibody staining against Zo-1 labels tight junctions. Phalloidin (red). **D-E'** Antibody staining against cadherin and β -catenin labels basolateral contacts and ‘bridge’ contacts between lumens. Phalloidin (green). Arrows indicate lumens, arrowheads indicate bridge contacts. Scale bars: 20 μ M.

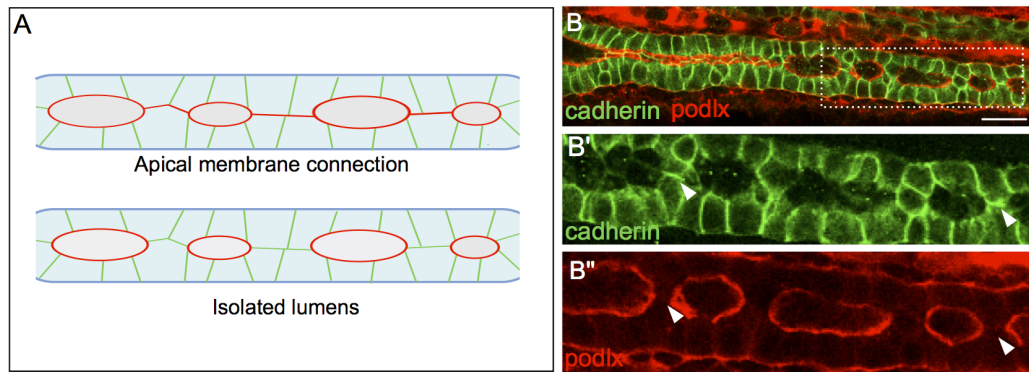


Figure 11- Basolateral adhesions separate adhesions on A-P axis

A- Cartoon depicting two scenarios of lumen fusion along the AP axis. Apical membrane (red) can be deposited on membranes between lumens (top) or lumens may arise isolated and fuse directly without an apical membrane linker (bottom). **B-B''** Whole-mount confocal image of a lumen resolution stage embryo expressing GFP-Podocalyxin (red) and stained for cadherin in green. Cadherin localizes to basolateral contacts separating lumens. Arrows indicate lumens, arrowheads indicate bridge contact. Scale bars: 20 μ M.

formation would require the disengagement of the cell-cell contacts between the adjacent lumens. To determine which scenario most accurately represents the process of lumen resolution along the intestine I performed whole-mount analysis of *Tg(hsp70l:GFP-podxl)pd1080* embryos stained for cadherin. Consistent with the transverse section data, lumens along the AP axis were frequently separated by Y- and T-shaped cadherin-positive contacts and GFP-Podxl was restricted to the membrane surrounding the lumens (Figure 11 B-B''). Thus, the organization of adjacent lumens seen in transverse sections is analogous to the organization of adjacent lumens along the AP axis. Furthermore, we found no evidence of apical membrane deposition between two lumens prior to lumen fusion.

Lumen fusion

Lumen resolution may occur via the expansion and direct fusion of luminal membranes, or through the reduction and breaking of contacts between the lumens or both. Prior to lumen fusion adjacent lumens expand and the connecting bridge appears to shrink. We observed that in regions where the basolateral bridge contact was particularly narrow, GFP-podxl-positive membranes protruded from the adjacent luminal surfaces toward a central area with diffuse cadherin signal, likely originating from the internalization of the contact (Figure 12A-A''). We termed this type of resolution event luminal fusion. Further analysis of cadherin-stained and *TgBAC(GFP-cldn15la)* embryos revealed that in some instances during the fusion process, cadherin and GFP-Cldn15la can still be found at the fusion site (Figure 13A-D). Co-localization with *Tg(hsp70l:Ras-RFP)* confirmed that cadherin remains at the membrane. Although the basolateral

proteins are not completely removed from the membrane, cell-cell adhesion is lost. This localization at the cell surface likely originates from the separated bridge contact, suggesting that the adhesions between the cells had snapped prior to their complete internalization (Figure 13B-D). We termed this type of resolution event adhesion snapping. Analysis of lumen resolution events in whole mount embryos revealed that luminal fusion seems to be the predominant mode of lumen resolution (65%), whereas adhesion snapping accounts for 35% of the resolution events (n=20). Together, these data indicate that lumen resolution involves remodeling of bridge contacts through both apical membrane expansion and the reduction of the adhesion contact.

3.3 Discussion

In this study we identify lumen resolution as a critical process during single lumen formation. Single lumen formation begins with multiple small lumens that enlarge through fluid accumulation driven by *Cldn15* and $\text{Na}^+/\text{K}^+\text{ATPase}$ (Fig. 7A). Prior to lumen coalescence, enlarged lumens are found along the length of the gut and are separated by basolateral bridge contacts. Our studies reveal that cell-cell bridge contacts lack apical and tight junction markers between the lumens, indicating that these bridge contacts do not change identity prior to lumen fusion. Instead, we observed that lumen fusion occurs through both apical membrane expansion and the shrinking and breaking of basolateral bridge contacts. The most common bridge cell arrangement involves cells that have one apical surface, however occasionally bridge cells exhibit two apical surfaces. Bipolar cells have also been observed during tubulogenesis in the *Ciona* notochord (Denker and Jiang, 2012). Although the mechanism by which a cell acquires two apical

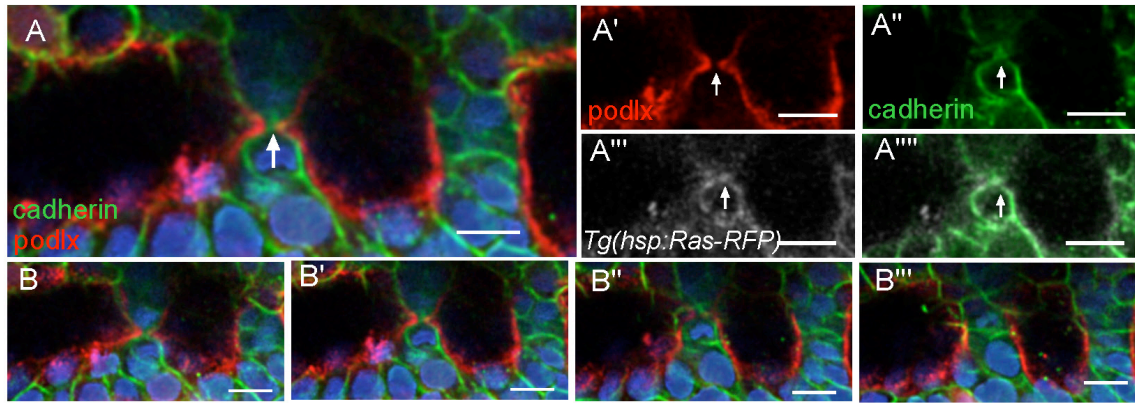


Figure 12- Lumen resolution through luminal fusion

A-A''' Whole mount confocal image of an embryo expressing GFP-Podocalyxin (false colored in red) and stained for cadherin (green) shows luminal expansion during a “lumen fusion” event. Ras-RFP (white) marks cell membranes. Arrows mark fusion event. Blue, DAPI. **B-B'''** Optical sections from a Z-stack surrounding a fusion event.

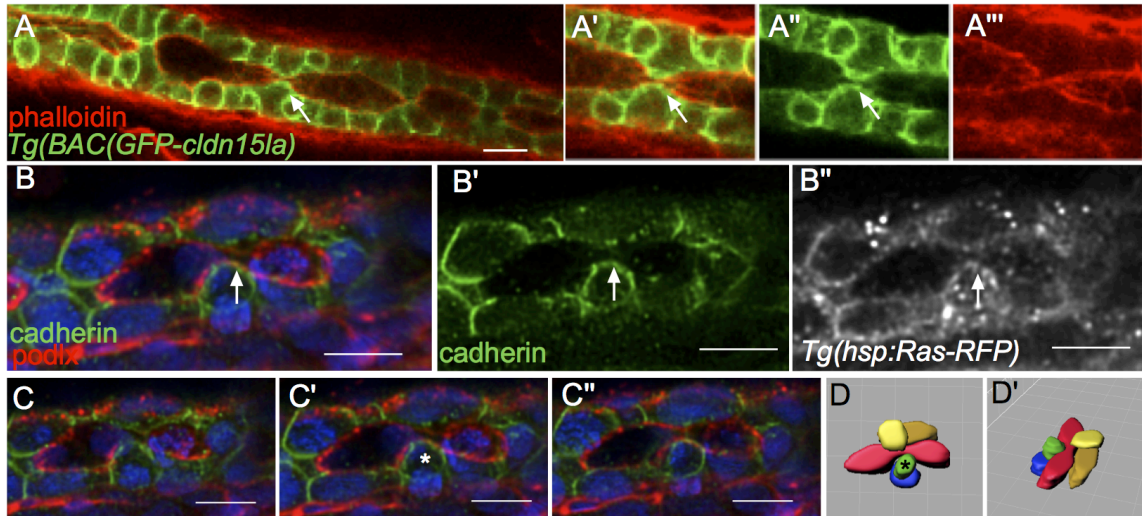


Figure 13- Lumen resolution through snapping

A-A'' Whole-mount confocal image of a *TgBAC(GFP-cldn15la)* embryo shows a putative adhesion snapping event during fusion. The arrow marks adhesion at the surface. **B-B''** Whole-mount confocal image of an embryo expressing GFP-Podocalyxin (red) and stained for cadherin (green) shows adhesion snapping during fusion. Ras-RFP (white) marks cell membranes. The arrow marks adhesion at the surface. **C-C''** Optical sections from Z-stack surrounding a fusion event. The asterisk marks a cell with adhesion. **D-D'** Space fill projection labeling cells surrounding the fusion event. Lumen, red. The asterisk marks a cell with adhesion. Scale bars: 10 μ M

membranes is unknown, it is possible that the cells between the lumens are unable to receive proper polarizing cues from the basement membrane.

During the resolution stage lumens may merge through either direct apical-apical membrane fusion or through fusion at cell junctions. Studies in the zebrafish vasculature and ascidian notochord provide insight into the possible mechanisms involved in membrane and junctional coalescence during lumen fusion. During ascidian notochord tubulogenesis, cellular remodeling involves a reduction of intracellular junctions between neighboring cells and the establishment of a new junction between two previously unconnected cells (Dong et al., 2009). Furthermore, work in the zebrafish dorsal longitudinal anastomotic vessel suggests that when two apical membrane compartments merge, a new junction is formed between two cells allowing for the detachment of a third cell at the new contact site (Herwig et al., 2011). However, a more detailed study will be needed to determine whether lumens merge through apical fusion in the zebrafish gut.

In the zebrafish intestine, lumens open at multiple sites within the gut tube rather than at a single initiation point as seen in other models of tube formation such as 3D cysts and the *C. elegans* excretory cell (Bryant et al., 2010; Khan et al., 2013; Kolotuev et al., 2013). Through live imaging and a detailed characterization of luminal architecture, we observed that lumens form along the entire length of the gut tube and are typically separated from each other by only one or two cells. This architecture allows lumens to fuse through localized cellular rearrangements, thus facilitating the generation of a continuous lumen within a long tube. Elucidating the mechanisms regulating continuous lumen formation is critical to understanding morphogenesis of various organs in

vertebrates. For example, in the mouse mammary gland, several small lumens form within the developing bud that must connect with each other to form a continuous luminal network (Hogg, 1983). Overall, the work in this chapter demonstrates that the zebrafish intestine serves as a powerful model to investigate the cellular processes involved in single continuous lumen formation in vertebrate tubes.

4. Molecular mechanisms regulating single lumen formation

In the prior chapter I identified a previously undescribed stage in single lumen formation characterized by enlarged un-fused lumens. I found that the fusion of these lumens requires the rearrangement of cellular contacts in between two lumens. In this chapter I investigate the molecular mechanisms that may be involved in contact rearrangement through the identification of a mutant exhibiting impaired lumen fusion and through the examination of the intracellular recycling pathway.

4.1 Introduction

De novo lumen formation is integral to the development of tubes that form from an unpolarized epithelium and the mechanism by which this occurs has been extensively studied *in vitro* in 3D cysts. In the cyst model, apical-basal cell polarity is established through the differential distribution of PIP2 and PIP3, as well as several polarity complexes both of which are required for the asymmetric targeting of membrane proteins (Joberty et al., 2000; Martin-Belmonte et al., 2007; Nelson, 2003). To initiate lumen formation, apical membrane proteins such as podocalyxin accumulate in Rab11 and Rab8a-positive vesicles. These vesicles are then delivered to the plasma membrane where, together with the exocyst and the Par3 complex, they fuse to generate an apical surface (Bryant et al., 2010). Once an early apical domain is established, the Par3-aPKC complex re-localizes tight junctions and oriented cell divisions reinforce the polarized architecture of the cyst (Jaffe et al., 2008; Martin-Belmonte and Mostov, 2008). Although these studies highlight the importance of apical membrane trafficking in lumen

formation, such *in vitro* systems cannot fully recapitulate the complexity of a three-dimensional organ. For example, in most 3D cyst models the lumen typically forms between two differentiated epithelial cells and does not involve processes of epithelial transformation and remodeling that are essential for tube formation *in vivo* in many organs.

Epithelial remodeling has been well studied in *Drosophila* models of tube morphogenesis. In the *Drosophila* salivary gland, lumen size and shape are controlled by regulating the localization of E-cadherin at adherens junctions and basolateral surfaces (Pirraglia et al., 2010). Apical elongation is promoted by reduced E-cadherin levels at adherens junctions and increased levels at the basolateral surface (Pirraglia et al., 2010). In the *Drosophila* trachea, trafficking of E-cadherin through Rab11-mediated recycling is known to regulate cell intercalation (Shaye et al., 2008). Together, these studies have highlighted the importance of endocytic trafficking and recycling of cadherin during epithelial remodeling. However, the cellular mechanisms controlling tubulogenesis in large un-branched tubes, particularly in vertebrates, remain poorly understood.

4.2 Results

smoothened mutants exhibit impaired lumen formation

We next sought to identify a genetic model to investigate the resolution stage of lumen formation in the intestine. The hedgehog pathway is a well-known regulator of gastrointestinal development in vertebrates. In mammals, the hedgehog (Hh) pathway is involved in intestinal patterning, regionalization, and villus formation, while in the zebrafish, Hh signaling regulates cloaca formation (Parkin et al., 2009; Ramalho-Santos

et al., 2000; Wallace and Pack, 2003). Therefore, we examined lumen formation in embryos mutant for *smoothened* (*smo*), the hedgehog co-receptor. We performed transverse sectional analyses of homozygous *smo*^{s294} (Aanstad et al., 2009) mutant embryos at 72 hpf, a time point when a single continuous lumen is well established in WT embryos. The *smo*^{s294} allele contains a mutation in a conserved cysteine residue in the extracellular domain of the protein and is essential for full activation of the Hh pathway (Aanstad et al., 2009). At 72 hpf, approximately 43% of *smo*^{s294} mutant embryos (n= 21 mutants) exhibit impaired lumen fusion in the intestine (Figure 14A,E). To confirm that the smoothened mutation is responsible for the lumen formation defect, we examined a null allele of smoothened, *smo*^{hi1640} (Chen et al., 2001) and found the same phenotype in a similar proportion of embryos (44% n=27) (data not shown). The *smo*^{s294} phenotype was similar to the class II WT intermediate, which indicates a failure at the resolution stage. To determine if un-fused lumens resolve at a later time in development, we also examined embryos beyond 72hpf. The un-fused lumen phenotype was observed at 85 hpf, 96 hpf, and 110 hpf (Figure 14B-D, F-H). At 96 hpf 27% of *smo*^{s294} embryos (n= 26 mutants) continued to exhibit un-fused lumens, indicating that impaired lumen fusion in mutants is not due to a developmental delay. In addition to transverse sectional analysis, we also examined *smo*^{s294} in whole-mount to determine if impaired lumen fusion was displayed along the entire intestine or was restricted to the anterior intestinal bulb. At 72 hpf, *smo*^{s294} mutants exhibited several un-fused lumens along the intestine (Figure 14I-J), which is consistent with the results observed in WT embryos at the resolution stage. It is important to note that in the intestine of *smo*^{s294} mutants, the un-fused lumens are fully

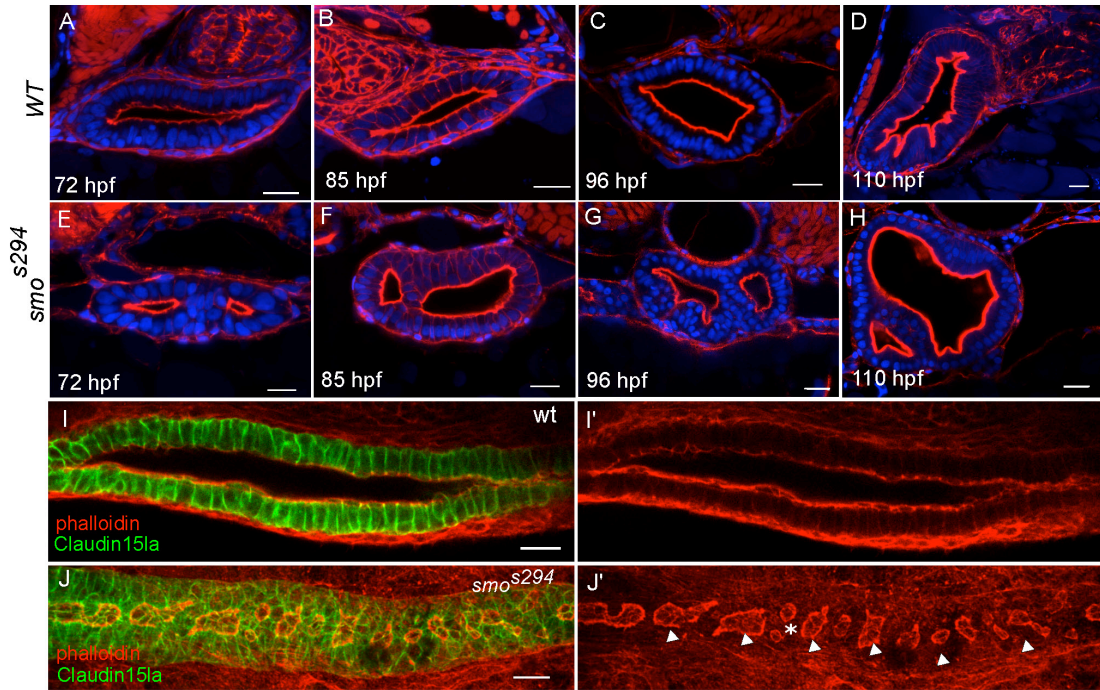


Figure 14- smoothed mutants exhibit a defect in lumen fusion

A-H Confocal cross sections of WT (top) and *smo*^{s294} (bottom) intestines at 72 hpf, 85 hpf, 96 hpf, and 110 hpf. Phalloidin (red). **I-J** Confocal whole-mount image of WT and *smo*^{s294} embryos expressing *TgBAC(cldn15la-GFP)* to highlight the cellular and luminal architecture of the intestine at 72 hpf. **I**- WT intestine, **J**- *smo*^{s294} intestine. Arrowheads: lumens, Asterisk: adjacent lumens. Scale bars: 20μM

open and continue to expand as cells divide (Figure 14E-H). These results indicate that the *smo*^{s294} phenotype results from a failure in lumen resolution and not from impaired fluid accumulation. Taken together, these data support the idea that fluid alone cannot drive single lumen formation in the intestine and reveal that lumen opening and lumen fusion are two distinct events required for single lumen formation that can be genetically uncoupled.

Characterization of *smo* guts

Hedgehog signaling occurs in a paracrine manner typically involving Hh expressing cells in the epithelium and signal receiving cells in the mesenchyme. To examine the spatiotemporal expression of *smo* in the gut we used a transgenic reporter line for the Hh pathway target gene, *patched* (Choi et al., 2013). At 48 and 72 hpf signaling was observed in the mesenchyme surrounding the gut epithelium which is consistent with established finding (Figure 15A-C). Hh signaling is known to play an important role in the differentiation of mesodermal precursors into smooth muscle. In *smo*^{s294} we observed that the mesenchymal layer contained fewer, more elongated cells compared to WT (Figure 14E-H). Therefore, we next examined the differentiation of the mesenchymal layer in *smo*^{s294} mutants. *in situ* hybridization revealed that expression of the smooth muscle marker α SMA is lacking in mutant embryos at 72 hpf compared to WT, indicating an absence of differentiated smooth muscle surrounding the gut (Figure 15D-E).

To determine if impaired lumen fusion in *smo*^{s294} mutants stems from an early endoderm migration defect, we examined expression of the endoderm marker, *foxa3*. At

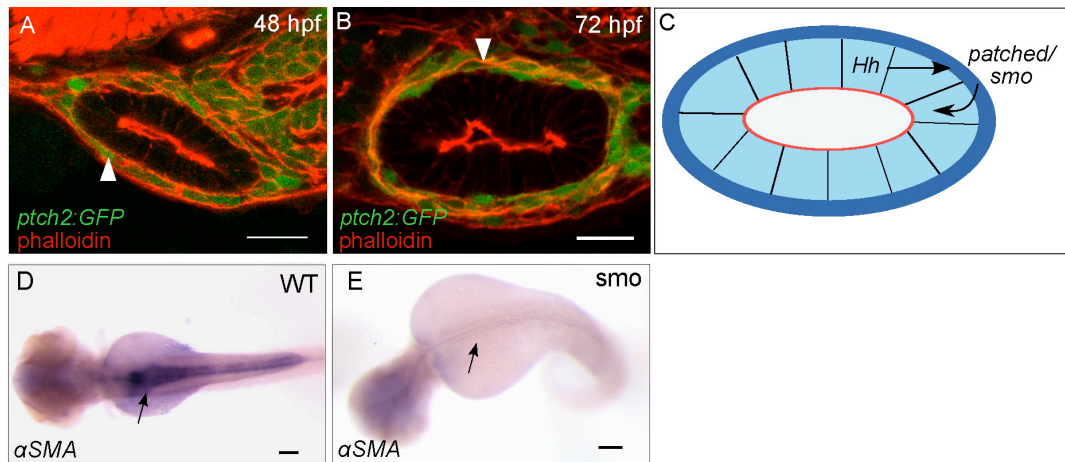


Figure 15- *smoothened* signaling acts in the surrounding mesenchyme

A-B Confocal cross section of the transcriptional reporter *Tg(GBS-ptch2:EGFP)umz23*. Phalloidin (red), DAPI (blue). Scale bar: 20 μ M. **C** *Hh* is expressed in the epithelium and binds to *ptch* in the mesenchyme to activate *smo* mediated downstream transcription. Thus, *smo* regulates the epithelium through epithelial-mesenchymal signaling pathways. **D-E** Dorsal view of an *in situ* hybridization showing α SMA expression in WT and *smo* mutant embryos at 72 hpf. Arrows point to smooth muscle. Scale bar: 100 μ M.

30 hpf *smo*^{s294} mutants show a single, midline localized endodermal rod that is overall similar in shape to that of WT embryos (Figure 16A-B). Examination of *TgBAC(cldn15la-GFP)* embryos at 48 hpf revealed that the intestinal epithelium is also similar in size and shape in WT and *smo*^{s294} mutants (Figure 16C-D, G). Furthermore, we determined that there is no significant difference in cell number, or cell proliferation between WT and *smo*^{s294} mutants (Figure 16E-F', H-I). There was also no observable apoptosis in the gut of WT or *smo*^{s294} embryos (data not shown). Therefore, the lumen fusion phenotype observed in *smo*^{s294} mutants does not result from defects in early endoderm migration, or impaired regulation of epithelial cell numbers.

Next we investigated whether the lumen defect in *smo*^{s294} mutants is linked to a failure in the establishment of apical-basal polarity. To determine if *smo*^{s294} mutants exhibit disrupted epithelial polarity we examined the localization of several apical and basolateral markers at 72 hpf. Staining for the tight junction protein ZO-1 showed proper localization to the junctions and no localization between lumens, similar to what we observe in WT intermediate embryos (Figure 17A-B). In addition, examination of *Tg(hsp70l:GFP-podx); smo*^{s294} embryos revealed proper localization of podocalyxin to the luminal surface (Figure 17C-D). However, the basolateral protein cadherin was localized to all basolateral surfaces, and was also found in a non-polarized distribution on the bridge cells between the lumens. These bridge cells express cadherin on all membranes, similar to the localization pattern in WT intermediate embryo (Figure 17E-F). Therefore, *smo*^{s294} mutants do not display extreme defects in cell polarity during lumen formation. The localization of polarity markers resembles what is seen in

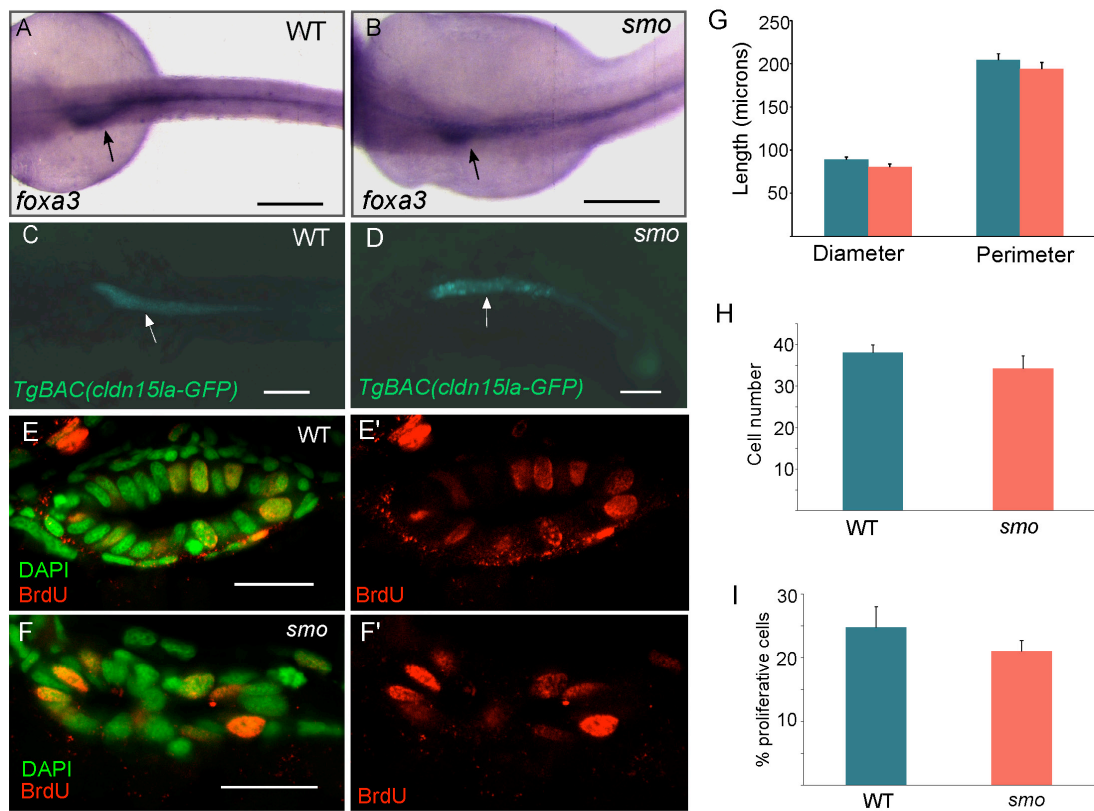


Figure 16- Gut tube shape and cell number are similar in WT and *smo* mutants

A-B In situ hybridization of WT and *smo* mutant embryos expressing *foxa3* at 30 hpf.

Scale bar: 200 μ M. **C-D** WT and *smo* mutant embryo expressing *TgBAC(cldn15la-GFP)*

at 48 hpf. Arrows indicate intestine. **E-F'** Cross section of WT and *smo* mutant guts at 72

hpf stained for BrdU to label proliferating cells. Scale bars: 20 μ M. (G) Quantification of the diameter and perimeter of WT and *smo* mutant guts from transverse cross sections.

Wt n=14, mutant n=18, diameter p>0.18, perimeter p >0.48. (H) Quantification of total cell number in WT and mutant guts. WT n=14, mutant n=18, p>0.30

(I) Quantification of the percent of BrdU positive cells in WT and *smo* mutant guts. WT n= 14, mutant n= 19, p> 0.32.

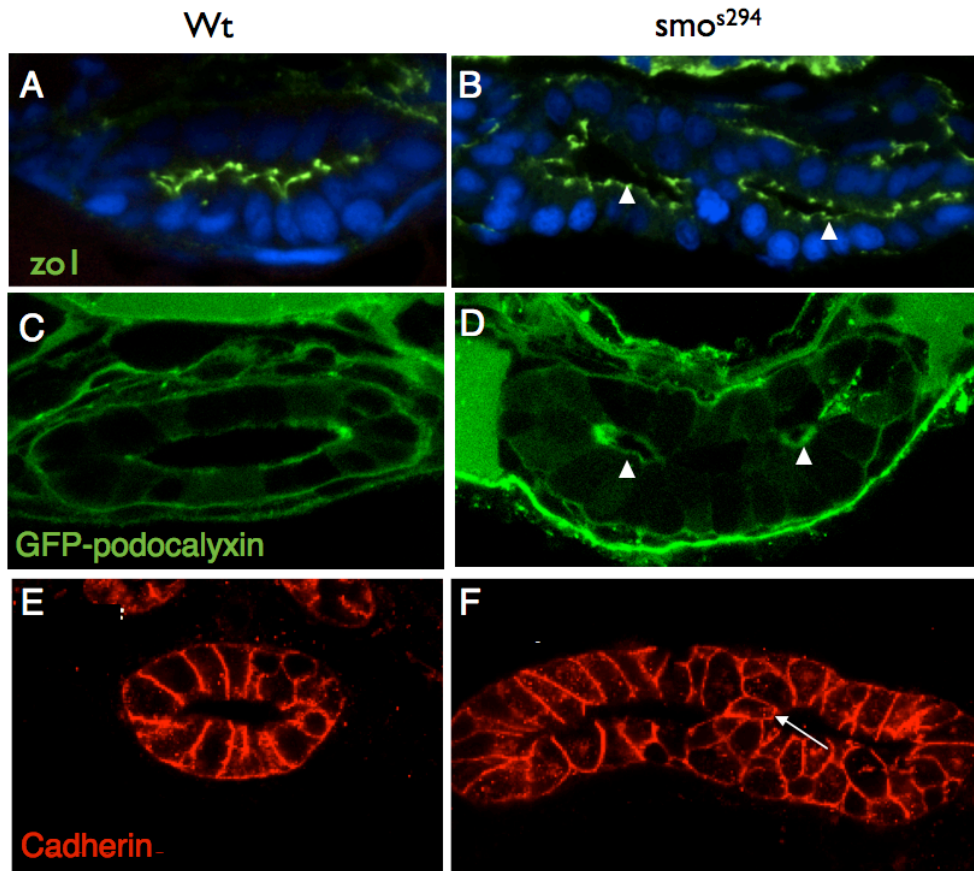


Figure 17- *smoothened* mutants do not display polarity defects

A-B Confocal cross sections of Wt and *smo* mutant embryos stained for the tight junction marker Zo-1 (green). **C-D** Confocal cross sections of Wt and *smo* mutant *Tg(hsp70l:GFP-podxl)* embryos (green). **E-F** Confocal cross section of Wt and *smo* mutant embryos stained for the basolateral marker cadherin (red).

intermediate stage WT embryos, further suggesting that the *smo*^{s294} lumen phenotype is representative of the lumen resolution stage of development. Taken together these results indicate that *smo* mutants exhibit mesenchymal defects, yet the intestinal epithelium is similar between WT and mutant embryos. However, despite the epithelial similarities *smo* mutants are distinct in their inability to undergo lumen fusion.

Endocytic degradation and recycling during lumen resolution

Because single lumen formation in the zebrafish gut occurs without apoptosis (Ng et al., 2005), lumen resolution must involve epithelial remodeling and the rearrangement of cellular contacts that are observed between the lumens. This remodeling can be achieved by changing the identity of bridge contacts, from basolateral to apical, or by breaking adhesions. To undergo remodeling, cellular contacts and adhesions can be internalized and trafficked to lysosomes for degradation or they can be recycled back to the cell surface (Le et al., 1999; Palacios et al., 2005). To determine if lysosomal degradation is important for lumen fusion we inhibited the degradation pathway by targeting a variety of mechanisms. First, we perturbed Rab7 function, which regulates late endosomal trafficking, (Bucci et al., 2000) using a dominant negative version of the protein (Rab7DN). Expression of Rab7DN was induced by heat shocking *Tg(hsp70l:GFP-Rab7aDN)* embryos at 48 hpf. Examination at 72 hpf revealed there was no difference in single lumen formation between WT and DN embryos (Figure 18A-B). To further probe the degradation pathway, we inhibited intracellular acidification. Acidification is critical to the proper function of intracellular compartments, and is primarily regulated by the vacuolar type H⁺ATPase. A low pH is essential to the function

lysosomes and other vesicles along the degradation pathway. Therefore, we impaired lysosomal acidification using the drug bafilomycin, which inhibits the vacuolar type H⁺ ATPase (V-H⁺ATPase). Embryos were bathed in a range of drug concentrations yet lumen defects were never observed (Figure 18C-D). It is difficult to determine if bafilomycin was able to reach the gut in sufficient quantities to adequately impair intracellular acidification, therefore we also examined embryos mutant for members of the V-H⁺ATPase complex (Nuckels et al., 2009). Analysis of embryos mutant for the v1f and v1e1 subunit of the V-H⁺ATPase complex again showed no lumen defects (Figure 18E-F). Taken together these results suggest that intracellular degradation and acidification are not critical to contact remodeling and lumen fusion.

Several studies have found that endocytic recycling and trafficking are important for epithelial remodeling during morphogenesis (Pirraglia et al., 2010; Shaye et al., 2008). The Rab11 family of small GTPases as well as the Rab11 effector proteins Rab11FIP and MyoVb are well known regulators of the recycling pathway (Hales et al., 2001; Lapierre et al., 2001; Ullrich et al., 1996) and have been shown to play a key role in both apical trafficking and basolateral recycling during epithelial morphogenesis (Kerman et al., 2008; Satoh et al., 2005). To determine if recycling is involved in single lumen formation, we utilized a dominant-negative construct to disrupt endogenous Rab11a function. We crossed *Tg(UAS:mcherry-rab11a-S25N)mw35* (Rab11aDN) (Clark et al., 2011) to a *Tg(hsp70l:gal4)* line to temporally control expression of Rab11aDN. Expression of Rab11aDN prior to the resolution stage resulted in an un-fused lumen phenotype, similar to that of *smo*^{s294} mutants and class II WT embryos, in 45% of

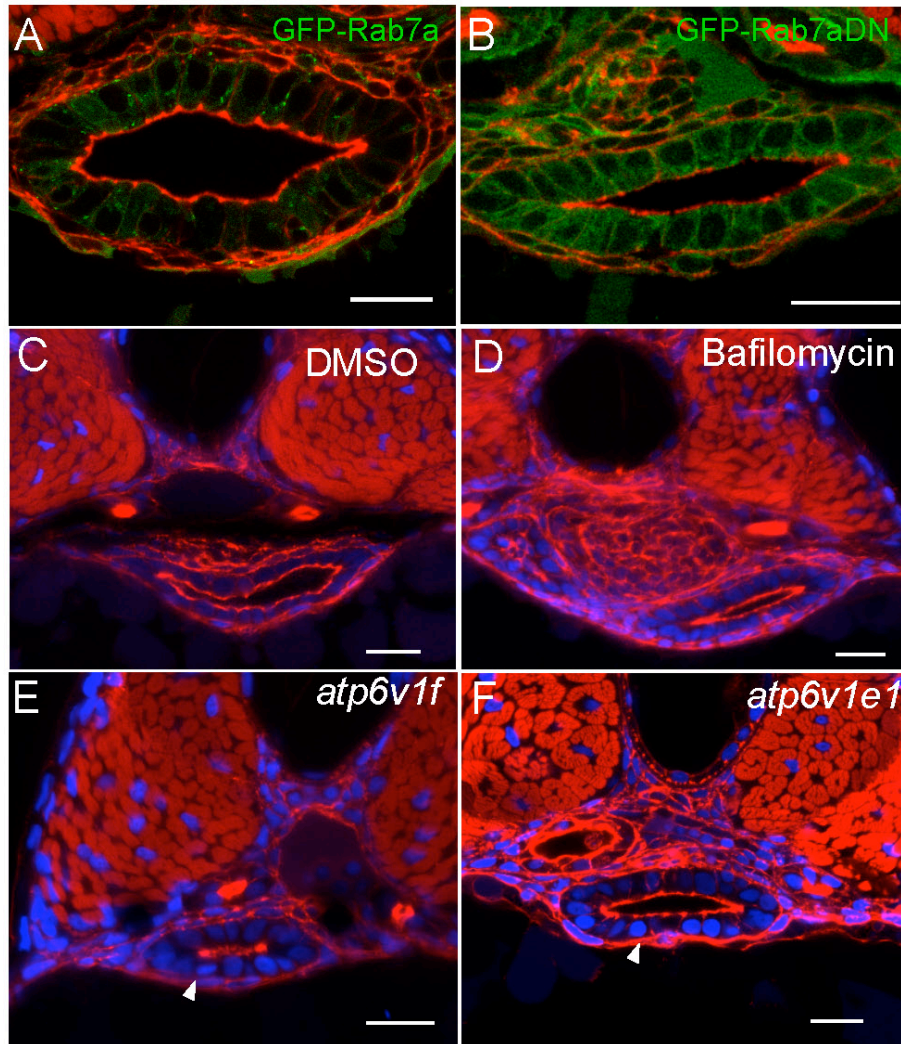


Figure 18- The degradation pathway is not involved in lumen formation

A-B Confocal cross sections from *Tg(hsp70l:GFP-Rab7)* and *Tg(hsp70l:GFP-Rab7DN)* embryos. Phalloidin (red). **C-D** Confocal cross sections from DMSO and bafilomycin treated embryos. **E-F** Confocal cross sections from *atp6^{v1f}* and *atp3^{v1e}* mutant embryos. Phalloidin (red). Scale bars: 20 μM

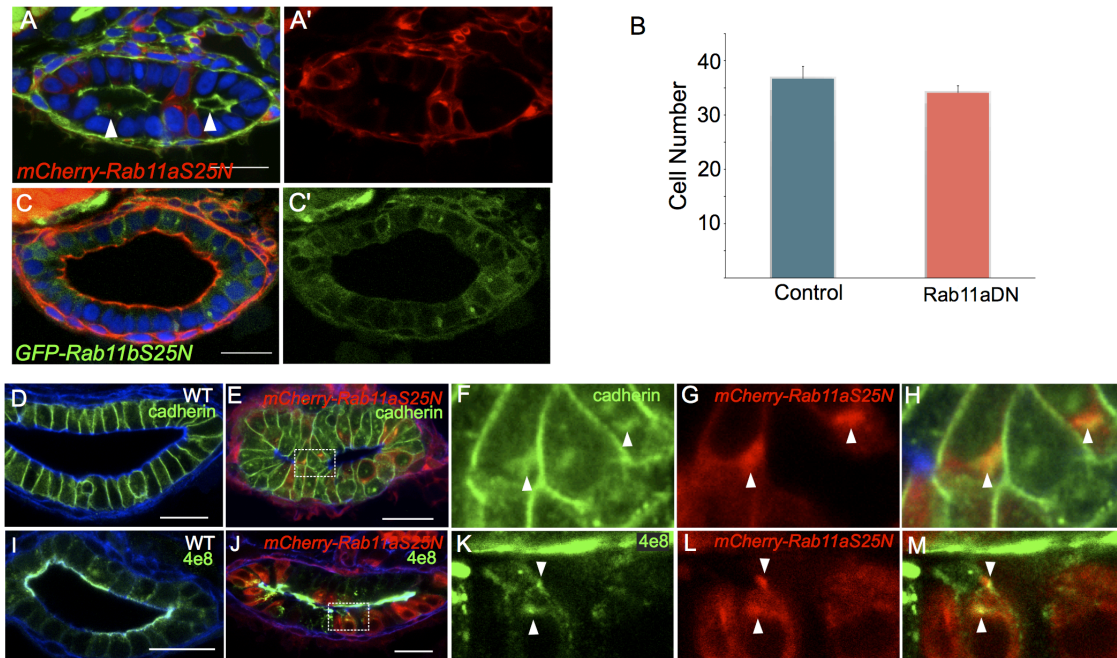


Figure 19- Rab11aDN embryos exhibit impaired lumen fusion

A-A' Confocal cross section of a *Tg(hsp70l:gal4); Tg(UAS:mcherry-rab11aS25N)* embryo. Phalloidin (green). **B** Quantification of total cell number in the gut in WT and Rab11aDN embryos. WT n=13, DN n=11, $p>0.32$. **C-C'** Confocal cross section of a *Tg(hsp70l:GFP-rab11bS25N)* embryo. Phalloidin (red) **D** Confocal cross section of a WT embryo at 72 hpf stained for cadherin. **E-H** Confocal cross section of a Rab11aDN embryo stained for cadherin. Arrowheads point to Rab11DN and cadherin co-localization in internal compartments. **I** Confocal cross section of a WT embryo at 72 hpf stained for 4e8. **J-M** Confocal cross section of a Rab11aDN embryo at 72 hpf stained for 4e8. Arrowheads point to Rab11DN and 4e8 co-localization in internal compartments Scale bars: 20 μ M

embryos (n=20) at 72 hpf (Figure 19A). These embryos contained the same number of epithelial cells in the gut as WT embryos, indicating that failed lumen resolution is not due to differences in cell numbers or a developmental delay (Figure 19B). Upon expression of Rab11aDN, cadherin accumulated intracellularly, indicating it is recycled in a Rab11a-dependent manner during lumen formation (Figure 19D-H). In addition, the apical protein 4e8 was also found to co-localize to Rab11aDN compartments (Figure 19I-M). We also tested the function of Rab11b, which is highly similar to Rab11a, yet resides in distinct apical vesicles in epithelial cells and co-localizes with different cargo proteins (Lai et al., 1994; Lapierre et al., 2003). Unlike DN-Rab11a, expression of DN-Rab11b did not cause a lumen formation phenotype (Figure 19C). Thus Rab11a mediated recycling of basolateral and apical membrane proteins is necessary for lumen fusion during single lumen formation.

The dynamic nature of cadherin at the membrane is based on its continual trafficking to and from the cell surface and this trafficking is essential to the regulation of adhesions during morphogenesis (Bryant and Stow, 2004). p120-catenin regulates cadherin stability at the membrane by masking an endocytic signal on the C-terminal tail of cadherin, preventing its internalization and degradation (Davis et al., 2003; Nanes et al., 2012; Xiao et al., 2003). To determine if cadherin stability is involved in lumen fusion we overexpressed p120-catenin during the resolution stage of lumen formation to stabilize cadherin at the surface. We examined *Tg(hsp70l:GFP-p120)pd1091* embryos in whole-mount and found that p120 localizes to the basolateral membranes and high expression of the protein impairs lumen fusion within the intestine compared to non-

expressing clutchmates (Figure 20A-B). Using this transgenic line, additional studies can be performed to determine if specific contacts expressing high levels of p120 are less likely to undergo remodeling.

Since *smo* mutants have mesenchymal defects, we next examined Rab11DN embryos to determine if impaired lumen fusion is linked to defects in mesenchymal differentiation. We performed in situ hybridization on Rab11aDN embryos to detect expression of α SMA, and found that Rab11DN embryos exhibited proper differentiation of the mesenchymal layer (Figure 21A-B). Furthermore, staining for smooth muscle myosin, Myh11, showed that mesenchymal cells specifically expressing Rab11aDN differentiated to a similar extent as controls (Figure 21C-D'). These data suggest that Rab11aDN expression does not affect the differentiation of the gut mesenchymal layer and that the lumen resolution phenotype observed in Rab11DN embryos is not solely due to mesenchymal defects.

Impaired Rab11a recycling in *smo* mutants

The similar lumen phenotype shared by *smo*^{s294} mutants and Rab11aDN-expressing embryos next led us to investigate whether defects in the recycling pathway contribute to the *smo*^{s294} phenotype. To this end we generated a GFP-RAB11a transgenic line, *Tg(hsp70l-GFP-RAB11a)pd1031*, to mark recycling endosomes. In WT embryos, GFP-RAB11a was localized to small sub-apical compartments surrounding the lumen (Figure 22A-A'). In contrast, *smo*^{s294} mutants exhibited abnormally enlarged GFP-RAB11a compartments that were dispersed from the apical surface (Figure 22B-B'). These enlarged Rab11a compartments in *smo* mutants contained the apical protein 4e8

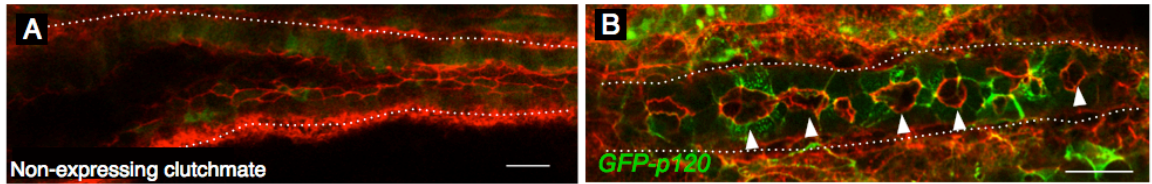


Figure 20- p120 expression impairs lumen fusion

A-B Whole mount confocal image of an embryo expressing *Tg(hsp70l:GFP-p120)* and a non-expressing clutchmate. Arrowheads point to un-fused lumens found in GFP-p120 expressing embryos.

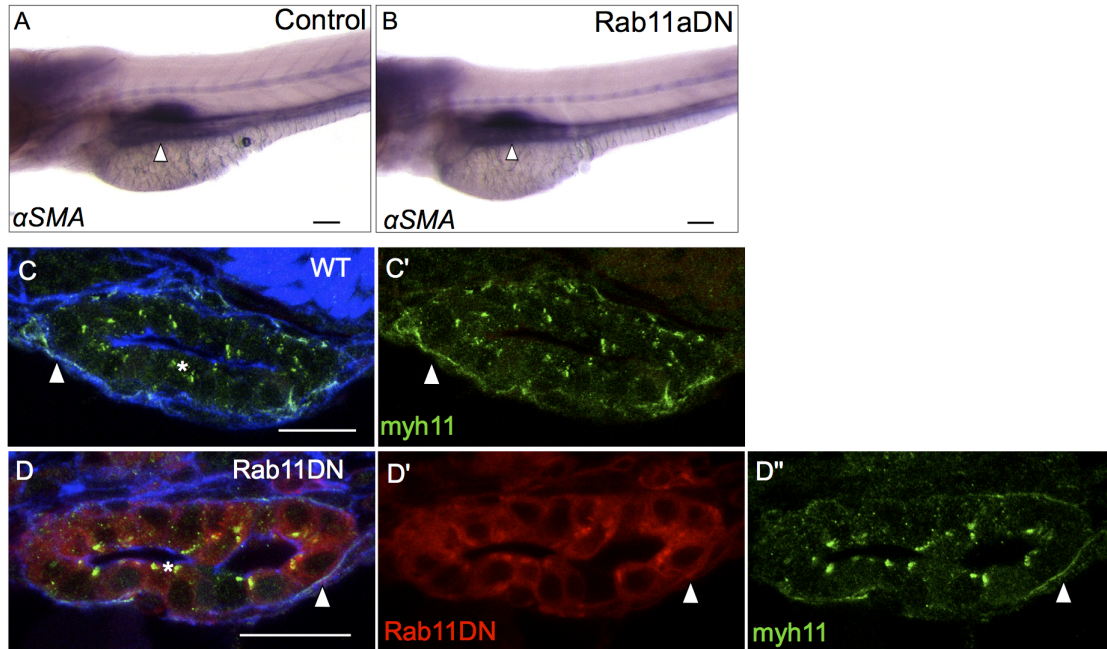


Figure 21- Mesenchymal differentiation is not impaired in Rab11aDN embryos

A-B- Lateral view of an *in situ* hybridization showing α SMA expression in WT and Rab11aDN embryos at 72 hpf. Arrow points to smooth muscle. Scale bar: 100 μ M. **C-D''-** Confocal section of WT and Rab11DN embryo stained for Myh11. Arrowhead points to Myh11 in the mesenchyme. Asterisk indicates non-specific epithelial staining as observed previously (Wallace et al., 2005) Scale bars: 20 μ M

indicating a defect in trafficking of apical membrane proteins (Figure 22 C-D'). Colocalization with cadherin was not as apparent (Figure 22E-F'). However, due to the transient nature of internalized cadherin, cadherin colocalization with recycling endosomes is often limited (Desclozeaux et al., 2008), which likely accounts for the minimal amount of colocalization with Rab11a compartments we observe. These data, together with the Rab11DN data suggests that Rab11 trafficking of both apical and basolateral proteins is important in lumen fusion.

Previous studies in the *Drosophila* trachea have shown a similar accumulation of Rab11 in enlarged compartments upon over-expression of the Rab11 effector protein Rip11, an ortholog of Rab11Fip1a (Shaye et al., 2008). Rab11Fip1a and MyoVb interact with Rab11 family members and regulate plasma membrane recycling (Hales et al., 2001; Lapierre et al., 2001). To investigate Rab11 effectors in *smo*^{s294} mutants we examined the expression levels of Rab11a, Rab11b, Rab11Fip1a and MyoVb in WT and *smo*^{s294} embryos. We used fluorescence-activated cell sorting (FACS) to isolate intestinal cells from homozygous mutant *TgBAC(cldn15la-GFP)pd1034; smo*^{s294} embryos and WT clutchmates. We isolated RNA and performed quantitative RT-PCR (qPCR) to evaluate differential gene expression specifically in the intestinal epithelium of *smo* mutants. In *smo*^{s294} cells, the expression of *rab11fip1a* was increased threefold. However, the expression of *rab11a*, *rab11b* and *myo5b* was not significantly different from that in WT cells (Figure 22I). To assess how an increase in Rab11fip1a levels may contribute to the *smo* gut phenotype, we overexpressed Rab11fip1a in *Tg(hsp70l:GFP-RAB11a)* embryos through RNA injection. Upon mild overexpression, GFP-Rab11a compartments became

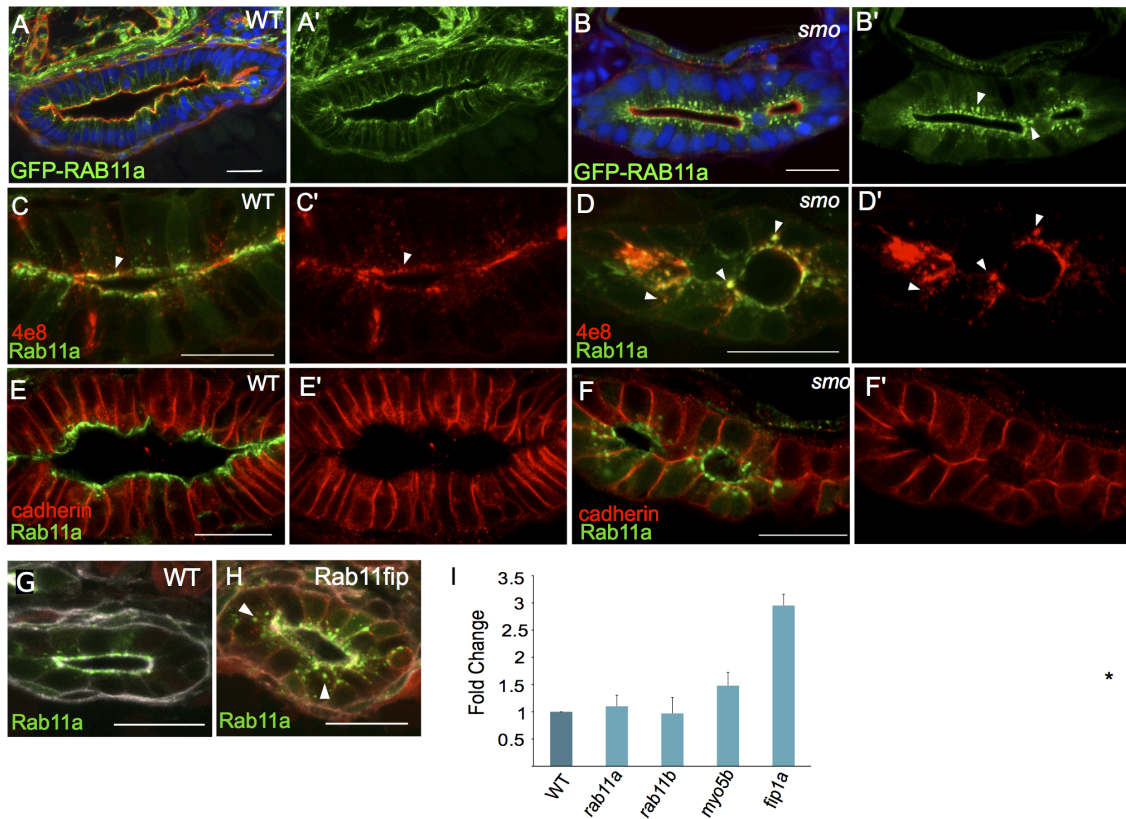


Figure 22- Rab11a is abnormally localized in *smo* mutants

A-B' Confocal cross sections of *smo*^{s294} and WT clutch-mates expressing *Tg(hsp70l:GFP-RAB11a)*. Arrowheads point to abnormal enlarged Rab11 positive vesicles in *smo*^{s294}. Phalloidin (red) **C-F'** Confocal cross section of WT and *smo*^{s294} embryos expressing *Tg(hsp70l:GFP-RAB11a)* stained for the apical marker 4e8 (C-D') or cadherin (E-F'). Arrowheads point to areas of colocalization. **G-H** Confocal cross sections of uninjected and RFP-Rab11fip1 injected *Tg(hsp70l:GFP-RAB11a)* embryos. Arrowheads point to dispersed compartments. **I** Expression levels of Rab11 family members in the intestinal epithelium of *smo*^{s294} mutants relative to WT clutch-mates. Rab11fip1a $p < 0.011$. All embryos are 72 hpf. Scale bars: 20 μ M

enlarged and disorganized compared to non-injected embryos, similar to that observed in *smo* mutants (Figure 22G-H). The data suggests that increased levels of Rab11fip1a are likely in part responsible for the abnormally enlarged GFP-RAB11a compartments observed in *smo*^{s294} mutants.

4.3 Discussion

The studies presented here have identified an intermediate stage in the process of single lumen formation and revealed that lumen resolution is a genetically-regulated process crucial for continuous lumen formation in the zebrafish gut. In addition, our findings show that intracellular recycling of apical and basolateral membrane proteins is involved in the remodeling process during lumen fusion. Finally, our data also highlight the role of *smoothened* signaling from the mesenchyme in the regulation of lumen morphogenesis in the gut epithelium.

Based on our studies, we propose that *smo* signaling facilitates the remodeling and weakening of bridge contacts as well as the enlargement of apical membrane via Rab11a-mediated trafficking and recycling. These signaling and trafficking events are essential to the generation of a single continuous lumen in the zebrafish gut (Figure 23A). In our model, basolateral recycling re-localizes the adhesion from the bridge to lateral surfaces, thus shrinking and weakening the contacts between the lumens. In addition, apical membrane is delivered to the luminal surface to facilitate membrane expansion. As adhesions shrink, the bridge contacts eventually break and lumens fuse (Figure 23B). This may also be facilitated by the insertion of anti-adhesive apical proteins on the edge

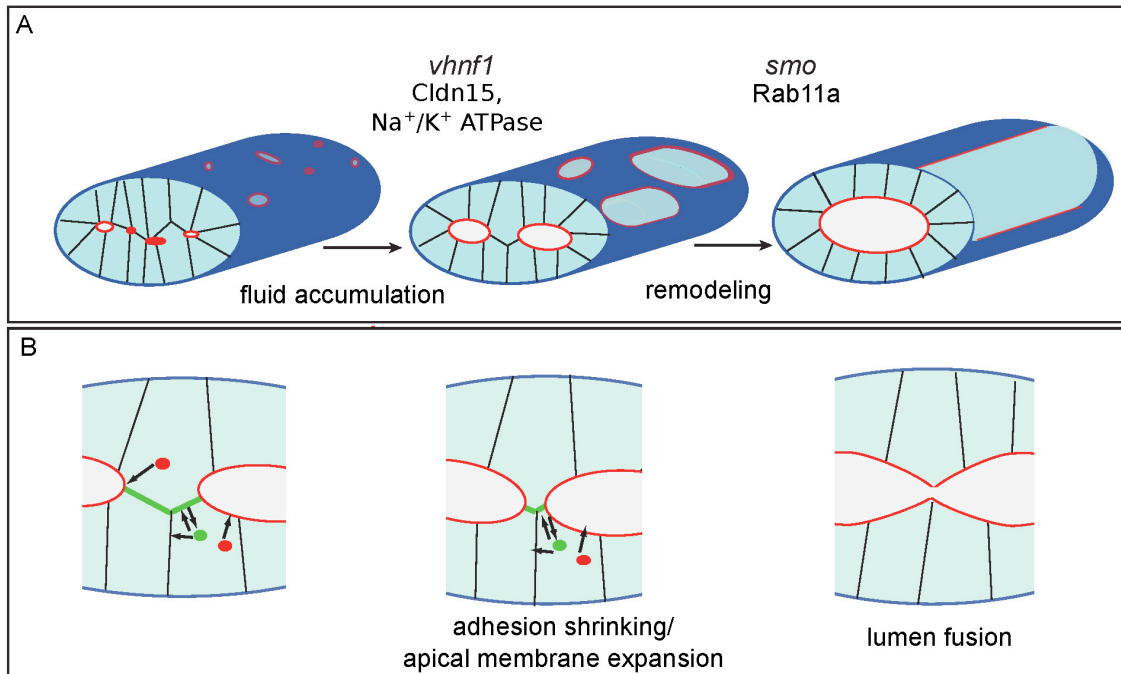


Figure 23- Lumens enlarge and fuse during single lumen formation

A- During single lumen formation, *vhnf1* drives lumen enlargement through Cldn15 and Na⁺/K⁺ATPase regulated fluid accumulation. Next *smoothened* regulates remodeling through Rab11a mediated trafficking to facilitate lumen fusion. Red indicates the luminal surface. **B-** During the fusion process, Rab11 traffics apical proteins (red) to the luminal surface and recycles basolateral proteins (green) from bridge contacts to lateral membranes. As the lumens expand, the bridge contacts between the lumens shrink and split, and the lumens fuse.

of the bridge contact as shown in blood vessels (Strilic et al., 2010). Interestingly, zebrafish mutant for aPKC λ , which regulates adherens and tight junctions, also exhibit a single lumen formation defect (Horne-Badovinac et al., 2001), underscoring that proper regulation of adherens is critical in single lumen formation.

Work in 3D cyst models has established the importance of functional Rab11 and recycling endosomes in E-cadherin trafficking, cyst morphogenesis and lumen formation (Bryant et al., 2010; Desclozeaux et al., 2008). In 3D cysts, Rab11 is critical for lumen initiation by mediating the relocation of apical membrane from the outer surface of cells to a central patch where a lumen subsequently forms (Bryant et al., 2010). However, in most *in vivo* tubular systems including the zebrafish intestine, mammalian pancreas and mammary gland, lumens initiate at several different sites within a rod of cells and must connect with each other to form a continuous luminal network. Our work shows that Rab11 mediated trafficking is needed to facilitate lumen resolution. Therefore, Rab11 may play a role in two distinct processes of lumen formation- lumen initiation and lumen resolution.

The examination of important recycling pathway members revealed differential expression of the Rab11 effector protein, Rab11fip1a, as well as an accumulation of enlarged Rab11a compartments in the *smo*^{s294} intestinal epithelium. Overexpression of Rab11fip1a caused a similar accumulation of Rab11a compartments compared to WT embryos but did not produce a lumen fusion phenotype. This suggests that either additional genes are also involved or that higher levels of Rab11fip1a expression are required to cause a lumen formation defect. In the *Drosophila* trachea, the overexpression

of the Rab11 effector protein, Rip11, causes an accumulation of large Rab11 vesicles, similar to what we observed in *smo*^{s294} mutants, and results in impaired morphogenesis (Shaye et al., 2008). Furthermore, expression of the pseudophosphorylated Rab11-FIP2(S227E) mutant results in multiple lumens and a disruption of tight and adherens junctions in cysts *in vitro* (Lapierre et al., 2012). Therefore, our findings in *smo*^{s294} mutants are consistent with previous studies and highlight the importance of effector protein levels in modulating endocytic recycling.

Although *smo*^{s294} mutants exhibit aberrant Rab11a localization and increased expression of Rab11 effector proteins, it is unclear how *smo* signaling regulates these recycling pathway members. In zebrafish, molecular interactions between epithelial Hh and mesenchymal Fgf10 regulate proliferation and differentiation in the esophagus and swimbladder (Korz et al., 2011). In addition, Hh signaling from the endoderm is required for posterior gut development in zebrafish embryos (Parkin et al., 2009). Using a transcriptional reporter we found that *smo* signaling acts in the surrounding mesenchyme but not in the intestinal epithelium. Thus, *smo* likely regulates lumen fusion through epithelial-mesenchymal interactions and/or morphogen signaling such as the Bmp or Fgf pathways. Signaling from the mesenchyme through secreted factors, and/or mechanical interactions are undoubtedly important for epithelial organization during tubulogenesis. Future studies should dissect the specific role both types of interactions play in regulating gut morphogenesis.

5. The role of Clic5 in the zebrafish gut

Early in our study of intestinal tubulogenesis, a microarray was performed on WT and *smo* mutant whole embryos to identify potential targets regulating lumen formation. One gene of interest that initially attracted our attention was the Chloride Intracellular Channel, *clic5*. In this chapter I describe our work with this protein and discuss its potential role in gut development. I will also discuss work that is currently being pursued in the lab to understand early polarization and lumen initiation in the gut and explain how *Clic5* may provide insight into this area of study.

5.1 Introduction

The chloride intracellular channel (CLIC) family of proteins was first identified as a class of intracellular anion channels consisting of 6 highly conserved family members (Cromer et al., 2002). CLIC proteins are highly conserved among vertebrates. The six paralogues are composed of approximately 240 amino acids with a conserved C terminal domain and a variable N-terminus, and many of these proteins have splice variants or additional N-terminal domains.

p64, also known as CLIC5B, was the first CLIC family member to be identified. p64 was purified from bovine kidney cells and was characterized as a chloride channel based on inhibition by indanyloxyacetic acid 94. Cloning of p64 revealed no similarity with other integral membrane proteins or any known ion channels, however reconstitution of these proteins in liposomes showed chloride channel activity (Landry et

al., 1993). Several additional proteins were then identified based on the presence of a characteristic CLIC module and had variable activity as an ion channel.

Interestingly, all CLIC proteins that have been studied exist in both a soluble globular confirmation and as integral membrane proteins with channel activity (Littler et al., 2010). The transition between these two confirmations is likely regulated by pH and redox conditions. However, CLIC proteins do not act as typical ion channels. They lack an N-terminal signal sequence and, unlike most ion channel proteins, which contain several clear transmembrane domains, CLIC proteins only have a putative transmembrane domain. In vitro experiments have shown that CLIC1,4, and 5 can form poorly selective integral membrane ion channels. However, it remains unknown whether these channels have any physiological activity in vivo.

Aside from channels, some studies have suggested that CLICs play a role in the interactions between the membrane and the cytoskeleton. For example, CLIC5 was first isolated from placental microvillus and shown to interact with the cortical cytoskeletal complex containing ezrin and actin (Berryman et al., 2004). Clc5a has also been identified in podocytes where it forms a complex with ezrin, podocalyxin and the actin cytoskeleton. Mice with a mutation in CLIC5a display abnormal podocyte morphology and proteinuria, indicating that CLIC5a plays a role in podocyte structure and function as a component of the cytoskeleton (Pierchala et al., 2010; Wegner et al., 2010).

Furthermore, CLICs are associated with intracellular vesicle membranes in both membrane bound and soluble forms. It is currently believed that CLICs are required for

formation and maintenance of intracellular vesicles, however the mechanism of this regulation is currently unknown (Littler et al., 2010).

Several studies have provided insight into the physiological functions of CLIC, which range from roles in tubulogenesis, acidification, and the actin cytoskeleton. In *C. elegans* the CLIC-like protein *exc4* was shown to be involved in the formation and maintenance of the intracellular tubular excretory vesicle (Berry et al., 2003). This study determined that the first 66 residues of Exc4, which includes the putative transmembrane domain, are essential to proper localization to the apical membrane. Following this study, vertebrate CLIC proteins, specifically CLIC4, were also investigated in tubulogenesis. For example, CLIC4^{-/-} mice were found to exhibit defects in angiogenesis due to impaired acidification along the intracellular tubulogenic pathway (Tung et al., 2009). The “jitterbug” mouse also provides insight into the function of Clic proteins. These mice arose from a spontaneous recessive mutation in *Clic5* and display a lack of coordination and progressively become deaf. It was discovered that these mice have a defect in inner hair cell stereocilia due to a lack of CLIC5 in the base of the hair bundle, which causes the stereocilia to degrade. Based on this phenotype, it was proposed that CLIC5 associates with radixin to help stabilize the linkage of the actin bundle to the plasma membrane in inner hair cells (Gagnon et al., 2006). Later studies also found that the jitterbug mouse displays reduced levels of phospho-ERM in podocytes (Wegner et al., 2010).

Together, these studies have provided clues to a wide range of physiological roles of CLIC proteins including roles in tubulogenesis and the actin cytoskeleton. Given

Clic's ability to regulate endosomal trafficking through its role as a possible intracellular channel, together with its connection to tubulogenesis, Clic5 was identified as a good candidate gene to study further as a mediator of lumen formation. In the following section, I investigate a potential role for Clic5 in lumen initiation and single lumen formation in the zebrafish gut.

5.2 Results

Prior to the generation of the *Tg(cldn15la:GFP)* line and the ability to sort intestine-specific cells, whole embryos were used to identify potential genes regulated by *smo* during single lumen formation. Microarray analysis was used to examine the gene expression pattern of *smo* mutant and WT embryos at 72 hpf. The analysis revealed no overlap with the transcriptional program of *vhnf1*. The array provided a list of genes that were up and down regulated in *smo* with respect to wt, many of which are implicated in endocytosis and recycling. To determine which genes may be playing a role during lumen formation, we examined the expression patterns of genes that were highly downregulated in *smo* mutants and focused our attention to those with gut expression. Here, I will discuss our work on Clic5, which showed a fourfold downregulation in *smo* mutants.

In vitro analysis of Clic5

To validate the results obtained from the microarray we used RT-QPCR to examine *clic5* transcript levels in WT and mutant embryos. Zebrafish have three *clic5* family members (Figure 24). *clic5a* and *clic5b* are splice variants while *clic5a1* (*zgc:101827*) is a gene duplication of *clic5a*. Clic5a and Clic5a1 are approximately 240

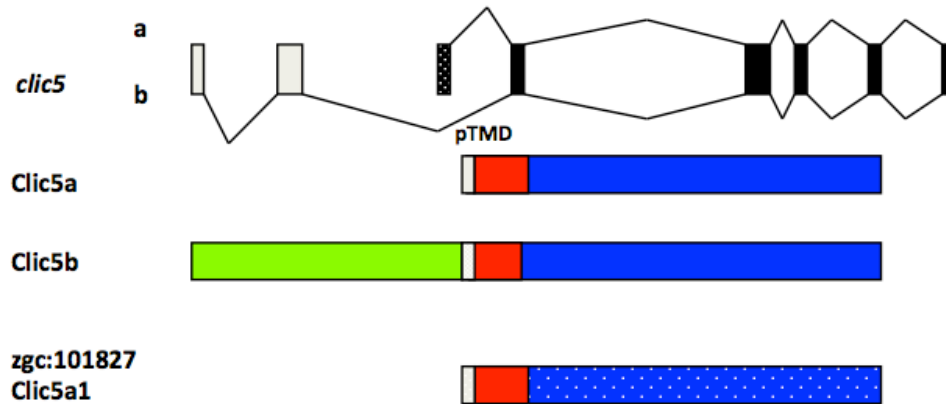


Figure 24- Zebrafish clic5

Zebrafish contain three *clic5* family members. Clic5a and Clic5b are splice variants which differ in a 200 amino acid N-terminal region. Clic5a1 (zgc:101827) is a gene duplication of Clic5a and shares 84% identity.

amino acids in length and have a conserved N-terminal region. Clic5b on the other hand is over 400 amino acids in length due to an additional N-terminal motif of approximately 200 amino acids. To determine the abundance of each isoform in WT embryos we made cDNA from 72 hpf whole embryos and performed qPCR. The expression level of *cli5a1* was 10-fold more abundant compared to *cllic5a* and *cllic5b* (Figure 25A). Next, we compared expression levels between WT and *smo* mutant embryos and found *cllic5a1* expression was reduced 2-fold in mutants, while *cllic5a* and *cllic5b* remained fairly unchanged relative to WT levels (Figure 25B). A time course analysis of *cllic5a1* expression from 2-5 dpf was also performed by qPCR to determine the stage in development in which *cllic5a1* is most highly expressed. This revealed that *cllic5a1* expression remains constant from 2-4 dpf then increases 2.5-fold at 5 dpf (Figure 25C). This increase in expression at 5 dpf may indicate that Clic5a1 is involved in additional morphological or physiological processes occurring later in gut development.

Since Clic proteins have been shown to be both intracellular channels and actin binding proteins, we next examined Clic5 localization to determine if it is found intracellularly or at the cell surface. To examine the localization of Clic5 in a polarized epithelium we generated a stable MDCK cell line expressing GFP-Clic5. When MDCK cells are grown on a 2D thin substrate they serve as an effective system to study apical basal polarity. When suspended in a thick 3D matrix, these cells aggregate to form cysts consisting of an epithelial monolayer surrounding a fluid filled cavity. When stable cells were grown on 2D filters, GFP-Clic5 co-localized with GP135 on the apical membrane (Figure 26A). Furthermore, when cells were cultured in a matrix, 3D cysts formed and

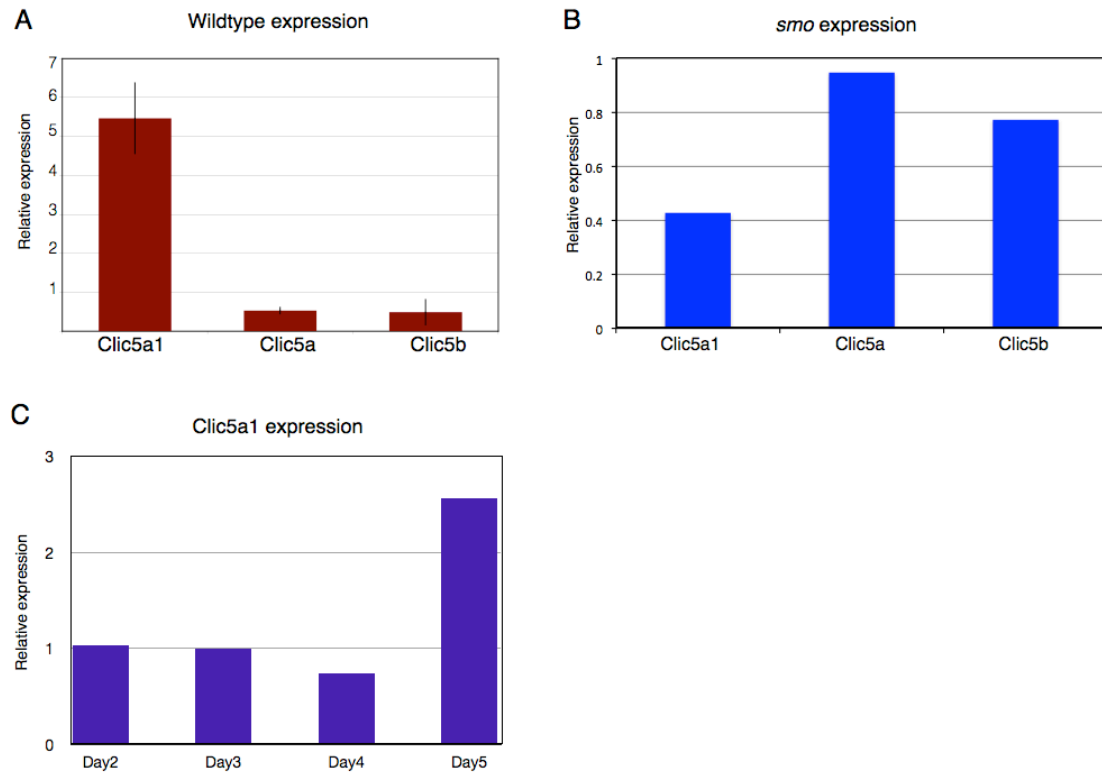


Figure 25- Gene expression analysis of clic5

A Relative expression levels of *clic5a1*, *clic5a*, and *clic5b* in whole embryos, normalized to β -actin. **B** Relative expression levels of *clic5a1*, *clic5a*, and *clic5b* in whole *smo* mutant embryos, normalized to WT clutchmates. **C** Relative expression level of *clic5a1* at 2,3,4 and 5 dpf. Expression normalized to 2 dpf levels.

GFP-Clic5 localized to the luminal surface. Thus, Clic5 localizes apically in polarized epithelial cells in vitro (Figure 26B). Next, we used the cyst model to determine if Clic5 is involved in lumen formation. GFP-Clic5 was overexpressed in Caco2 intestinal epithelial cells and the cells were grown into 3D cysts. After several days of growth, the overexpression of Clic5 resulted in cysts containing multiple lumens, while non-transfected controls properly formed single lumens (Figure 26C-D). This result suggests that misregulation of Clic5 expression may interfere with lumen initiation or lumen coalescence.

Is Clic5 a chloride channel?

To investigate the potential of Clic5 acting as an ion channel we examined whether GFP-Clic5 functions as a peripheral or integral membrane protein. We created a homogenate of HEK 293 cells expressing GFP-Clic5, laid it on a sucrose cushion and centrifuged the lysate to isolate the membrane fraction. The majority of Clic5 protein was found in the top fraction of the sucrose cushion, indicating that Clic5 associates with the membrane (Figure 27C). We then pelleted the membrane fraction and resuspended the proteins in a high alkaline buffer to isolate peripheral proteins from integral membrane proteins. Most of the Clic5 protein was solubilized by the high pH, indicating that Clic5 is peripherally associated (Figure 27D). Taken together, these data suggest that Clic5 is not an ion channel but does associate with the membrane, possibly as a regulator of ion channel activity. However, given Clic5's known interaction with the actin

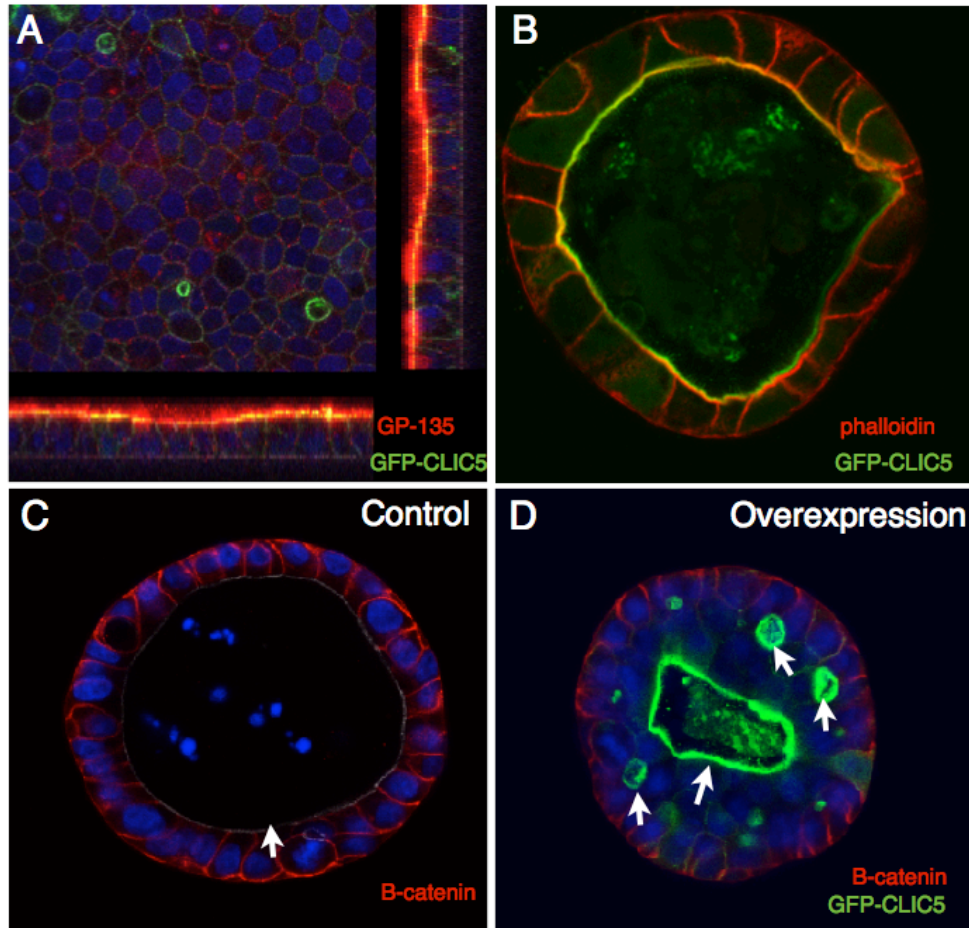


Figure 26- in vitro expression of Clic5

A Confocal image and orthogonal plane view of GFP-Clic5 localized to the apical surface of polarized MDCK cells grown on a filter. The apical marker Gp-135 is in red. **B** Confocal image of GFP-Clic5 localized to the apical membrane of cells in a 3D MDCK cyst. Phalloidin is in red. **C-D** 3D Caco2 cyst overexpressing GFP-Clic5 and a non-transfected control. β -catenin is in red. Arrows point to lumens.

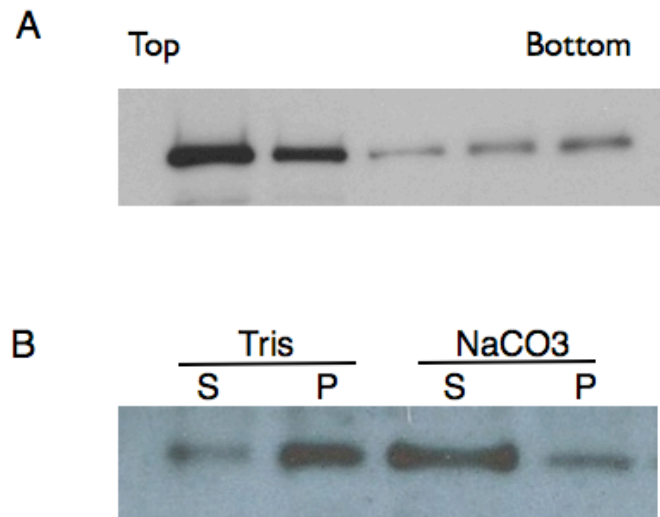


Figure 27- Clic5 associates peripherally with the membrane

A- GFP-Clic5 cells were homogenized and spun on a sucrose gradient. Fractions were collected from the top to bottom of the gradient and blotted for GFP expression. **B-** The membrane fraction from (A) was treated with Tris buffer or Tris + NaCO₃ and pelleted. In neutral conditions, GFP expression was detected in the pellet and in high pH conditions GFP was detected in the supernatant. S-supernatant, P- pellet

cytoskeleton and its identity as a peripheral membrane protein, Clic5 may also be acting as a scaffold protein that couples the membrane with the cytoskeleton.

In vivo analysis of Clic5

Our in vitro analysis revealed that Clic5 localizes to the apical membrane and overexpression of Clic5 impairs single lumen formation in 3D cysts. Therefore, we next investigated Clic5 during lumen formation in the zebrafish gut. To examine endogenous protein expression, we obtained an antibody against full length human Clic5. We stained cross sections of 72 and 96 hpf embryos and found that Clic5a1 localization changes over the course of development. At 72 hpf, the protein is found in a punctate pattern in the cytoplasm with only slight apical expression (Figure 28A). After 96 hpf, the protein localizes predominantly to the apical membrane of the gut (Figure 28B). This point in development correlates with the formation of microvilli at the apical surface suggesting that Clic5 may associate with the actin cytoskeleton as previously reported (Berryman et al., 2004).

Although antibody staining suggests that Clic5 is found primarily at the apical surface of the gut at 4 dpf, it is often difficult to achieve high quality antibody staining in the zebrafish gut. To support our Clic5a1 antibody localization data, we created a stable transgenic line expressing GFP-Clic5a1 under control of the heat shock promoter, *Tg(hsp70l:GFP-clic5a1)*. We heat shocked embryos at various time points to observe the localization of Clic5a1 during gut development. At 2 dpf, Clic5a1 localized weakly to the apical surface (Figure 29A-A'). By 3dpf, Clic5a1 localization at the apical surface was stronger and was also faintly observed in the cytoplasm, and by day 4, Clic5a1 strongly is

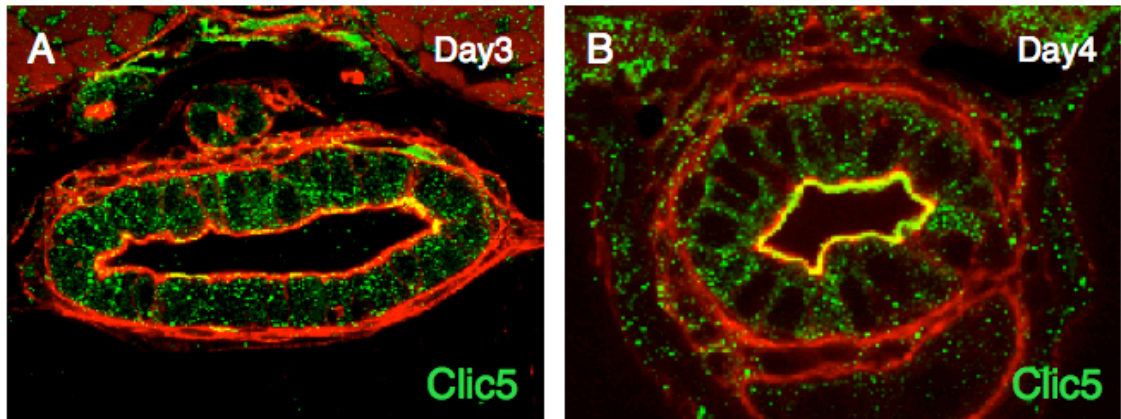


Figure 28- Clic5a1 localizes to the apical membrane in the gut

A. Confocal cross section of 3 dpf embryo stained for Clic5 (green). **B** Confocal cross section of 4 dpf embryos stained for Clic5 (green). Phalloidin is in red.

unaffected in mutant embryos (Figure 29D-D'). These data support our antibody staining and suggest that Clic5a is strongly polarized to the apical surface, likely due to its interaction with actin.

Studies in both mice and worms have suggested that Clic proteins play a role in tubulogenesis. Therefore, we continued our studies in zebrafish to determine if Clic5 is involved in lumen formation in the gut. We knocked down Clic5a1 expression with antisense morpholinos against *clic5a1*, *clic5a*, and *clic5b*. Morpholinos against each isoform were individually injected at the one cell stage and cross sections of 72 hpf embryos were examined for lumen defects. Knockdown of both *clic5a* and *clic5a1* resulted in impaired lumen resolution similar to *smo* mutants (Figure 30A-C). However, *clic5b* knockdown did not produce a lumen phenotype (Figure 30D). These preliminary results need to be confirmed using additional knockdown technologies (e.g., TALENs). Taken together, these data suggest Clic5 may be involved in tubulogenesis in the zebrafish gut, however the mechanism by which this is occurring warrants further investigation.

5.3 Discussion

In this study we investigated the role of Clic5 in single lumen formation. We show that Clic5 expression is reduced in *smo* mutants and localizes to the apical surface of epithelial cells both in vivo and in vitro. Furthermore, we show that Clic5 acts as a peripheral membrane protein and knockdown of Clic5 may impair lumen formation. However, additional studies need to be performed to further elucidate the role of Clic5 in single lumen formation.

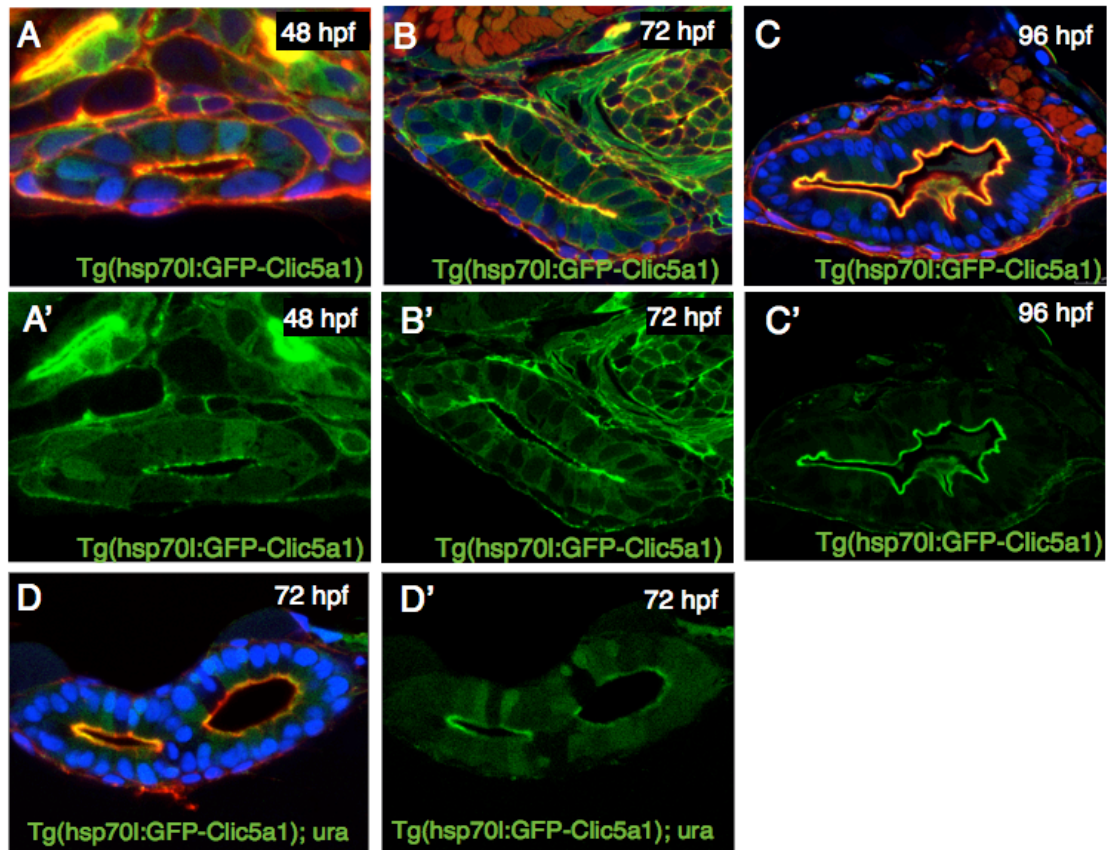


Figure 29- Expression of Tg(hsp70l:GFP-clic5a1) during gut development

A-C' Confocal cross sections of *Tg(hsp70l:GFP-Clic5a1)* embryos at 48, 72, and 96 hpf. Phalloidin is in red, DAPI is in blue. **D-D'** Confocal cross section of *Tg(hsp70l:GFP-Clic5a1; ura)* mutant embryos at 3 dpf. Phalloidin is in red DAPI is in blue.

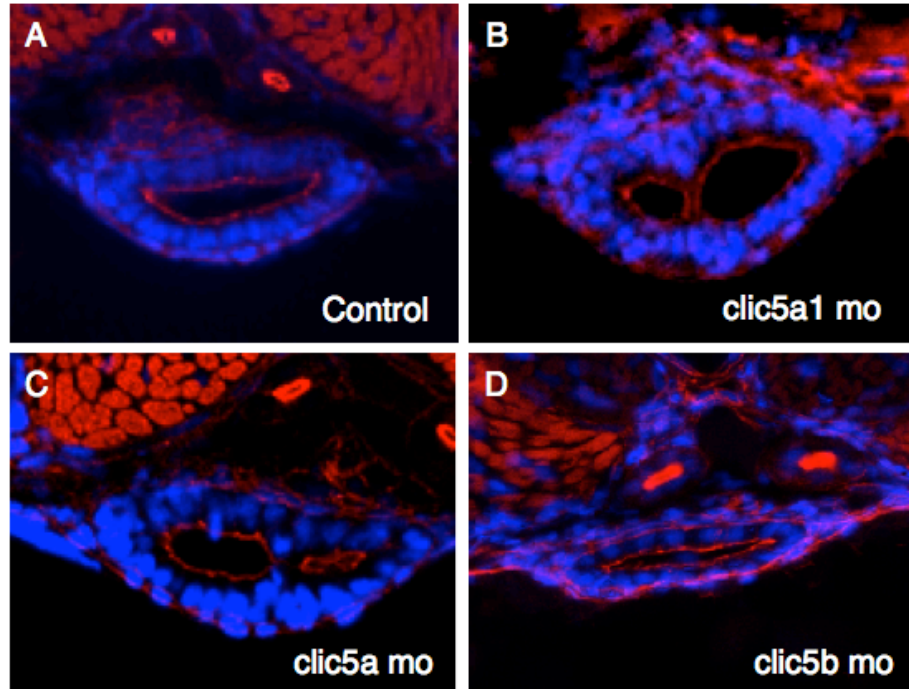


Figure 30- Morpholino knockdown of clic5 impairs lumen formation

A-D Confocal cross sections of embryos injected with a morpholino against clic5a1, clic5a or clic5b and a non-injected control. Clic5a1 produced 3/13 lumen defects and clic5a produced 6/18 lumen defects.

Clic5a1 was identified as an interesting candidate gene due to the potential of CLIC proteins functioning as chloride channels. The microarray identifying Clic5 used RNA from whole embryos and was not specific to the gut. However, subsequent examination of Clic5 expression from sorted gut-specific cells revealed that *clic5a* and *clic5a1* are enriched in the intestinal epithelium. It was hypothesized that Clic5's function as a chloride channel was involved in the regulation of intracellular acidification, which is essential to endocytic trafficking during epithelial remodeling. However, recent studies question Clic5's role as a chloride channel and suggest that if Clic5 forms a channel, it is poorly selective at best (Singh et al., 2007). Our work further supports a non-channel role for Clic5 through the identification of Clic5 as a peripheral membrane protein rather than an integral membrane protein. One possibility is that Clic5 is not an ion channel itself, but rather helps modulate ion channel activity as shown with Clic2 (Board et al., 2004). Alternatively, Clic5 may not associate with channels at all, and may instead function as an actin binding protein. Interestingly, we found that Clic5 is enriched at the apical membrane and in microvilli, suggesting that Clic5 may be involved in brush border formation or stabilization through its known interactions with the actin cytoskeleton. Regardless of Clic5's function at the apical membrane, the generation of *Tg(hsp70l:GFP-clic5a1)* has proven useful as an apical marker in other zebrafish organs such as Kupffer's vesicle where it's been used to demonstrate proper apical polarity in the epithelium.

To determine the function of Clic5 we used morpholinos to knock down each *clic5* family member. Morpholinos are commonly used to quickly analyze the function of

genes early in development. However, morpholino knockdown is only effective at early stages in development and frequently presents off target effects and sequence-specific toxicity. The possibility that the lumen phenotype is the result of an overall delay in development rather than a gut specific phenotype still needs to be addressed. However, our morpholino results could not be replicated in subsequent experiments, likely due to a loss of morpholino activity over time. Therefore, to accurately determine the role of *Clic5* in lumen formation, a *Clic5* mutant is required. Using TALENs, *Clic5* can be specifically targeted to create several stable mutant lines and then the guts of the mutant embryos can be observed for lumen initiation, lumen fusion, or brush border defects.

Further examination of *Clic5* in the gut may also provide insight into the importance of actin binding during the process of lumen initiation. Work involving the *has* mutant has shown that actin foci and junction clustering is essential to the early formation of a single lumen (Horne-Badovinac et al., 2001). In addition, the *CLIC5a*^{-/-} mouse has shown that in the absence of *CLIC5a*, podocyte structure and function is impaired, likely due to a defect in actin binding (Pierchala et al., 2010). Together this suggests that *Clic5* may play a role in actin targeting and binding during the early stages of lumen initiation. In this case, loss of *Clic5* in zebrafish may result in either an inability to properly form actin foci or weaken actin foci, ultimately leading to impaired single lumen formation.

6. Conclusion and Future Directions

The work that I have presented here has not only provided insight into the process of lumen formation but has also spurred new questions regarding additional mechanisms regulating lumenogenesis and gut development. Fortunately, several tools have been generated throughout the course of my work, which can help address questions regarding the additional mechanisms involved in single lumen formation.

6.1 Apical polarity and lumen initiation

The establishment of cell polarity is critical to the formation and function of tubular organs. A key aspect in polarity establishment is the asymmetric distribution of Phosphatidylinositol-phosphates (PIPs), which regulate the proper targeting of membrane proteins. PIP3 localizes to the basolateral surface and PIP2 is enriched at the apical surface. The asymmetric distribution of PIPs is regulated by the PAR complex and the recruitment of PTEN to tight junctions (Martin-Belmonte et al., 2007).

Following protein synthesis, proteins are sorted from the TGN to their target surface. Basolateral protein sorting is dictated by a well-established, relatively simple set of sorting signals found on the cytoplasmic tail. In contrast, apical sorting signals are much more numerous and complex, and can be found on the luminal, membrane, or cytosolic region of the protein (Rodriguez-Boulan et al., 2005). Basolateral proteins are typically transported from the TGN directly to the plasma membrane or through an intermediate basolateral early endosome. However, the transport of apical proteins is not as straight forward. Some apical proteins can be trafficked directly to the surface, while

others go through a recycling endosome before being sorted to the plasma membrane. In addition, some proteins are trafficked non-specifically to all membranes and then are endocytosed and transported to the apical surface (Cao et al., 2012). The proper targeting of the apical protein podocalyxin has been shown to be essential for lumen formation in MDCK cysts. When trafficking of podocalyxin is impaired through dominant negative versions of Rab11 and Rab8, multiple lumens result (Bryant et al., 2010).

During our studies, we noticed that at the intermediate stage of lumen development basolateral proteins are specifically targeted to the basolateral surface, yet some apical markers remain weakly polarized and are found on both the apical and basolateral surfaces of the cell. For example, the basolateral proteins MICA and Aquaporin3 are found at the basolateral surface at 60 hpf (Figure 32A-B). However, when we examined the apical transmembrane protein p75 at 60 hpf, we found expression on both the apical and basolateral surface (Figure 32D). At day 5 however, this protein is fully polarized at the apical surface (Figure 32E). Furthermore, we found that PIP2 localizes to both apical and basolateral membranes in a non-polarized manner at 60 hpf (Figure 32 C). These initial results suggest that basolateral protein sorting is predominant early in gut development and that the apical sorting machinery in the gut is not fully functional until later in development when lumens have already been initiated. Furthermore, this also suggests that the establishment of apical membrane is dispensable for early lumen initiation, which raises the question, how is a luminal surface

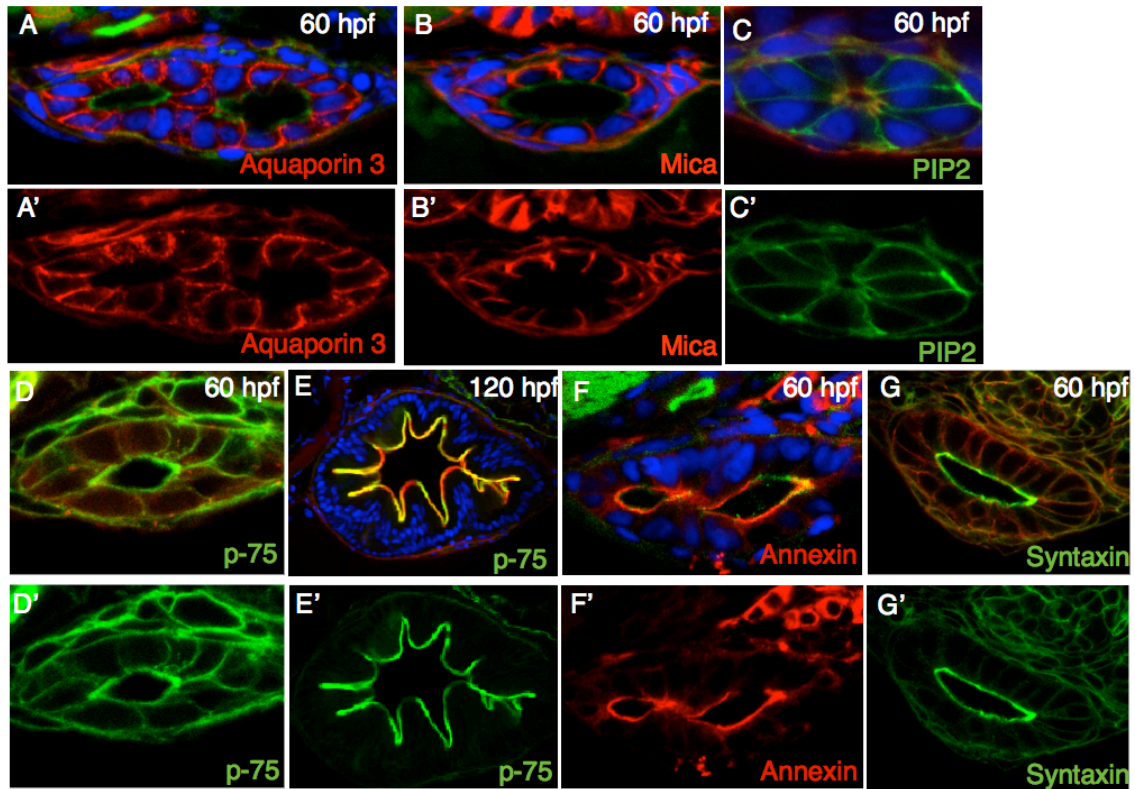


Figure 31- p-75 is unpolarized during early gut development

A-B- Confocal cross sections of 60 hpf embryos expressing the basolateral proteins Aquaporin3 and Mica. **C-** Confocal cross section of a 60 hpf embryo expressing GFP-PIP2. **D-** Confocal cross section of a 60 hpf embryo expressing the apical protein p-75. **E-** Confocal cross section of a 120 hpf embryo expressing the apical protein p-75. **F-G** Confocal cross sections of 60 hpf embryos expressing the apical proteins Annexin and Syntaxin.

established without full apical membrane polarization. We hypothesize that the establishment of the basolateral membrane is the primary requirement necessary for polarity and lumen initiation, whereas full apical membrane establishment is not essential for early stages of lumen formation.

Both Rab8 and Syntaxin 3 have been shown to be essential for proper apical membrane targeting (Sato et al., 2007; Sharma et al., 2006). To address the need of the apical membrane during lumen initiation, dominant negative versions of Rab8 and Syntaxin 3 have been generated in the lab to impair apical sorting. Rab8 and Syntaxin 3 mutant lines can be crossed to fish expressing tagged apical membrane proteins to determine if apical sorting is impaired upon expression of the dominant negative. We can also observe lumen initiation in dominant negative embryos. If mutant embryos are unable to establish an apical surface, but can still initiate lumen formation, this would suggest that apical membrane is not required for the early stages of lumen formation.

There are several apical proteins that do localize early in gut development. As shown in the previous chapters, the apical proteins Podocalyxin, and Clic5a1 are strictly localized to the apical surface during early gut development. Furthermore, examination of the apical proteins Annexin A2 and Syntaxin 3 also appear to localize apically at 60 hpf (Figure 32F-G). Interestingly, Clic5a1 and Podocalyxin are both known to interact with ERM proteins and the actin cytoskeleton, and Annexin A2 is a known regulator of actin dynamics, suggesting that actin binding and clustering may play an important role during lumen initiation (Grieve et al., 2012; Pierchala et al., 2010).

Overall, given our preliminary data and the tools recently generated in the lab, apical polarity establishment, apical protein sorting and actin binding during lumen initiation are all areas that can be easily investigated in future studies.

6.2 The role of the mesenchyme in lumen formation

A major question that still remains from our studies is how smoothed expression in the mesenchyme controls lumen resolution in the epithelium. It is hypothesized that smoothed regulates the epithelium indirectly by regulating signaling from the mesenchyme to the epithelium. It has been well established that the mesenchyme is critical for proper gut development. However, the relationship between the mesenchyme and lumen formation has not been investigated. The mesenchyme can potentially regulate single lumen formation through signaling mechanisms or through mechanical interactions. *smo* mutants lack mesenchyme around the gut and are unable to undergo lumen fusion. Therefore, it is difficult to determine if the lumen defects are a result of a physical lack of mesenchyme or if the defects are caused by a loss of the source of signaling factors.

Several studies have shown that members of the Fgf and BMP family of proteins are frequently involved in mesenchyme to epithelium signaling in the gut. For example, in mice Fgf10 in the mesenchyme signals to the epithelium through FgfR2b to drive proliferation during cecal budding (Zhang et al., 2006). Similarly, in zebrafish, Ihh and Fgf10 interact during swimbladder and esophagus morphogenesis. It is suggested that Ihh from the epithelium interacts with mesenchymal Fgf10, which in turn, is secreted by the mesoderm to affect the Fgfr2 expressing cells of the gastrointestinal endoderm (Korz et

al., 2011). Furthermore, work from Madison et al. showed that hedgehog signaling via Gli2 and Gli3 directly regulates *foxf1* and *foxl1* in the mesenchyme (Madison et al., 2009). Gli and Fox transcription factors regulate secreted morphogens including BMPs and Wnts that signal back to the endoderm. Mutations in the Fox family of genes are known to cause delays in epithelial organization (Kaestner et al., 1997).

To identify potential mesenchymal signals involved in lumen formation, we used BAC recombineering to generate a Myh11-GFP fusion protein. Based on in situ data, we expect stable transgenic embryos to express Myh11-GFP specifically in the mesenchyme around the gut. Using this line, we can sort GFP+ cells and isolate mesenchymal RNA for microarray analysis to identify genes that are highly expressed in the mesenchyme. Using the microarray results, together with our knowledge of known intestinal signaling molecules involved in other vertebrate systems, we can identify candidate genes that may be involved in mesenchymal regulation of lumen formation. We can also use the *mhy11* containing BAC to create a Myh11-Gal4 fusion using BAC recombineering. Transgenic embryos expressing this fusion protein can be crossed to UAS expressing transgenics to specifically regulate expression of any gene of interest in the mesenchyme. Together, these tools will provide us with ability to further investigate the role of the mesenchyme during various stages of gut development.

Aside from signaling, the mesenchyme may also provide physical forces that are essential for epithelial organization and lumen formation. For example, the mesenchyme may be required to constrain the epithelium and provide an inward force that drives cellular rearrangements and lumen fusion. In this scenario, the absence of mesenchyme

would allow separate lumens to enlarge without any force to promote fusion. However, this hypothesis is difficult to address since it is challenging to measure forces in vivo. Furthermore, we are unable to perform ablation experiments since any ablation of the mesenchyme would not only affect mechanical interactions, but also mesenchymal-epithelial signaling. Future advances in tools and technologies may soon allow this question to be addressed.

6.3 Regulation of Rab11

In our study of single lumen formation we showed that Rab11 is necessary for proper lumen fusion. However, there is currently no evidence that links the hedgehog pathway to Rab11 or endocytic recycling. To find a possible connection between smoothed signaling and Rab11 regulation we compared the expression levels of two Rab11 effector proteins in WT and *smo* embryos and found that *rab11-fip1a* was up regulated in mutant embryos. Additional studies need to be performed to more thoroughly address how differential expression of Rab11 effector proteins, as well as other recycling related genes affect lumen formation. Aside from *fip1a* and *myoVb*, several other Rab11 effector proteins including Rabphilin, phosphoinositide 4 kinase, SEC15, and 5 FIP family members, can be examined as possible smoothed targets. If specific effectors exhibit reduced expression in *smo* mutants, overexpression experiments can be performed to rescue lumen fusion. Likewise, knockdown of these effectors may also induce abnormal accumulations GFP-Rab11 in *Tg(hsp70l:GFP-Rab11aWT)* embryos.

6.4 Claudin 15la and single lumen formation

The Claudin15la-GFP transgenic line was initially generated as a tool to better facilitate live imaging of the early zebrafish gut. Similar to most Claudin proteins, 15la was expected to localize at the apical membrane, thus providing a way to visualize the process of lumen fusion. However, examination of transgenic stable lines revealed that Cldn15la localizes to the basolateral membrane. Furthermore, we noticed that the localization of Cldn15la changes over the course of development. At 48 hpf, Cldn15la accumulates at what appears to be tight junctions around the lumen and the basolateral surface (Figure 31A-A'). However, over time the localization at the tight junctions decreases and by 72 hpf Cldn15la is uniformly expressed on the lateral surface (Figure 31B-D'). Similar localization patterns have been observed in a variety of organs. For example, Claudin 3 exhibits basolateral expression in the rat small intestine (Rahner et al., 2001), and Claudin 7 localizes to both the basolateral membrane and tight junction region of pancreatic ductal cells and rat epididymal cells (Inai et al., 2007; Westmoreland et al., 2012). Interestingly, studies in the rat uterus found that the localization of several Claudin proteins change from tight junction to basolateral localization over the course of the estrous cycle. The authors suggest that these changes in the localization of Claudins and other tight junction proteins may occur in response to the changes in uterine morphology and luminal fluid levels that take place during the estrous cycle (Mendoza-Rodriguez et al., 2005). It is proposed that the basolateral localization of Claudin provides an excess pool of the protein, which can be quickly relocated and utilized at the tight junction when needed.

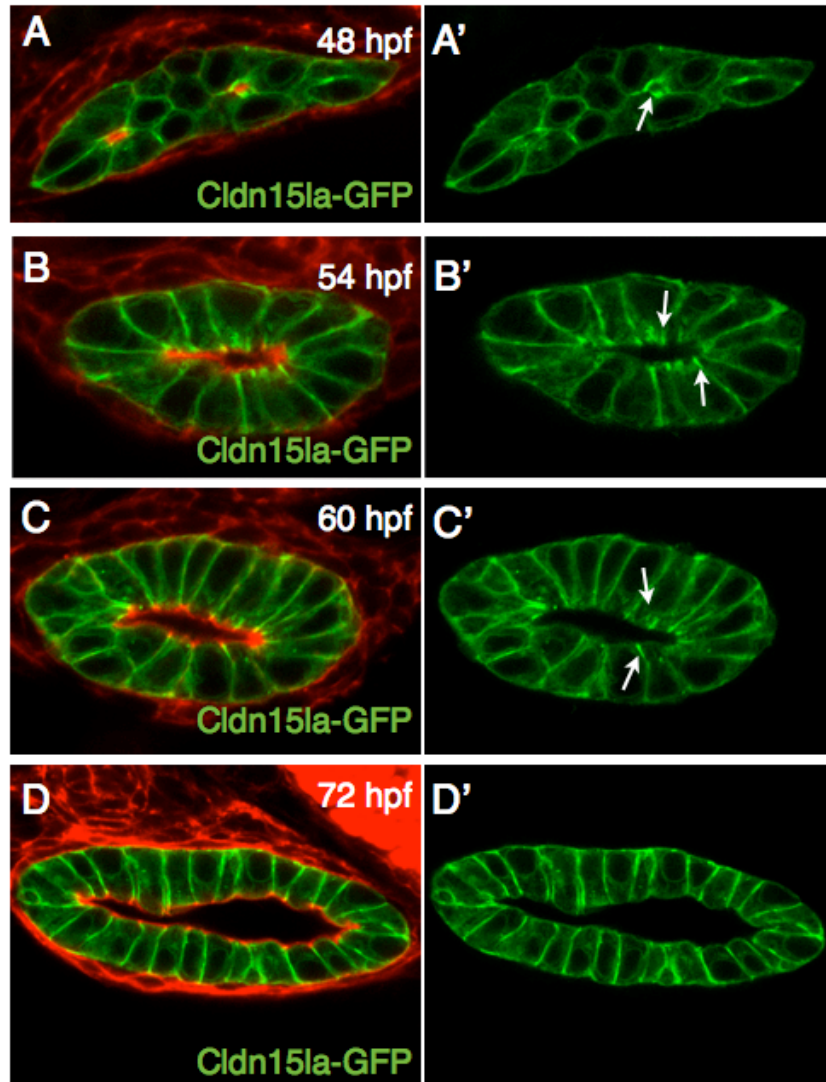


Figure 32- Claudin15la-GFP localization during development

A-D Confocal cross sections of *TgBAC(cldn15la-GFP)* embryos at 48, 54, 60, and 72 hpf. Arrows point to tight junction localization of Cldn15la. Phalloidin is in red.

There are several possible roles for Claudin in the gut during the period of lumen formation. For example, as a basolateral protein, Cldn15la could be involved in cell-cell adhesion during epithelial remodeling. Alternatively, Cldn15la could regulate lumen initiation through its interaction with the actin-based cytoskeleton. The early localization to the tight junctions could suggest a role for Cldn15la in the regulation of paracellular ion and fluid flow into the lumen. Similar to the rat uterus, Cldn15 may relocate from tight junctions to the basolateral membrane based on a need for paracellular fluid flow during lumen expansion. To address the function of Cldn15la in the gut, we can generate a TALEN mutant and examine the processes of lumen initiation, fluid accumulation, and lumen fusion in mutant embryos. Since expression of Cldn15la is highly specific to the gut, we would not expect any problems with viability or non-specific effects from other organ systems.

The early and specific expression pattern of Cldn15la also allows us to generate valuable tools to study intestine development. We have created a Cldn15la-Gal4 fusion construct through BAC recombineering to regulate the expression of genes specifically in the gut. The majority of experiments described previously used the heat shock promoter to temporally control gene expression, but ubiquitous expression in response to heat shock is not ideal in all situations. The Cldn15la-Gal4 transgenic line will allow us to express dominant negative forms of essential genes, such as Rab5, dynamin, and cadherin, specifically in the intestine to avoid problems with early lethality and non-specific effects. This line will not only provide a better tool to investigate the molecular

regulators of lumen formation but can also be utilized in several other gut related projects in the lab.

6.5 Investigation of Array Targets

During our lumen formation study we took advantage of our ability to sort gut specific cells to determine gene expression levels under a variety of conditions. Our first array compared gene expression in intestinal and non-intestinal cells at 3 and 5 dpf. The purpose of this array was to identify genes highly specific to the gut that may play critical roles during the early and later stages of gut development, and many of the genes from the array required further investigation. The serine/threonine kinase, *stk24*, exhibited the greatest fold change with a 595-fold upregulation in the gut compared to non-gut cells. In situ hybridization confirmed its expression in the gut and a TALEN mutant was created to examine loss of function. At this point, no observable lumen phenotype has been found in the gut based strictly on morphology. However, more experiments need to be performed to determine if *stk24a* mutants exhibit any physiological abnormalities, including defects in cell differentiation, endocytosis, or fluid regulation. Several additional genes from the array have also been targeted for future studies. Expression of the actin associated lipid binding protein, *anax2b*, was enriched 300-fold in gut cells while the scaffold protein *pdzk1* was 170 fold more expressed. Anaxa2b localizes apically early in lumen formation and can be used as a marker in studies involving polarity initiation and apical sorting machinery as described above. *pdzk1* can also be studied in terms of polarity establishment and maintenance. Pdzk1 is a scaffold protein containing 4 PDZ domains and mediates the clustering of proteins at the cell surface. A

pdzk1 TALEN mutant has been created but does not have any morphological defects. To further study the role of *pdzk1* in the gut, mutants can be crossed to transgenic lines expressing various polarity markers, such as Podxl, Syntaxin3, and Clic5. If these markers fail to polarize or if they accumulate intracellularly it would indicate that actin scaffolding is critical for proper apical targeting. Furthermore, if lumens are still able to form despite intracellular retention of apical proteins such as podocalyxin, it would imply that apical membrane establishment is not required for lumen initiation. Alternatively, *pdzk1* could also be involved in polarity maintenance, which can potentially have functional effects later in gut development. As such, embryos can be examined beyond 5 dpf for defects in barrier function, absorption, and fluid regulation.

We also performed a second microarray to compare gene expression levels of WT and *smo* mutant intestinal cells. This array was only minimally analyzed, and further analysis this array can provide additional information that can initiate future studies on single lumen formation and Hh signaling in the gut. Several collagen family members were highly downregulated in *smo* mutants, suggesting a potential defect in the basement membrane. Studies in the mouse intestine have showed that inhibition of the hedgehog pathway leads to a downregulation of basement membrane genes including integrin and collagen, and an upregulation of MMPs. This suggests that loss of Hh signaling causes a degradation of the basement membrane through expression of MMPs (Kosinski et al., 2010). Furthermore, work in MDCK cysts have established that cues from the ECM are essential in regulating the intracellular signaling that controls apical-basal polarity. In such a system, integrin and collagen interactions activate Rac-1 to induce laminin

assembly, which is required for polarity (O'Brien et al., 2001). Therefore, the basement membrane is an area of study that may provide additional insight into the regulation of single lumen formation in the zebrafish gut.

6.6 Conclusions

In this study, I have thoroughly examined the process of lumenogenesis in the zebrafish gut and identified a previously uncharacterized stage of single lumen formation. The resolution stage of lumen formation is characterized by enlarged unfused lumens separated by basolateral cell contacts. This stage of lumen formation requires cellular remodeling to facilitate lumen coalescence, which can occur through lumen fusion or adhesion snapping events. Furthermore, I have shown that the Hh signaling pathway is required for lumen fusion and have established lumen fusion and lumen enlargement as two genetically separable events. In addition, Rab11 mediated recycling was found to be impaired in *smo* mutants and critical to the process of lumen fusion. Finally, through this study I have generated novel tools and assays to specifically address questions during early gut development, which has provided insight into the molecular processes regulating cellular rearrangement during lumen resolution and has elicited new questions for future areas of study.

The knowledge gained from the studies presented here not only expand our understanding of zebrafish gut development, but can also be applied to human organ development and disease. Cord hollowing, for example, occurs during human pancreas development. The pancreatic ductal network forms via epithelial remodeling and fusion of secondary lumens with a primary duct, which is similar to what is observed in the

zebrafish gut. Therefore, work uncovering the cellular and molecular mechanisms regulating lumen formation in the zebrafish gut could provide insight into pancreatic duct development in humans. Furthermore, greater knowledge of the mechanisms regulating lumen formation can also help to elucidate causes of tubular diseases such as polycystic kidney disease. Aside from lumen formation, our studies on intracellular recycling and remodeling in the gut can also be applied to mammalian systems. Cadherin regulation and trafficking, which we show is important for lumen fusion, is involved in a large number of developmental processes across organisms. Furthermore, improper regulation of cadherin and other adhesion proteins leads to severe morphogenic defects, diseases, and tumor progression. Taken together, our study of lumen formation in the zebrafish gut can provide insight into mammalian development and has applications in organ morphogenesis and disease in humans.

Appendix

Microarray data

In this section I have included data obtained from two microarrays associated with studies presented here. The first array compared gene expression levels in non-intestinal epithelial cells with intestinal epithelial cells to identify genes that are highly enriched in the gut. The data sets shown in Table 1 and 2 list the top upregulated and downregulated genes in the intestinal epithelium relative to the rest of the embryo. I used the DAVID bioinformatics database to analyze the top and bottom most genes from the array to identify functionally related gene groups and pathways that are common amongst genes within each set. The most upregulated group of genes, and therefore most specific to the gut, include genes associated with metabolism and biosynthesis (Figure 33).

Interestingly, the most downregulated genes in the gut compared to the rest of the embryo include many genes associated with cell-cell adhesion, the ECM, and the Hh pathway (Figure 34).

The second set of array data presented in this section was obtained from intestinal epithelial cells from WT and *smo* mutant embryos. Table 3 and 4 shows the most upregulated and downregulated genes in mutant embryos compared to WT. DAVID analysis of unregulated genes in the *smo* intestine showed an enrichment of general metabolic genes (Figure 35). Analysis of downregulated genes on the other hand revealed an enrichment of genes associated with endocytosis (specifically the recycling pathway) and cell adhesion amongst others, which is in line with our experimental data (Figure 36

and 37). However, additional analysis of this array will be necessary for a more in-depth interpretation of the data.

Table 1- Downregulated genes in the intestinal epithelium

Gene Name	Fold downregulated
nephrosin-like	53.55
transient receptor potential cation channel, subfamily V,	48.36
collagen, type IX, alpha 1	44.75
collagen, type IX, alpha 1	44.10
similar to cathepsin L	40.81
cathepsin L, 1 b	39.01
protein tyrosine phosphatase, receptor type, C	37.15
keratin 5	35.95
collagen, type XI, alpha 1a	29.68
daz-like gene	28.15
collagen, type I, alpha 1b	27.97
pre-B-cell leukemia homeobox interacting protein 1a	27.90
collagen type II, alpha-1a	27.78
hypothetical protein LOC553366	27.32
retinol dehydrogenase 8 like	27.23
type I cytokeratin	26.60
hatching enzyme 1b	26.29
matrilin 1	26.18
matrix metalloproteinase 13a	25.65
calymmin	25.51
claudin i	24.88
collagen, type I, alpha 2	24.85
Sperm acrosome membrane-associated protein 4-like	24.43
lysophosphatidic acid receptor 6 like	24.29
retinol binding protein 4, plasma	24.23
periostin, osteoblast specific factor	23.96
PLAC8-like protein 1-like	23.88
aminopeptidase N-like	23.87
integrin beta 3b	23.73
hatching enzyme 1a	23.45
collagen type II, alpha-1b	23.39
odorant receptor, family H, subfamily 132, member 4	23.33
spleen focus forming virus proviral integration oncogene spil	22.65
matrilin 3b	21.90
rhodopsin	21.74
neurexin 3b	21.68
Rhesus blood group, B glycoprotein	21.30
claudin 1	21.25
collagen, type IX, alpha 3	21.11
cholinergic receptor, nicotinic, alpha 10	21.07
lysozyme	21.03

Table 2- Upregulated genes in intestinal epithelial cells

Gene Name	Fold upregulated
serine/threonine kinase 24a (STE20 homolog, yeast)	595.56
carbonic anhydrase IV b	586.66
claudin 15-like a	372.47
annexin A2b	354.99
caudal type homeobox 1 b	320.69
hypothetical LOC794295	306.67
caudal type homeo box transcription factor 1 a	245.92
angiotensin I converting enzyme (peptidyl-dipeptidase A) 2	212.02
hexose-binding lectin 3	205.36
hexose-binding lectin 3	199.70
alanyl (membrane) aminopeptidase	195.64
bridging integrator 2a	179.41
bloodthirsty-related gene family, member 6	176.50
PDZ domain containing 1	173.59
fatty acid binding protein 6, ileal (gastrotropin)	161.93
claudin 15b	160.25
solute carrier family 34 (sodium phosphate), member 2a	150.89
claudin 15a	137.73
solute carrier family 47, member 1	134.30
acyl-CoA synthetase long-chain family member 5	134.10
sialidase 3.3	132.35
cytochrome P450, family 7, subfamily A, polypeptide 1a	128.38
Neu3.4	124.01
UDP glucuronosyltransferase 5 family, polypeptide A2	113.88
indoleamine 2,3-dioxygenase 1	103.75
transmembrane protein 86B	101.07
villin 1 like	101.01
hypothetical LOC561946	97.07
complement component bfb	95.41
cadherin 17, LI cadherin (liver-intestine)	88.23
myosin VIIa-like	87.98
monoacylglycerol O-acyltransferase 2	86.08
solute carrier family 5 member 1	85.30
caudal type homeo box transcription factor 4	85.24
solute carrier family 13, member 2	84.36
dipeptidyl-peptidase 4	80.41
glutamyl aminopeptidase	79.29
similar to leucine rich repeat containing 24	76.95
plastin 1 (I isoform)	76.34
sb:cb166	72.91
tetraspanin 13a	72.85
crystallin, gamma M3	72.70
indoleamine 2,3-dioxygenase 1	71.16
cytochrome P450, family 2, subfamily J, polypeptide 22	68.21
membrane guanylyl cyclase-like	67.64
pyruvate carboxylase	67.45

Term	RT	Genes	Count	%	P-Value
PPAR signaling pathway	RT		25	1.3	6.4E-9
Fatty acid metabolism	RT		18	0.9	2.0E-8
Valine, leucine and isoleucine degradation	RT		20	1.0	2.7E-8
Tryptophan metabolism	RT		19	1.0	4.2E-8
Steroid biosynthesis	RT		11	0.6	1.8E-6
Aminoacyl-tRNA biosynthesis	RT		16	0.8	6.5E-6
Metabolism of xenobiotics by cytochrome P450	RT		12	0.6	1.0E-5
Drug metabolism	RT		12	0.6	1.0E-5
Ascorbate and aldarate metabolism	RT		9	0.5	1.0E-5
beta-Alanine metabolism	RT		11	0.6	1.5E-5
One carbon pool by folate	RT		9	0.5	5.1E-5
Propanoate metabolism	RT		13	0.7	9.6E-5
Retinol metabolism	RT		12	0.6	1.1E-4
Cysteine and methionine metabolism	RT		15	0.8	1.3E-4
Glutathione metabolism	RT		14	0.7	1.6E-4
Histidine metabolism	RT		10	0.5	3.0E-4
Biosynthesis of unsaturated fatty acids	RT		9	0.5	4.9E-4
Linoleic acid metabolism	RT		8	0.4	7.8E-4
Drug metabolism	RT		12	0.6	8.4E-4
Primary bile acid biosynthesis	RT		7	0.4	1.2E-3
Terpenoid backbone biosynthesis	RT		7	0.4	2.0E-3
Pentose and glucuronate interconversions	RT		7	0.4	2.0E-3
Arginine and proline metabolism	RT		16	0.8	2.4E-3
Arachidonic acid metabolism	RT		11	0.6	2.5E-3
alpha-Linolenic acid metabolism	RT		6	0.3	3.2E-3
Butanoate metabolism	RT		10	0.5	3.3E-3
Porphyrin and chlorophyll metabolism	RT		10	0.5	4.3E-3

Figure 33- Common biological pathways associated with upregulated genes in the intestinal epithelium

Screenshot from the DAVID bioinformatics database showing biological pathways that are associated with 1900 upregulated genes in the intestinal epithelium

Term	RT	Genes	Count	%	P-Value
Cell adhesion molecules (CAMs)	RT		45	1.2	2.4E-9
Focal adhesion	RT		73	1.9	9.1E-9
Hedgehog signaling pathway	RT		28	0.7	1.3E-6
ECM-receptor interaction	RT		27	0.7	2.5E-5
Melanogenesis	RT		40	1.0	8.2E-5
Cytokine-cytokine receptor interaction	RT		37	1.0	4.4E-4
Tight junction	RT		42	1.1	5.1E-4
Regulation of actin cytoskeleton	RT		58	1.5	1.8E-3
Cardiac muscle contraction	RT		24	0.6	9.5E-3
Glycosphingolipid biosynthesis	RT		8	0.2	1.3E-2
Keratan sulfate biosynthesis	RT		7	0.2	1.6E-2
Nitrogen metabolism	RT		9	0.2	2.0E-2
Calcium signaling pathway	RT		52	1.4	3.3E-2
Wnt signaling pathway	RT		39	1.0	4.9E-2
Glycolysis / Gluconeogenesis	RT		17	0.4	5.5E-2
SNARE interactions in vesicular transport	RT		14	0.4	6.3E-2
Neuroactive ligand-receptor interaction	RT		55	1.4	7.5E-2
Fructose and mannose metabolism	RT		12	0.3	7.6E-2

Figure 34- Common biological pathways associated with downregulated genes in the intestinal epithelium

Screenshot from the DAVID bioinformatics database showing biological pathways that are associated with 3200 downregulated genes in the intestinal epithelium

Table 3- Downregulated genes in *smo* mutant intestinal epithelial cells

Gene Name	Fold Downregulated
fatty acid binding protein 11b	95.29
collagen, type X, alpha 1	61.83
claudin 15b	29.94
interleukin 1 receptor accessory protein-like 2	29.44
collagen, type XI, alpha 1a	25.69
septin 7a	24.04
collagen, type I, alpha 1b	23.64
myoglobin	20.37
NK6 transcription factor related, locus 2	19.93
dynactin 1a	19.85
actin, alpha 2, smooth muscle, aorta	19.22
decorin	19.11
MYC binding protein 2	18.64
sodium channel, voltage-gated, type III, beta	18.37
proprotein convertase subtilisin/kexin type 2	18.12
chymotrypsin-like	18.06
chymotrypsinogen B1	17.43
solute carrier family 40 (iron-regulated transporter)	17.39
crystallin, gamma S3	16.96
capthepsin B, b	16.58
parvalbumin 8	16.46
solute carrier family 12, member 10.1	16.25
period homolog 1a (Drosophila)	14.61
collagen, type IV, alpha 5 (Alport syndrome)	14.22
adaptor-related protein complex 2, beta 1 subunit	14.15
transmembrane protein 68	13.80
myomesin 1a (skelemin)	13.20
scavenger receptor class B, member 1	12.82
paired box gene 7a	12.81
solute carrier family 16, member 10	12.73
NCK-associated protein 1	12.52
ubiquitin specific peptidase 22	12.47
fep15 selenoprotein	12.28
distal-less homeobox gene 1a	12.09
retinoblastoma 1	12.01
solute carrier family 40, member 1	11.99
spectrin, beta, non-erythrocytic 1	11.86
pyrroline-5-carboxylate reductase-like	11.85
collagen type II, alpha-1a	11.79
KH-type splicing regulatory protein	11.74
opsin 1 (cone pigments), short-wave-sensitive 1	11.61
protein phosphatase 2, regulatory subunit B'	11.50
kinesin family member 1C	11.44
axin 2 (conductin, axil)	11.35
vestigial like 4 (Drosophila)	11.29
ankyrin repeat domain 1b (cardiac muscle)	11.29
homeo box B13a	11.27

Table 4- Upregulated genes in *smo* mutant intestinal epithelial cells

Gene Name	Fold Upregulated
ribosomal protein S3A	45.84
immunoresponsive gene 1, like	31.10
programmed cell death 2	31.08
claudin k	30.34
keratin 8	30.14
influenza virus NS1A binding protein a	27.79
glyceraldehyde-3-phosphate dehydrogenase,	27.72
nuclear receptor binding factor 2	25.41
guanine nucleotide binding protein, beta polypeptide 2-like 1	24.79
growth arrest and DNA-damage-inducible, beta a	24.79
ribosomal protein L7	24.54
protein tyrosine phosphatase, mitochondrial 1	24.16
lactate dehydrogenase Ba	23.95
alpha-1-microglobulin/bikunin precursor, like	23.93
ASF1 anti-silencing function 1 homolog Ba (<i>S. cerevisiae</i>)	23.23
microtubule-associated protein 1 light chain 3 beta	22.83
lysyl-tRNA synthetase	22.22
cysteine conjugate-beta lyase 2	22.22
complement factor B	21.91
transferrin-a	20.77
trm2 tRNA methyltransferase 2 homolog A (<i>S. cerevisiae</i>)	19.98
coagulation factor V	19.96
proliferation associated nuclear element	19.88
solute carrier family 25 alpha, member 5	19.71
complement factor D (adipsin) like	19.31
fibrinogen, B beta polypeptide	19.27
prodynorphin	19.25
protein phosphatase 2, catalytic subunit, beta isoform	19.19
type I cytokeratin, enveloping layer	19.13
TatD DNase domain containing 1	18.86
interferon induced transmembrane-like	18.65
HIRA interacting protein 5	18.59
LYR motif containing 1	18.54
tumor necrosis factor a (TNF superfamily, member 2)	18.52
malonyl CoA:ACP acyltransferase (mitochondrial)	18.47
caspase Xa	18.27
eukaryotic translation elongation factor 2b	17.82
keratin 18	17.50
suppressor of defective silencing 3 homolog (17.07
nuclear cap binding protein subunit 2	17.03
THO complex 5	17.00
glucose phosphate isomerase a	17.00
preprohepcidin 2	16.98
secreted immunoglobulin domain 4	16.87

Term	RT	Genes	Count	%	P-Value
Ribosome	RT		37	1.4	1.3E-7
Glycolysis / Gluconeogenesis	RT		29	1.1	2.5E-7
Fatty acid metabolism	RT		16	0.6	1.9E-4
Proteasome	RT		21	0.8	3.7E-4
beta-Alanine metabolism	RT		11	0.4	5.4E-4
Valine, leucine and isoleucine degradation	RT		17	0.6	9.3E-4
Limonene and pinene degradation	RT		9	0.3	9.8E-4
Pyruvate metabolism	RT		16	0.6	1.2E-3
Amino sugar and nucleotide sugar metabolism	RT		18	0.7	1.3E-3
Butanoate metabolism	RT		13	0.5	1.6E-3
Propanoate metabolism	RT		13	0.5	4.3E-3
Aminoacyl-tRNA biosynthesis	RT		14	0.5	7.9E-3
Glyoxylate and dicarboxylate metabolism	RT		7	0.3	1.6E-2
Tryptophan metabolism	RT		13	0.5	2.5E-2
NOD-like receptor signaling pathway	RT		16	0.6	2.6E-2
Lysine degradation	RT		14	0.5	3.5E-2
Pyrimidine metabolism	RT		24	0.9	4.0E-2
Porphyrin and chlorophyll metabolism	RT		10	0.4	5.5E-2
Glycosphingolipid biosynthesis	RT		5	0.2	5.7E-2
Histidine metabolism	RT		8	0.3	6.1E-2
Glycosaminoglycan degradation	RT		8	0.3	6.1E-2
Lysosome	RT		30	1.1	7.6E-2
Fructose and mannose metabolism	RT		12	0.4	8.0E-2

Figure 35- Common biological pathways associated with upregulated genes in *smo*

Screenshot from the DAVID bioinformatics database showing biological pathways that are associated with 2600 upregulated genes in *smo* mutants.


Term	RT	Genes	Count	%	P-Value
Wnt signaling pathway	RT		40	1.4	2.8E-3
Ubiquitin mediated proteolysis	RT		31	1.1	6.3E-3
Focal adhesion	RT		46	1.6	1.5E-2
Spliceosome	RT		28	1.0	2.0E-2
Oocyte meiosis	RT		29	1.0	2.3E-2
Circadian rhythm	RT		7	0.2	4.2E-2
ECM-receptor interaction	RT		16	0.6	6.9E-2
Endocytosis	RT		46	1.6	7.4E-2
Adherens junction	RT		21	0.7	7.6E-2
RNA degradation	RT		14	0.5	9.6E-2

Figure 36- Common biological pathways associated with downregulated genes in *smo*

Screenshot from the DAVID bioinformatics database showing biological pathways that are associated with 2800 downregulated genes in *smo* mutants.

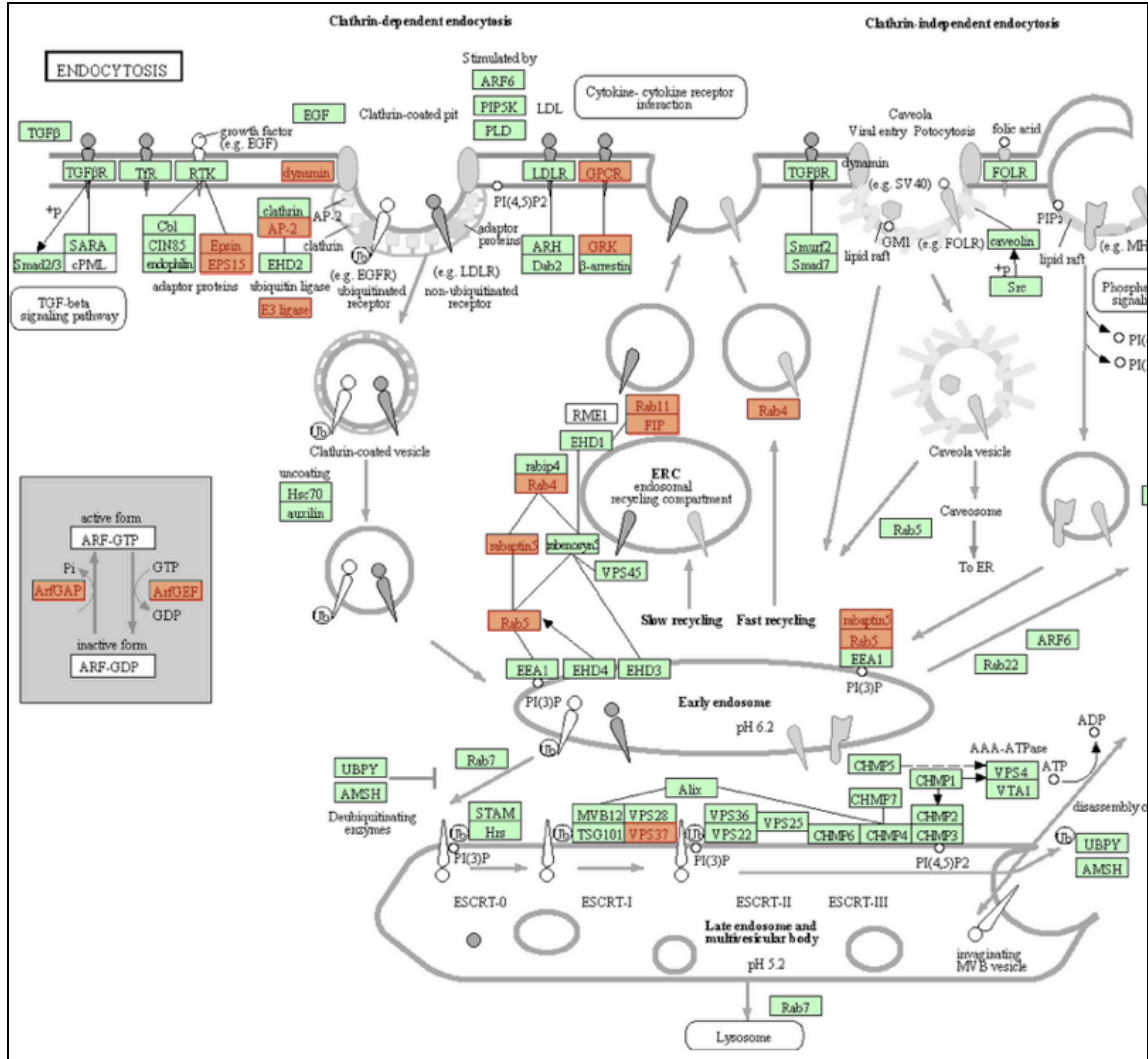


Figure 37- The endocytic pathway is downregulated in *smo* mutants

Snapshot from DAVID bioinformatics database showing the endocytic pathway. Genes in red are downregulated in *smo* mutants.

References

- Aanstad, P., Santos, N., Corbit, K. C., Scherz, P. J., Trinh, L. A., Salvenmoser, W., Huisken, J., Reiter, J. F. and Stainier, D. Y. R. (2009). The extracellular domain of Smoothed regulates ciliary localization and is required for high-level Hh signaling. *Curr Biol* 19, 1034-1039.
- Aridor, M. and Hannan, L. A. (2002). Traffic jams II: an update of diseases of intracellular transport. *Traffic* 3, 781-790.
- Bagnat, M., Cheung, I. D., Mostov, K. E. and Stainier, D. Y. R. (2007). Genetic control of single lumen formation in the zebrafish gut. *Nat Cell Biol* 9, 954-960.
- Bagnat, M., Navis, A., Herbstreith, S., Brand-Arzamendi, K., Curado, S., Gabriel, S., Mostov, K., Huisken, J. and Stainier, D. Y. (2010). Cse11 is a negative regulator of CFTR-dependent fluid secretion. *Curr Biol* 20, 1840-1845.
- Berry, K. L., Bülow, H. E., Hall, D. H. and Hobert, O. (2003). A *C. elegans* CLIC-like protein required for intracellular tube formation and maintenance. *Science* 302, 2134-2137.
- Berryman, M., Bruno, J., Price, J. and Edwards, J. C. (2004). CLIC-5A functions as a chloride channel in vitro and associates with the cortical actin cytoskeleton in vitro and in vivo. *J Biol Chem* 279, 34794-34801.
- Bitgood, M. J. and McMahon, A. P. (1995). Hedgehog and Bmp genes are coexpressed at many diverse sites of cell-cell interaction in the mouse embryo. *Dev Biol* 172, 126-138.
- Board, P. G., Coggan, M., Watson, S., Gage, P. W. and Dulhunty, A. F. (2004). CLIC-2 modulates cardiac ryanodine receptor Ca²⁺ release channels. *The international journal of biochemistry & cell biology* 36, 1599-1612.
- Bryant, D. M., Datta, A., Rodríguez-Fraticelli, A. E., Peränen, J., Martín-Belmonte, F. and Mostov, K. E. (2010). A molecular network for de novo generation of the apical surface and lumen. *Nature cell biology*.
- Bryant, D. M. and Stow, J. L. (2004). The ins and outs of E-cadherin trafficking. *Trends Cell Biol* 14, 427-434.
- Bucci, C., Parton, R. G., Mather, I. H., Stunnenberg, H., Simons, K., Hoflack, B. and Zerial, M. (1992). The small GTPase rab5 functions as a regulatory factor in the early endocytic pathway. *Cell* 70, 715-728.

- Bucci, C., Thomsen, P., Nicoziani, P., McCarthy, J. and van Deurs, B. (2000). Rab7: a key to lysosome biogenesis. *Mol Biol Cell* 11, 467-480.
- Buckley, C. E., Ren, X., Ward, L. C., Girdler, G. C., Araya, C., Green, M. J., Clark, B. S., Link, B. A. and Clarke, J. D. (2013). Mirror-symmetric microtubule assembly and cell interactions drive lumen formation in the zebrafish neural rod. *The EMBO journal* 32, 30-44.
- Buechner, M. (2002). Tubes and the single *C. elegans* excretory cell. *Trends Cell Biol* 12, 479-484.
- Calhoun, B. C., Lapierre, L. A., Chew, C. S. and Goldenring, J. R. (1998). Rab11a redistributes to apical secretory canaliculus during stimulation of gastric parietal cells. *The American journal of physiology* 275, C163-170.
- Cao, X., Surma, M. A. and Simons, K. (2012). Polarized sorting and trafficking in epithelial cells. *Cell research* 22, 793-805.
- Chen, W., Burgess, S. and Hopkins, N. (2001). Analysis of the zebrafish smoothed mutant reveals conserved and divergent functions of hedgehog activity. *Development* 128, 2385-2396.
- Cheung, I. D., Bagnat, M., Ma, T. P., Datta, A., Evason, K., Moore, J. C., Lawson, N. D., Mostov, K. E., Moens, C. B. and Stainier, D. Y. (2012). Regulation of intrahepatic biliary duct morphogenesis by Claudin 15-like b. *Dev Biol* 361, 68-78.
- Choi, W. Y., Gemberling, M., Wang, J., Holdway, J. E., Shen, M. C., Karlstrom, R. O. and Poss, K. D. (2013). In vivo monitoring of cardiomyocyte proliferation to identify chemical modifiers of heart regeneration. *Development* 140, 660-666.
- Clark, B. S., Winter, M., Cohen, A. R. and Link, B. A. (2011). Generation of Rab-based transgenic lines for in vivo studies of endosome biology in zebrafish. *Developmental dynamics : an official publication of the American Association of Anatomists* 240, 2452-2465.
- Classen, A. K., Anderson, K. I., Marois, E. and Eaton, S. (2005). Hexagonal packing of *Drosophila* wing epithelial cells by the planar cell polarity pathway. *Dev Cell* 9, 805-817.
- Cromer, B. A., Morton, C. J., Board, P. G. and Parker, M. W. (2002). From glutathione transferase to pore in a CLIC. *Eur Biophys J* 31, 356-364.

- Crosnier, C., Vargesson, N., Gschmeissner, S., Ariza-McNaughton, L., Morrison, A. and Lewis, J. (2005). Delta-Notch signalling controls commitment to a secretory fate in the zebrafish intestine. *Development* 132, 1093-1104.
- Davis, M. A., Ireton, R. C. and Reynolds, A. B. (2003). A core function for p120-catenin in cadherin turnover. *J Cell Biol* 163, 525-534.
- Denker, E. and Jiang, D. (2012). *Ciona* intestinalis notochord as a new model to investigate the cellular and molecular mechanisms of tubulogenesis. *Semin Cell Dev Biol* 23, 308-319.
- Desclozeaux, M., Venturato, J., Wylie, F. G., Kay, J. G., Joseph, S. R., Le, H. T. and Stow, J. L. (2008). Active Rab11 and functional recycling endosome are required for E-cadherin trafficking and lumen formation during epithelial morphogenesis. *American journal of physiology. Cell physiology* 295, C545-556.
- Dong, B., Horie, T., Denker, E., Kusakabe, T., Tsuda, M., Smith, W. C. and Jiang, D. (2009). Tube formation by complex cellular processes in *Ciona intestinalis* notochord. *Dev Biol* 330, 237-249.
- Dong, P. D., Munson, C. A., Norton, W., Crosnier, C., Pan, X., Gong, Z., Neumann, C. J. and Stainier, D. Y. (2007). Fgf10 regulates hepatopancreatic ductal system patterning and differentiation. *Nat Genet* 39, 397-402.
- Feng, Y., Press, B. and Wandinger-Ness, A. (1995). Rab 7: an important regulator of late endocytic membrane traffic. *J Cell Biol* 131, 1435-1452.
- Field, H. A., Dong, P. D. S., Beis, D. and Stainier, D. Y. R. (2003). Formation of the digestive system in zebrafish. ii. pancreas morphogenesis☆. *Developmental Biology* 261, 197-208.
- Furuse, M., Fujita, K., Hiiragi, T., Fujimoto, K. and Tsukita, S. (1998). Claudin-1 and -2: novel integral membrane proteins localizing at tight junctions with no sequence similarity to occludin. *J Cell Biol* 141, 1539-1550.
- Gagnon, L. H., Longo-Guess, C. M., Berryman, M., Shin, J.-B., Saylor, K. W., Yu, H., Gillespie, P. G. and Johnson, K. R. (2006). The chloride intracellular channel protein CLIC5 is expressed at high levels in hair cell stereocilia and is essential for normal inner ear function. *J Neurosci* 26, 10188-10198.
- Georgijevic, S., Subramanian, Y., Rollins, E. L., Starovic-Subota, O., Tang, A. C. and Childs, S. J. (2007). Spatiotemporal expression of smooth muscle markers in developing zebrafish gut. *Developmental dynamics : an official publication of the American Association of Anatomists* 236, 1623-1632.

- Georgiou, M., Marinari, E., Burden, J. and Baum, B. (2008). Cdc42, Par6, and aPKC regulate Arp2/3-mediated endocytosis to control local adherens junction stability. *Curr Biol* 18, 1631-1638.
- Gorvel, J. P., Chavrier, P., Zerial, M. and Gruenberg, J. (1991). rab5 controls early endosome fusion in vitro. *Cell* 64, 915-925.
- Gregory, M., Dufresne, J., Hermo, L. and Cyr, D. (2001). Claudin-1 is not restricted to tight junctions in the rat epididymis. *Endocrinology* 142, 854-863.
- Grieve, A. G., Moss, S. E. and Hayes, M. J. (2012). Annexin A2 at the interface of actin and membrane dynamics: a focus on its roles in endocytosis and cell polarization. *International journal of cell biology* 2012, 852430.
- Hales, C. M., Griner, R., Hobdy-Henderson, K. C., Dorn, M. C., Hardy, D., Kumar, R., Navarre, J., Chan, E. K., Lapierre, L. A. and Goldenring, J. R. (2001). Identification and characterization of a family of Rab11-interacting proteins. *J Biol Chem* 276, 39067-39075.
- Harris, K. P. and Tepass, U. (2008). Cdc42 and Par proteins stabilize dynamic adherens junctions in the Drosophila neuroectoderm through regulation of apical endocytosis. *J Cell Biol* 183, 1129-1143.
- Herwig, L., Blum, Y., Krudewig, A., Ellertsdottir, E., Lenard, A., Belting, H. G. and Affolter, M. (2011). Distinct cellular mechanisms of blood vessel fusion in the zebrafish embryo. *Curr Biol* 21, 1942-1948.
- Hogan, B. L. M. and Kolodziej, P. A. (2002). Organogenesis: molecular mechanisms of tubulogenesis. *Nat Rev Genet* 3, 513-523.
- Hogg, N. A., Harrison, C. J. and Tickle, C. (1983). Lumen formation in the developing mouse mammary gland. *Journal of embryology and experimental morphology* 73, 39-57.
- Horne-Badovinac, S., Lin, D., Waldron, S., Schwarz, M., Mbamalu, G., Pawson, T., Jan, Y., Stainier, D. Y. and Abdelilah-Seyfried, S. (2001). Positional cloning of heart and soul reveals multiple roles for PKC lambda in zebrafish organogenesis. *Current biology : CB* 11, 1492-1502.
- Huang, P., Xiao, A., Zhou, M., Zhu, Z., Lin, S. and Zhang, B. (2011). Heritable gene targeting in zebrafish using customized TALENs. *Nature biotechnology* 29, 699-700.
- Huisken, J. and Stainier, D. Y. (2007). Even fluorescence excitation by multidirectional selective plane illumination microscopy (mSPIM). *Opt Lett* 32, 2608-2610.

- Hutagalung, A. H. and Novick, P. J. (2011). Role of Rab GTPases in membrane traffic and cell physiology. *Physiol Rev* 91, 119-149.
- Inai, T., Sengoku, A., Hirose, E., Iida, H. and Shibata, Y. (2007). Claudin-7 expressed on lateral membrane of rat epididymal epithelium does not form aberrant tight junction strands. *Anatomical record* 290, 1431-1438.
- Iruela-Arispe, M. L. and Beitel, G. J. (2013). Tubulogenesis. *Development* 140, 2851-2855.
- Ishizuya-Oka, A. and Hasebe, T. (2008). Sonic hedgehog and bone morphogenetic protein-4 signaling pathway involved in epithelial cell renewal along the radial axis of the intestine. *Digestion* 77 Suppl 1, 42-47.
- Jaffe, A. B., Kaji, N., Durgan, J. and Hall, A. (2008). Cdc42 controls spindle orientation to position the apical surface during epithelial morphogenesis. *The Journal of Cell Biology* 183, 625-633.
- Joberty, G., Petersen, C., Gao, L. and Macara, I. G. (2000). The cell-polarity protein Par6 links Par3 and atypical protein kinase C to Cdc42. *Nat Cell Biol* 2, 531-539.
- Kaestner, K. H., Silberg, D. G., Traber, P. G. and Schutz, G. (1997). The mesenchymal winged helix transcription factor Fkh6 is required for the control of gastrointestinal proliferation and differentiation. *Genes Dev* 11, 1583-1595.
- Kamei, M., Saunders, W. B., Bayless, K. J., Dye, L., Davis, G. E. and Weinstein, B. M. (2006). Endothelial tubes assemble from intracellular vacuoles in vivo. *Nature* 442, 453-456.
- Kedinger, M., Duluc, I., Fritsch, C., Lorentz, O., Plateroti, M. and Freund, J. N. (1998). Intestinal epithelial-mesenchymal cell interactions. *Annals of the New York Academy of Sciences* 859, 1-17.
- Kerman, B. E., Cheshire, A. M., Myat, M. M. and Andrew, D. J. (2008). Ribbon modulates apical membrane during tube elongation through Crumbs and Moesin. *Dev Biol* 320, 278-288.
- Khan, L. A., Zhang, H., Abraham, N., Sun, L., Fleming, J. T., Buechner, M., Hall, D. H. and Gobel, V. (2013). Intracellular lumen extension requires ERM-1-dependent apical membrane expansion and AQP-8-mediated flux. *Nat Cell Biol* 15, 143-156.
- Kolotuev, I., Hyenne, V., Schwab, Y., Rodriguez, D. and Labouesse, M. (2013). A pathway for unicellular tube extension depending on the lymphatic vessel determinant Prox1 and on osmoregulation. *Nat Cell Biol* 15, 157-168.

- Kolterud, A., Grosse, A. S., Zacharias, W. J., Walton, K. D., Kretovich, K. E., Madison, B. B., Waghray, M., Ferris, J. E., Hu, C., Merchant, J. L., et al. (2009). Paracrine Hedgehog signaling in stomach and intestine: new roles for hedgehog in gastrointestinal patterning. *Gastroenterology* 137, 618-628.
- Korz, S., Winata, C. L., Zheng, W., Yang, S., Yin, A., Ingham, P., Korzh, V. and Gong, Z. (2011). The interaction of epithelial Ihha and mesenchymal Fgf10 in zebrafish esophageal and swimbladder development. *Dev Biol* 359, 262-276.
- Kosinski, C., Stange, D. E., Xu, C., Chan, A. S., Ho, C., Yuen, S. T., Mifflin, R. C., Powell, D. W., Clevers, H., Leung, S. Y., et al. (2010). Indian hedgehog regulates intestinal stem cell fate through epithelial-mesenchymal interactions during development. *Gastroenterology* 139, 893-903.
- Kwan, K. M., Fujimoto, E., Grabher, C., Mangum, B. D., Hardy, M. E., Campbell, D. S., Parant, J. M., Yost, H. J., Kanki, J. P. and Chien, C. B. (2007). The Tol2kit: a multisite gateway-based construction kit for Tol2 transposon transgenesis constructs. *Developmental dynamics : an official publication of the American Association of Anatomists* 236, 3088-3099.
- Lai, F., Stubbs, L. and Artzt, K. (1994). Molecular analysis of mouse Rab11b: a new type of mammalian YPT/Rab protein. *Genomics* 22, 610-616.
- Landry, D., Sullivan, S., Nicolaides, M., Redhead, C., Edelman, A., Field, M., al-Awqati, Q. and Edwards, J. (1993). Molecular cloning and characterization of p64, a chloride channel protein from kidney microsomes. *J Biol Chem* 268, 14948-14955.
- Lapierre, L. A., Avant, K. M., Caldwell, C. M., Oztan, A., Apodaca, G., Knowles, B. C., Roland, J. T., Ducharme, N. A. and Goldenring, J. R. (2012). Phosphorylation of Rab11-FIP2 regulates polarity in MDCK cells. *Mol Biol Cell* 23, 2302-2318.
- Lapierre, L. A., Dorn, M. C., Zimmerman, C. F., Navarre, J., Burnette, J. O. and Goldenring, J. R. (2003). Rab11b resides in a vesicular compartment distinct from Rab11a in parietal cells and other epithelial cells. *Experimental cell research* 290, 322-331.
- Lapierre, L. A., Kumar, R., Hales, C. M., Navarre, J., Bhartur, S. G., Burnette, J. O., Provance, D. W., Jr., Mercer, J. A., Bahler, M. and Goldenring, J. R. (2001). Myosin vb is associated with plasma membrane recycling systems. *Mol Biol Cell* 12, 1843-1857.
- Le, T. L., Yap, A. S. and Stow, J. L. (1999). Recycling of E-cadherin: a potential mechanism for regulating cadherin dynamics. *J Cell Biol* 146, 219-232.

- Littler, D. R., Harrop, S. J., Goodchild, S. C., Phang, J. M., Mynott, A. V., Jiang, L., Valenzuela, S. M., Mazzanti, M., Brown, L. J., Breit, S. N., et al. (2010). The enigma of the CLIC proteins: Ion channels, redox proteins, enzymes, scaffolding proteins? *FEBS letters*.
- Lubarsky, B. and Krasnow, M. A. (2003). Tube morphogenesis: making and shaping biological tubes. *Cell* 112, 19-28.
- Madara, J. L., Neutra, M. R. and Trier, J. S. (1981). Junctional complexes in fetal rat small intestine during morphogenesis. *Dev Biol* 86, 170-178.
- Madison, B. B., McKenna, L. B., Dolson, D., Epstein, D. J. and Kaestner, K. H. (2009). FoxF1 and FoxL1 link hedgehog signaling and the control of epithelial proliferation in the developing stomach and intestine. *J Biol Chem* 284, 5936-5944.
- Marshansky, V. and Futai, M. (2008). The V-type H⁺-ATPase in vesicular trafficking: targeting, regulation and function. *Curr Opin Cell Biol* 20, 415-426.
- Martin-Belmonte, F., Gassama, A., Datta, A., Yu, W., Rescher, U., Gerke, V. and Mostov, K. (2007). PTEN-mediated apical segregation of phosphoinositides controls epithelial morphogenesis through Cdc42. *Cell* 128, 383-397.
- Martin-Belmonte, F. and Mostov, K. (2008). Regulation of cell polarity during epithelial morphogenesis. *Curr Opin Cell Biol* 20, 227-234.
- Melnick, M. and Jaskoll, T. (2000). Mouse submandibular gland morphogenesis: a paradigm for embryonic signal processing. *Critical reviews in oral biology and medicine : an official publication of the American Association of Oral Biologists* 11, 199-215.
- Mendoza-Rodriguez, C. A., Gonzalez-Mariscal, L. and Cerbon, M. (2005). Changes in the distribution of ZO-1, occludin, and claudins in the rat uterine epithelium during the estrous cycle. *Cell Tissue Res* 319, 315-330.
- Miller, J. C., Tan, S., Qiao, G., Barlow, K. A., Wang, J., Xia, D. F., Meng, X., Paschon, D. E., Leung, E., Hinkley, S. J., et al. (2011). A TALE nuclease architecture for efficient genome editing. *Nature biotechnology* 29, 143-148.
- Mohler, J. and Vani, K. (1992). Molecular organization and embryonic expression of the hedgehog gene involved in cell-cell communication in segmental patterning of *Drosophila*. *Development* 115, 957-971.

- Munson, C., Huisken, J., Bit-Avragim, N., Kuo, T., Dong, P. D., Ober, E. A., Verkade, H., Abdelilah-Seyfried, S. and Stainier, D. Y. (2008). Regulation of neurocoel morphogenesis by Pard6 gamma b. *Dev Biol* 324, 41-54.
- Nanes, B. A., Chiasson-MacKenzie, C., Lowery, A. M., Ishiyama, N., Faundez, V., Ikura, M., Vincent, P. A. and Kowalczyk, A. P. (2012). p120-catenin binding masks an endocytic signal conserved in classical cadherins. *J Cell Biol* 199, 365-380.
- Navis, A., Marjoram, L. and Bagnat, M. (2013). Cftr controls lumen expansion and function of Kupffer's vesicle in zebrafish. *Development* 140, 1703-1712.
- Nelson, W. J. (2003). Epithelial cell polarity from the outside looking in. *News in physiological sciences : an international journal of physiology produced jointly by the International Union of Physiological Sciences and the American Physiological Society* 18, 143-146.
- Ng, A. N., de Jong-Curtain, T. A., Mawdsley, D. J., White, S. J., Shin, J., Appel, B., Dong, P. D., Stainier, D. Y. and Heath, J. K. (2005). Formation of the digestive system in zebrafish: III. Intestinal epithelium morphogenesis. *Dev Biol* 286, 114-135.
- Nuckels, R. J., Ng, A., Darland, T. and Gross, J. M. (2009). The vacuolar-ATPase complex regulates retinoblast proliferation and survival, photoreceptor morphogenesis, and pigmentation in the zebrafish eye. *Invest Ophthalmol Vis Sci* 50, 893-905.
- O'Brien, L. E., Jou, T. S., Pollack, A. L., Zhang, Q., Hansen, S. H., Yurchenco, P. and Mostov, K. E. (2001). Rac1 orientates epithelial apical polarity through effects on basolateral laminin assembly. *Nat Cell Biol* 3, 831-838.
- Pack, M., Solnica-Krezel, L., Malicki, J., Neuhauss, S. C., Schier, A. F., Stemple, D. L., Driever, W. and Fishman, M. C. (1996). Mutations affecting development of zebrafish digestive organs. *Development* 123, 321-328.
- Palacios, F., Tushir, J. S., Fujita, Y. and D'Souza-Schorey, C. (2005). Lysosomal targeting of E-cadherin: a unique mechanism for the down-regulation of cell-cell adhesion during epithelial to mesenchymal transitions. *Molecular and cellular biology* 25, 389-402.
- Parkin, C. A., Allen, C. E. and Ingham, P. W. (2009). Hedgehog signalling is required for cloacal development in the zebrafish embryo. *The International journal of developmental biology* 53, 45-57.
- Paterson, A. D., Parton, R. G., Ferguson, C., Stow, J. L. and Yap, A. S. (2003). Characterization of E-cadherin endocytosis in isolated MCF-7 and chinese

- hamster ovary cells: the initial fate of unbound E-cadherin. *J Biol Chem* 278, 21050-21057.
- Pierchala, B. A., Munoz, M. R. and Tsui, C. C. (2010). Proteomic analysis of the slit diaphragm complex: CLIC5 is a protein critical for podocyte morphology and function. *Kidney Int* 78, 868-882.
- Pirraglia, C., Walters, J. and Myat, M. M. (2010). Pak1 control of E-cadherin endocytosis regulates salivary gland lumen size and shape. *Development* 137, 4177-4189.
- Pokutta, S. and Weis, W. I. (2007). Structure and mechanism of cadherins and catenins in cell-cell contacts. *Annual review of cell and developmental biology* 23, 237-261.
- Rahner, C., Mitic, L. L. and Anderson, J. M. (2001). Heterogeneity in expression and subcellular localization of claudins 2, 3, 4, and 5 in the rat liver, pancreas, and gut. *Gastroenterology* 120, 411-422.
- Ramalho-Santos, M., Melton, D. A. and McMahon, A. P. (2000). Hedgehog signals regulate multiple aspects of gastrointestinal development. *Development* 127, 2763-2772.
- Reichenbach, B., Delalande, J. M., Kolmogorova, E., Prier, A., Nguyen, T., Smith, C. M., Holzschuh, J. and Shepherd, I. T. (2008). Endoderm-derived Sonic hedgehog and mesoderm Hand2 expression are required for enteric nervous system development in zebrafish. *Dev Biol* 318, 52-64.
- Rodriguez-Boulan, E., Kreitzer, G. and Musch, A. (2005). Organization of vesicular trafficking in epithelia. *Nat Rev Mol Cell Biol* 6, 233-247.
- Sato, T., Mushiake, S., Kato, Y., Sato, K., Sato, M., Takeda, N., Ozono, K., Miki, K., Kubo, Y., Tsuji, A., et al. (2007). The Rab8 GTPase regulates apical protein localization in intestinal cells. *Nature* 448, 366-369.
- Satoh, A. K., O'Tousa, J. E., Ozaki, K. and Ready, D. F. (2005). Rab11 mediates post-Golgi trafficking of rhodopsin to the photosensitive apical membrane of *Drosophila* photoreceptors. *Development* 132, 1487-1497.
- Sawyer, J. M., Harrell, J. R., Shemer, G., Sullivan-Brown, J., Roh-Johnson, M. and Goldstein, B. (2010). Apical constriction: a cell shape change that can drive morphogenesis. *Dev Biol* 341, 5-19.
- Scheer, N. and Campos-Ortega, J. A. (1999). Use of the Gal4-UAS technique for targeted gene expression in the zebrafish. *Mechanisms of development* 80, 153-158.

- Scott, C. C. and Gruenberg, J. (2011). Ion flux and the function of endosomes and lysosomes: pH is just the start: the flux of ions across endosomal membranes influences endosome function not only through regulation of the luminal pH. *BioEssays : news and reviews in molecular, cellular and developmental biology* 33, 103-110.
- Sharma, N., Low, S. H., Misra, S., Pallavi, B. and Weimbs, T. (2006). Apical targeting of syntaxin 3 is essential for epithelial cell polarity. *J Cell Biol* 173, 937-948.
- Shaye, D. D., Casanova, J. and Llimargas, M. (2008). Modulation of intracellular trafficking regulates cell intercalation in the Drosophila trachea. *Nat Cell Biol* 10, 964-970.
- Shimeld, S. M. (1999). The evolution of the hedgehog gene family in chordates: insights from amphioxus hedgehog. *Development genes and evolution* 209, 40-47.
- Singh, H., Cousin, M. A. and Ashley, R. H. (2007). Functional reconstitution of mammalian 'chloride intracellular channels' CLIC1, CLIC4 and CLIC5 reveals differential regulation by cytoskeletal actin. *FEBS J* 274, 6306-6316.
- Strahle, U., Blader, P. and Ingham, P. W. (1996). Expression of axial and sonic hedgehog in wildtype and midline defective zebrafish embryos. *The International journal of developmental biology* 40, 929-940.
- Strilic, B., Eglinger, J., Krieg, M., Zeeb, M., Axnick, J., Babal, P., Muller, D. J. and Lammert, E. (2010). Electrostatic cell-surface repulsion initiates lumen formation in developing blood vessels. *Curr Biol* 20, 2003-2009.
- Tung, J. J., Hobert, O., Berryman, M. and Kitajewski, J. (2009). Chloride intracellular channel 4 is involved in endothelial proliferation and morphogenesis in vitro. *Angiogenesis* 12, 209-220.
- Ullrich, O., Reinsch, S., Urbe, S., Zerial, M. and Parton, R. G. (1996). Rab11 regulates recycling through the pericentriolar recycling endosome. *J Cell Biol* 135, 913-924.
- van der Sluijs, P., Hull, M., Webster, P., Male, P., Goud, B. and Mellman, I. (1992). The small GTP-binding protein rab4 controls an early sorting event on the endocytic pathway. *Cell* 70, 729-740.
- Villasenor, A., Chong, D. C., Henkemeyer, M. and Cleaver, O. (2010). Epithelial dynamics of pancreatic branching morphogenesis. *Development* 137, 4295-4305.
- Wallace, K. N., Akhter, S., Smith, E. M., Lorent, K. and Pack, M. (2005). Intestinal growth and differentiation in zebrafish. *Mech Dev* 122, 157-173.

- Wallace, K. N. and Pack, M. (2003). Unique and conserved aspects of gut development in zebrafish. *Dev Biol* 255, 12-29.
- Walton, K. D., Croce, J. C., Glenn, T. D., Wu, S. Y. and McClay, D. R. (2006). Genomics and expression profiles of the Hedgehog and Notch signaling pathways in sea urchin development. *Dev Biol* 300, 153-164.
- Wang, E., Brown, P. S., Aroeti, B., Chapin, S. J., Mostov, K. E. and Dunn, K. W. (2000). Apical and basolateral endocytic pathways of MDCK cells meet in acidic common endosomes distinct from a nearly-neutral apical recycling endosome. *Traffic* 1, 480-493.
- Wegner, B., Al-Momany, A., Kulak, S. C., Kozlowski, K., Obeidat, M., Jahroudi, N., Paes, J., Berryman, M. and Ballermann, B. J. (2010). CLIC5A, a component of the ezrin-podocalyxin complex in glomeruli, is a determinant of podocyte integrity. *American journal of physiology. Renal physiology* 298, F1492-1503.
- Wells, J. M. and Melton, D. A. (1999). Vertebrate endoderm development. *Annual review of cell and developmental biology* 15, 393-410.
- Westerfield, M. (2000). *The Zebrafish Book. A guide for the laboratory use of zebrafish (Danio rerio)*. Eugene, OR: University of Oregon Press.
- Westmoreland, J. J., Drosos, Y., Kelly, J., Ye, J., Means, A. L., Washington, M. K. and Sosa-Pineda, B. (2012). Dynamic distribution of claudin proteins in pancreatic epithelia undergoing morphogenesis or neoplastic transformation. *Developmental dynamics : an official publication of the American Association of Anatomists* 241, 583-594.
- Xiao, K., Allison, D. F., Buckley, K. M., Kottke, M. D., Vincent, P. A., Faundez, V. and Kowalczyk, A. P. (2003). Cellular levels of p120 catenin function as a set point for cadherin expression levels in microvascular endothelial cells. *J Cell Biol* 163, 535-545.
- Yap, A. S., Briehner, W. M. and Gumbiner, B. M. (1997). Molecular and functional analysis of cadherin-based adherens junctions. *Annual review of cell and developmental biology* 13, 119-146.
- Yu, W., Datta, A., Leroy, P., O'Brien, L. E., Mak, G., Jou, T. S., Matlin, K. S., Mostov, K. E. and Zegers, M. M. (2005). Beta1-integrin orients epithelial polarity via Rac1 and laminin. *Mol Biol Cell* 16, 433-445.
- Yudowski, G. A., Puthenveedu, M. A., Henry, A. G. and von Zastrow, M. (2009). Cargo-mediated regulation of a rapid Rab4-dependent recycling pathway. *Mol Biol Cell* 20, 2774-2784.

Zerial, M. and McBride, H. (2001). Rab proteins as membrane organizers. *Nat Rev Mol Cell Biol* 2, 107-117.

Zhang, X., Stappenbeck, T. S., White, A. C., Lavine, K. J., Gordon, J. I. and Ornitz, D. M. (2006). Reciprocal epithelial-mesenchymal FGF signaling is required for cecal development. *Development* 133, 173-180.

Biography

Ashley Alvers Lento was born on February 28th, 1984 in Miami, Florida to the parents of Steve and Louanne Alvers. She graduated in 2002 from the Agriscience and Biotechnology academy at Coral Reef High School and attended The University of Florida. At UF, Ashley majored in Integrative Biology, minored in Anthropology and participated in undergraduate research in the lab of Dr. Loius Guillette. Following graduation in 2006, she became a research technician for one year before entering the Development and Stem Cell Biology program at Duke University in 2007. She joined the Bagnat lab in the Department of Cell Biology in 2008.

PUBLICATIONS

- Alvers, A. L., Ryan, S., Scherz, P. J., Huisken, J. and Bagnat, M.** (2014). Single continuous lumen formation in the zebrafish gut is mediated by smoothed-dependent tissue remodeling. *Development*.
- Alvers, A.L. and M. Bagnat.** Translational Gastroenterology, from Development to Disease. Chapter- GI development and disease-zebrafish. *Wiley. In press*
- Aris, J. P., Alvers, A. L., Ferraiuolo, R. A., Fishwick, L. K., Hanvivatpong, A., Hu, D., Kirlew, C., Leonard, M. T., Losin, K. J., Marraffini, M., et al.** (2013). Autophagy and leucine promote chronological longevity and respiration proficiency during calorie restriction in yeast. *Experimental gerontology* **48**, 1107-1119.
- Moore, B. C., Kohno, S., Cook, R. W., Alvers, A. L., Hamlin, H. J., Woodruff, T. K. and Guillette, L. J.** (2010). Altered sex hormone concentrations and gonadal mRNA expression levels of activin signaling factors in hatchling alligators from a contaminated Florida lake. *Journal of experimental zoology. Part A, Ecological genetics and physiology* **313**, 218-230.
- Alvers, A. L., Wood, M. S., Hu, D., Kaywell, A. C., Dunn, W. A., Jr. and Aris, J. P.** (2009b). Autophagy is required for extension of yeast chronological life span by rapamycin. *Autophagy* **5**, 847-849.

Alvers, A. L., Fishwick, L. K., Wood, M. S., Hu, D., Chung, H. S., Dunn, W. A., Jr. and Aris, J. P. (2009a). Autophagy and amino acid homeostasis are required for chronological longevity in *Saccharomyces cerevisiae*. *Aging cell* **8**, 353-369

Maatouk, D. M., DiNapoli, L., Alvers, A., Parker, K. L., Taketo, M. M. and Capel, B. (2008). Stabilization of beta-catenin in XY gonads causes male-to-female sex-reversal. *Human molecular genetics* **17**, 2949-2955.